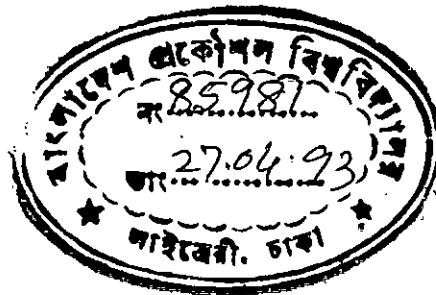


MICROWAVE DIPLEXER USING FORWARD COUPLED
MICROSTRIP COMBLINES



A Thesis submitted to the
Electrical and Electronic Engineering department of
BUET Dhaka, in partial fulfilment of the
requirements for the degree of
Master of Science in Engineering (Electrical and Electronic)

Md. Sayeed Akmal

March 1993



628.849.
1993
SAY

Declaration

I hereby declare that this work has not been submitted elsewhere for the award of any degree or diploma or for publication.


Md. Sayeed Akmal

Approval

The thesis MICROWAVE DIPLEXER USING FORWARD COUPLED MICROSTRIP COMBLINES submitted by Md. Sayeed Akmal, Roll No. 891319p, Session '87-88 to the Department of Electrical and Electronic Engineering of BUET has been accepted as satisfactory for partial fulfilment of the requirements for the degree of Master of Science in Engineering (Electrical and Electronic).

Board of Examineres

- | | | |
|--|---------------------------------|--------------------------------|
| 1. Dr. Saiful Islam
Professor and Head
Department of EEE
B.U.E.T., Dhaka 1000 | Chairman
(Supervisor) | <u>Saiful Islam</u>
29-3-93 |
| 2. Dr. Saiful Islam
Head
Department of EEE
B.U.E.T., Dhaka 1000 | Member
(Ex-officio) | <u>Saiful Islam</u>
29-3-93 |
| 3. Dr. A. B. M. Siddique Hossain
Professor and Dean
Faculty of EEE
B.U.E.T., Dhaka 1000 | Member | <u>[Signature]</u>
22/3/20 |
| 5. Dr. Shamsuddin Ahmed
Head
Department of EEE
ICTVTR, Gazipur | Member
(External) | <u>[Signature]</u>
22/3/20 |

Acknowledgement

With deep sincerity, the author wishes to acknowledge his profound gratitude to Professor Dr. Saiful Islam of Electrical and Electronic Engineering Department BUET for his incessant and meticulous guidance in completing this work. The author thanks him for his outstanding suggestions in the computation and design procedure of a forward coupled microstrip combline diplexer. The author also feels proud to acknowledge him for his expert opinion in designing the diplexer at every step of the entire research.

Thanks are given to Dr. Mohammad Ali Chowdhury, Mr. Mainul Hasan and Mr. Mohsin Mollah for their support and cooperation. Also thanks are given to the friends and colleagues who helped the author to complete this work.

Contents

Declaration	(i)
Approval	(ii)
Acknowledgement	(iii)
Contents	(iv)
Abstract	(vii)
Chapter 1: Introduction	
1.1 Historical review of multiplexers	1
1.2 Diplexer	3
1.3 Microstrip comb- and herringbone- lines	5
1.4 Compline diplexer	8
1.5 Objective of this research	9
1.6 Introduction to this work	9
Chapter 2: Review of the theory of n-coupled complines	
2.1 Introduction	12
2.2 Theory of n -coupled lines	13
2.3 The wave-propagation matrix \underline{J}	21
2.4 Capacitance and inductance matrices of an n -coupled compline system	23
2.5 The forward scattering matrix of forward coupled microstrip complines	25
2.6 Power and relative phase characteristics of an n -coupled compline system	26
2.7 Obtaining the line parameters of an n -coupled compline system from the \underline{J} matrix	28
2.8 Defining the \underline{e} vector for an n -coupled compline system	31
2.9 Summary	32

Chapter 3: Forward scattering matrix and line parameters of a combline diplexer

3.1	Introduction	33
3.2	Obtaining the forward scattering matrix of a combline diplexer from its wave-propagation matrix	35
3.3	The \underline{e} vector of a combline diplexer	37
3.4	Scaling a \underline{J} matrix	38
3.4.1	Scaling by scalar multiplication of a \underline{J} matrix	38
3.4.2	Scaling by adding a constant value with all the diagonal elements of a \underline{J} matrix	39
3.5	Determination of the parameters of a forward coupled microstrip combline diplexer from its wave propagation matrix	39
3.6	Summary	44

Chapter 4: Designing a combline diplexer by computer optimization

4.1	Introduction	45
4.2	Possible methods of optimization	47
4.2.1	Golden section search	49
4.2.2	Gradient methods	50
4.3	Selection of optimization algorithm	52
4.4	Optimization algorithm used in this work	52
4.5	The effect of changing the elements of \underline{e} vector on the characteristics of a diplexer	55
4.6	Starting value of the \underline{e} vector	77
4.7	Optimization of \underline{e} vector	78
4.8	Computation of the error function	80
4.9	The optimization program	85
4.10	Examples of optimization	86
4.11	Summary	97

Chapter 5: Obtaining the physical dimensions of a combline diplexer

5.1	Introduction	99
5.2	Modeling a solitary combline using the microstrip T-junction equivalent circuit	101
5.3	Necessary equations for obtaining the finger length and main-line characteristic impedance of a solitary microstrip combline	105
5.4	Obtaining the dimensions of a solitary microstrip combline	110
5.5	Obtaining the dimensions of a pair of coupled microstrip comblines . .	111
5.6	The computer program used in this work for computing the physical dimensions of a diplexer	112
5.7	Relationship between coupling capacitance and finger overlap of a pair of coupled combines	115
5.8	Summary	116

Chapter 6: Designing the diplexer

6.1	Introduction	117
6.2	Choice of Cu-clad laminate board, finger periodicity, finger line width and lower band edge frequency	117
6.3	Practical considerations for designing	118
6.4	Considerations regarding scaling and shifting	119
6.5	The design values	130
6.6	Summary	134

Chapter 7: Discussions and suggestions for future work

7.1	Discussions	135
7.2	Suggestions for future work	136
7.2.1	Developing an analytical design method	136
7.2.2	Developing a design method for a microstrip combline triplexer	137
7.2.3	Developing a designing method for microstrip combline quadruplexers, quintuplexers and n -channel multiplexers	137

References	157
------------------	-----

Appendices

Appendix A	List of the computer program for obtaining the power and relative phase characteristics of the ports of a diplexer	139
Appendix B	List of the computer program for optimizing the \underline{e} vector of a diplexer	144
Appendix C	List of the computer program for obtaining the line parameters of a diplexer from its \underline{e} vector	150

Abstract

A design method for a novel type of microwave diplexer using coupled microstrip comblines has been developed. The resulting diplexer is small in size, compact in structure and easy to fabricate by using photolithographic and etching techniques. This type of diplexer is suitable for use in Microwave Integrated Circuits (MIC) as well as Microwave Monolithic Integrated Circuits (MMIC).

For developing the new design method for the microstrip diplexers, the forward coupling properties of a pair of microstrip comblines are taken as the basis. In a previous work it has been shown that the characteristics of a pair of coupled microstrip comblines may be represented by a wave propagation matrix known as \underline{J} matrix. This \underline{J} matrix contains necessary information regarding the nature of propagation of waves in the coupled comblines.

In this work a diplexer is formed with the help of two coupled comblines. The \underline{J} matrix of such a diplexer is formed with the help of self line parameters of the two lines, the coupled line parameters and the length of the diplexer. It has been observed that the \underline{J} matrix obtained for a matched forward combline directional coupler in an earlier work provides a good starting \underline{J} matrix for this work. Using the \underline{J} matrix *scaling* and *shifting techniques* and also adjusting the coupled length, the operating band of the directional coupler is brought in between the required operating frequency ranges of the two output channels of the diplexer. The resulting \underline{J} matrix is then taken for optimization. In this work it has been found that a computer optimization technique using simple steepest descent algorithm works well for converting the directional coupler characteristics into the desired diplexer characteristics. The steps and techniques of the optimization procedure are presented. The matrix obtained after this optimization is next used for obtaining line parameters of the coupled comblines. The required equations for this purpose are also presented. After computing the physical dimensions of a microstrip combline diplexer it has been observed that the structure is physically realizable.

CHAPTER 1

Introduction



1.1 Historical review of multiplexers

In microwave engineering *multiplexers* are often required to split a single channel carrying many frequencies into a number of separate channels carrying narrow-band frequencies. When a band of microwave signals is fed into the input port of an n -channel multiplexer, it divides the signal-band into n -number of channels among n -number of output ports as per the design of the multiplexer. Generally filters of different characteristics are connected in series or in parallel to achieve multiplexing. A generalized block diagram of an n -channel multiplexer is shown in figure 1.1. Multiplexers may be of *contiguous channel* type or *non-contiguous channel* type. In contiguous type there is no frequency gap between two adjacent channels of the multiplexer. On the other hand, in non-contiguous type, guard bands are available between adjacent channels.

From the basic concept of multiplexer one might consider designing a multiplexer using a number of band pass filters having passbands in the ranges of the required multiplexer outputs. However, in practice, difficulties arise in such designs and usually special techniques are employed to avoid undesirable interactions between the filters which could result in very poor performance.

Several types of multiplexers [1] have been developed so far. One type of multiplexers uses *directional filters* [1]. These directional filters have a constant resistance input impedance provided that their output ports are terminated in their proper resistance terminations. When all the filters of such a multiplexer are designed for the same terminating resistance, the filters can be cascaded as shown in figure 1.2 to form a multiplexer where filter interaction problems are avoided. Each filter provides proper termination for its preceding neighbour and so there occurs no residual *Voltage Standing Wave Ratio* (VSWR) due to design and manufacturing imperfections. The system thus become reflectionless. In figure 1.2, Filter

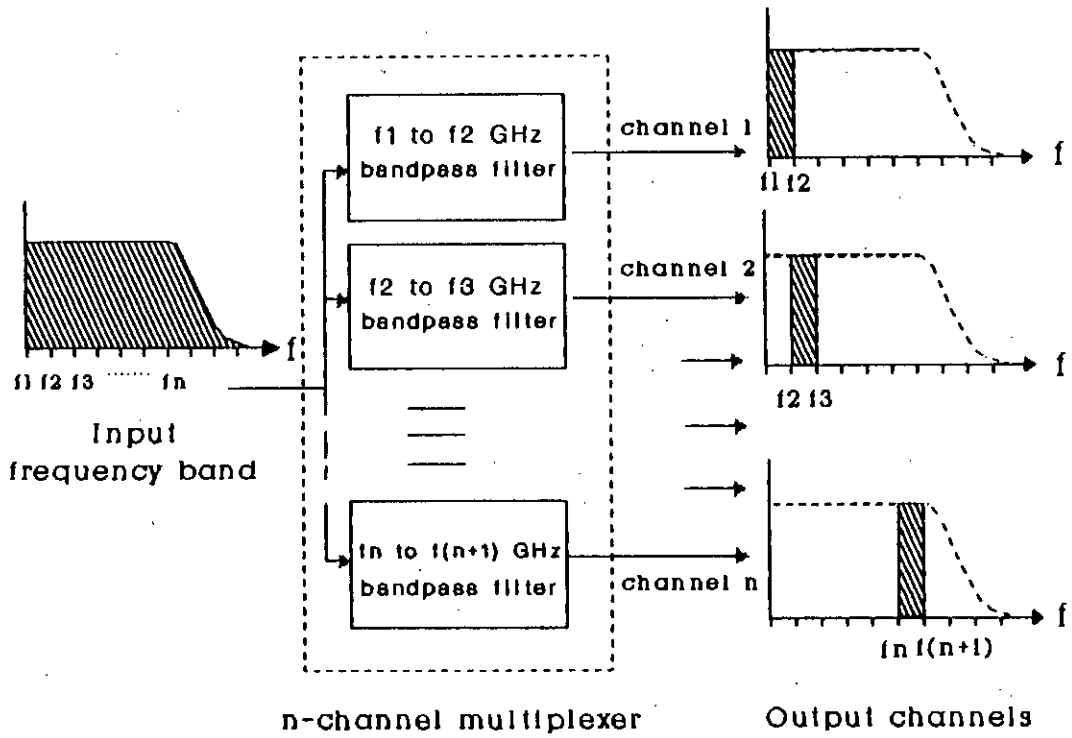


Fig. 1.1 Block diagram of an n -channel frequency multiplexe

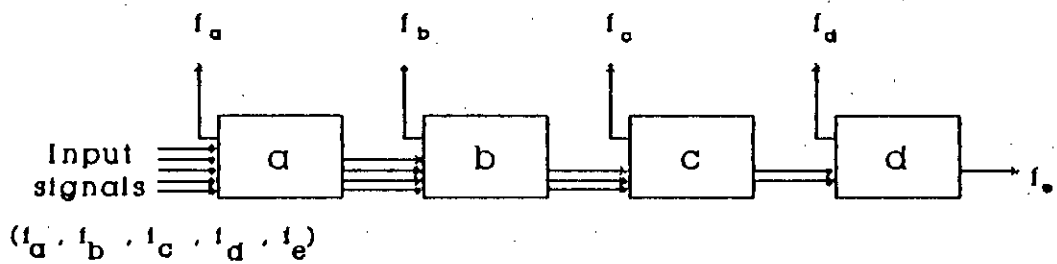


Fig. 1.2 Block diagram of a multiplexer using directional filters

a removes all of the energy at frequency f_a , but passes on the energy at all other frequencies. Filter b removes the energy at frequency f_b and so on. The use of directional filters for multiplexing is a simple way of solving multiplexing problem. In many cases it is also a very pragmatic solution, though by no means always the most practical way. The greatest practical drawback of directional filter is that each resonator of each filter has two different orthogonal modes, and if more than one or two resonators are required per filter, the tuning of the filters [1] may become very difficult.

There are also multiplexers which use *reflecting narrow-band filters*, with guard band between channels (noncontiguous) [1]. These multiplexers are used where the channels of a multiplexer are very narrow (say, of the order of 1% of the main bandwidth or less) and if the channels are separated by guard bands which are several times the pass band width of the individual filters. *Iris-coupled* type filters may be used in this type of multiplexers. A three-channel waveguide multiplexer is shown in figure 1.3. At frequency f_a , the Filter a has a pass-band while the other two filters, *Filter b and Filter c have their stop-bands. Similarly at frequency f_b the Filter b has a pass-band while the other two filters have their stop-bands. Filter c also behaves in a similar manner. If it is desired to add more channels, they can be mounted on the main waveguide at additional points corresponding to various odd multiples of $\lambda_g/4$ from the rightmost filter, i.e., Filter a in figure 1.3, (where λ_g is the *guide wavelength* at the midband frequency of the filter in question).

Another type proposed by J. F. Cline [2] employs *decoupling technique* which is achieved by a decoupling resonator adjacent to each filter. These type of multiplexers are also used for narrow-band channels with guard bands between channels. There are also some other types of multiplexers involving complicated features. It is difficult to fabricate multiplexers of the above mentioned configurations because of their complicated shape and geometry. The most difficult part is to design and fabricate the input and output sections. The problem that occurs in devising the feed junctions (the junctions where input signals are fed into and output signals are extracted from) is particularly very difficult to overcome. Due to these problems it is often quite difficult to fabricate such a multiplexer in planar configuration.

In order to get rid of these difficulties, a new type of multiplexer structure is considered in the present work. Such a multiplexer may be fabricated using forward coupled microstrip combines with the help of masking and etching techniques.

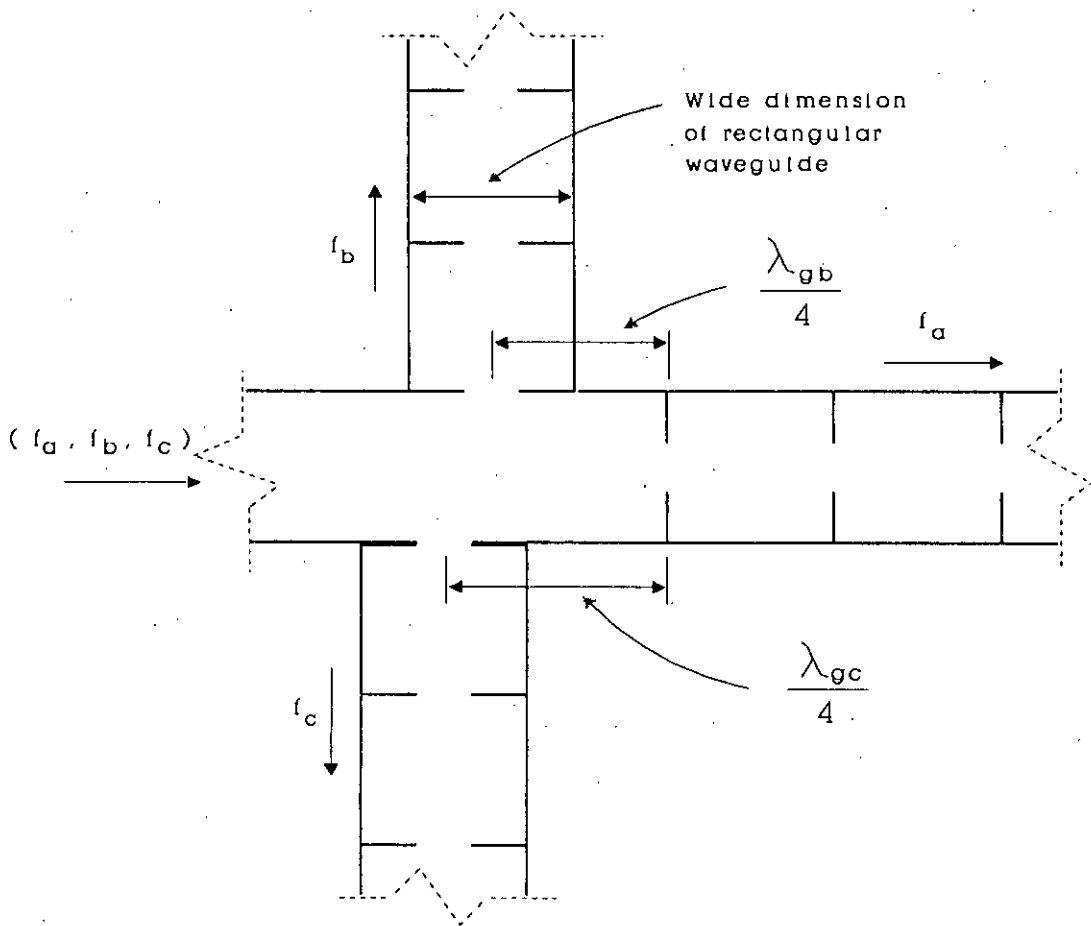


Figure 1.3 A multiplexer with narrow-band waveguide filters mounted so as to eliminate filter interaction.

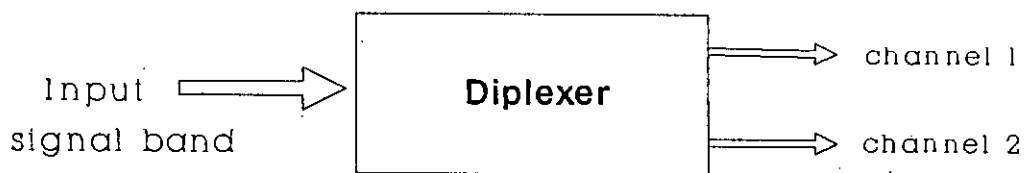


Figure 1.4 Block diagram of a diplexer.

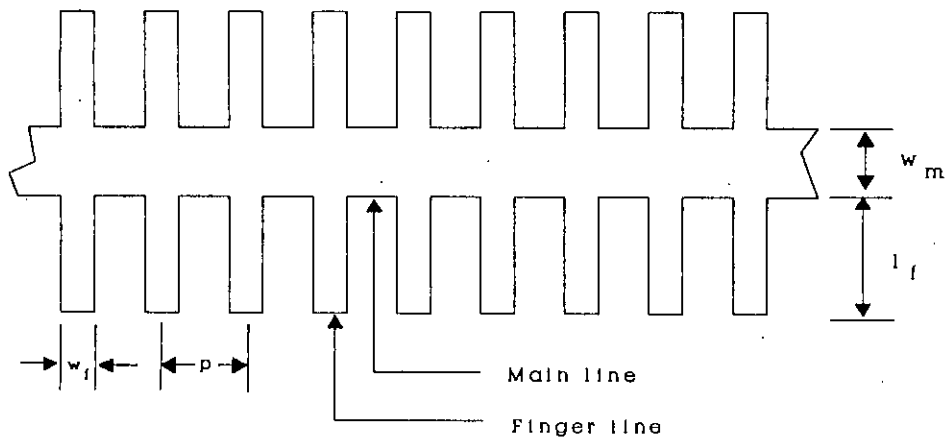


Figure 1.5 Top metalization pattern of a herringbone-line.

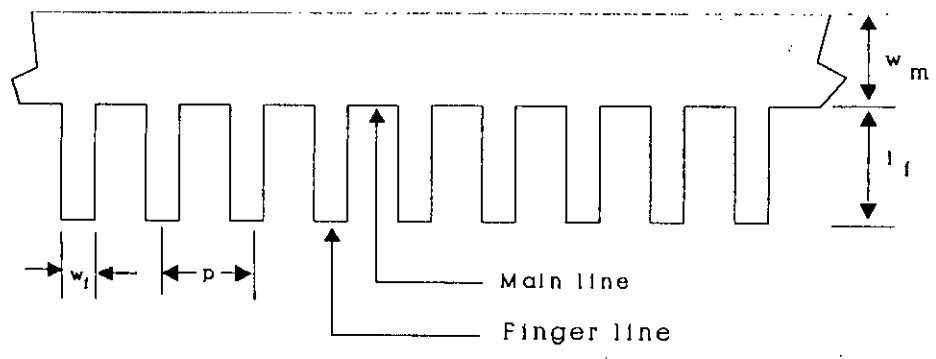


Figure 1.6 Top metalization pattern of a combline.

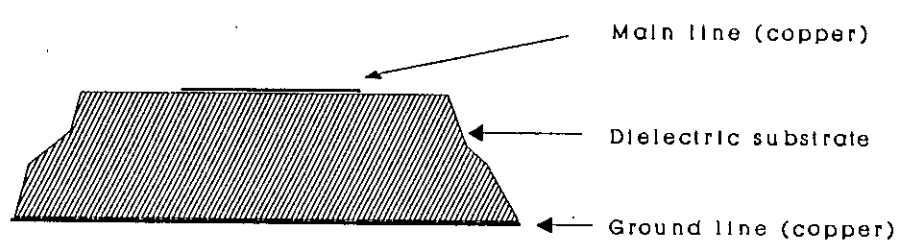


Figure 1.7 Transverse section of an open microstrip line.

1.2 Diplexer

A *diplexer* is a special form of multiplexer which has only two output channels. In fact a diplexer is the simplest form of multiplexer. So, the techniques for multiplexers discussed in section 1.1 may also be employed for designing diplexers. The block diagram of a diplexer is shown in figure 1.4.

A design method for developing a microwave diplexer using forward coupled microstrip comblines is undertaken in this research. The diplexer under consideration is a passive device which separates an incoming microwave band of signal between two channels according to the desired power ratio. Similarly, a *triplexer* would divide an input band of microwave signal among three channels and a *quadruplexer* would divide the input signal among four channels.

1.3 Microstrip Comb- and Herringbone- lines

A microstrip combline [6] consists of a *main line* and many *finger lines* periodically placed perpendicularly along its length as shown in figure 1.5 and figure 1.6. The finger lines are usually located at equal intervals which is known as the finger periodicity (p). The dimension of the mainline width (w_m), finger line width (w_f), length of finger (L_f) and finger periodicity (p) are in millimeter ranges. Slight variation of any of these parameters significantly affect the characteristic of the comblines. The difference between a *Comblines* and *Herringbone line* can be seen from the top metalization pattern, in open microstrip configuration from figure 1.5 and figure 1.6. The herringbone line has fingers in both sides of the main line (like the spine of a Herring fish as implied by its name) and the actual combline has fingers only on one side of the main line (similar to a comb). The mode of propagation is supported by the dielectric material between the conductor plate at the bottom and the conducting comblines. The transverse section of an open microstrip line is shown in figure 1.7.

The finger lines are actually small segments of open circuit transmission lines. Usually, the main line and the finger lines when considered separately, are microstrip lines having different characteristic impedances (assuming that the width of the two lines are different). The effective dielectric constant for main and finger lines, for such a case, is different. For the remaining part of this thesis the term Comblines will be used to represent both Comb- and Herringbone- lines if not specified explicitly.

A combline can be designed for a wide range of effective phase velocities and impedance values. This is one of the major advantages of this type of lines over *uniform microstrip lines*¹. Actually the finger lines may be considered as lumped shunt capacitances (C_0) added at periodic intervals without affecting the value of inductance (L). If the finger periodicity (p), i.e., the spacing between the added lumped capacitors is small compared with the wavelength, it may be anticipated that the line will appear to be smooth, with a *phase velocity* [3]

$$v_p = [(C + C_0/p)L]^{-1/2} \quad (1.1)$$

where, C_0/p is the amount of lumped capacitance added per unit length and C is the shunt capacitance per unit length of the main line. However, with very short lengths of fingers the phase velocity of a combline can be close to $c/\sqrt{\epsilon_r}$ (where c is the speed of light). With longer fingers much lower phase velocity can be achieved which may be realized from above equation. Practically, values of phase velocities in the range of 50% to 90% of the velocity in the dielectric material (e.g. 1.1×10^8 m/s to 2×10^8 m/s in substrate of dielectric constant 2.5) can be easily obtained. An important advantage of microstrip combines over uniform microstrip lines is that, due to the presence of the finger lines the former can achieve higher coupling capacitance per unit length between neighbouring lines. For example, coupling capacitance upto 60 pF/m can easily be obtained between two combines made with a 1.5 mm thick dielectric substrate ($\epsilon_r = 2.55$), having 2.4 mm finger periodicity and 1 mm wide fingers. Due to these advantages, microstrip lines of this category have been selected for realizing forward coupled diplexers. The aforementioned advantages make the microstrip combline configuration the right choice for realizing forward coupled diplexers and that is why it is undertaken in this research.

The two major disadvantages of a combline are *stop-bands* and *finger resonance*. Stop-band is a function of finger periodicity of this type of lines. Following the solution of waves in periodic structure presented by Collin and Carroll [2], it may be shown that the stop band in a combline occurs when β_e is equal to π (where β_e is the *effective propagation constant* of the combline). This means that a periodicity of value equal to π/β_e will produce stop-band at the frequency at which computation is done. Sub-periodicity which subsequently causes stop-bands may sometimes be introduced due to constructional defects. If the fingers are made too

¹Uniform microstrip lines are those where finger lines are absent i.e., where the microstrip line has the main line only

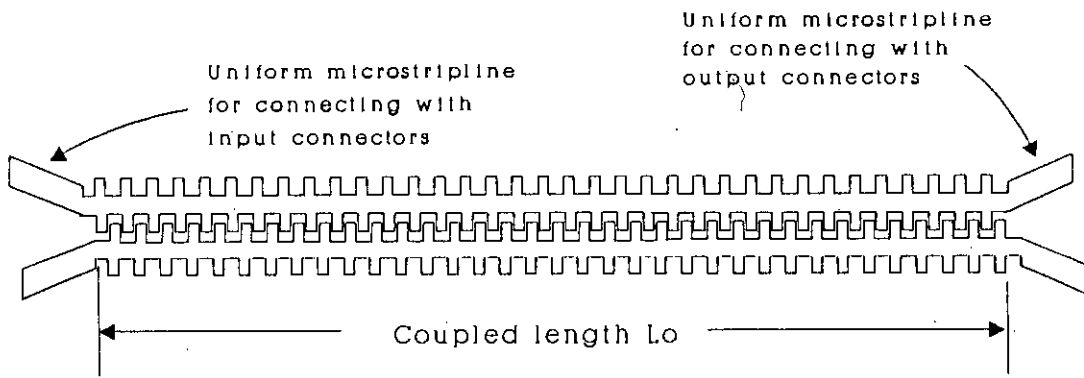


Figure 1.8 Coupled comblines in planar geometry will be used to realize a diplexer.

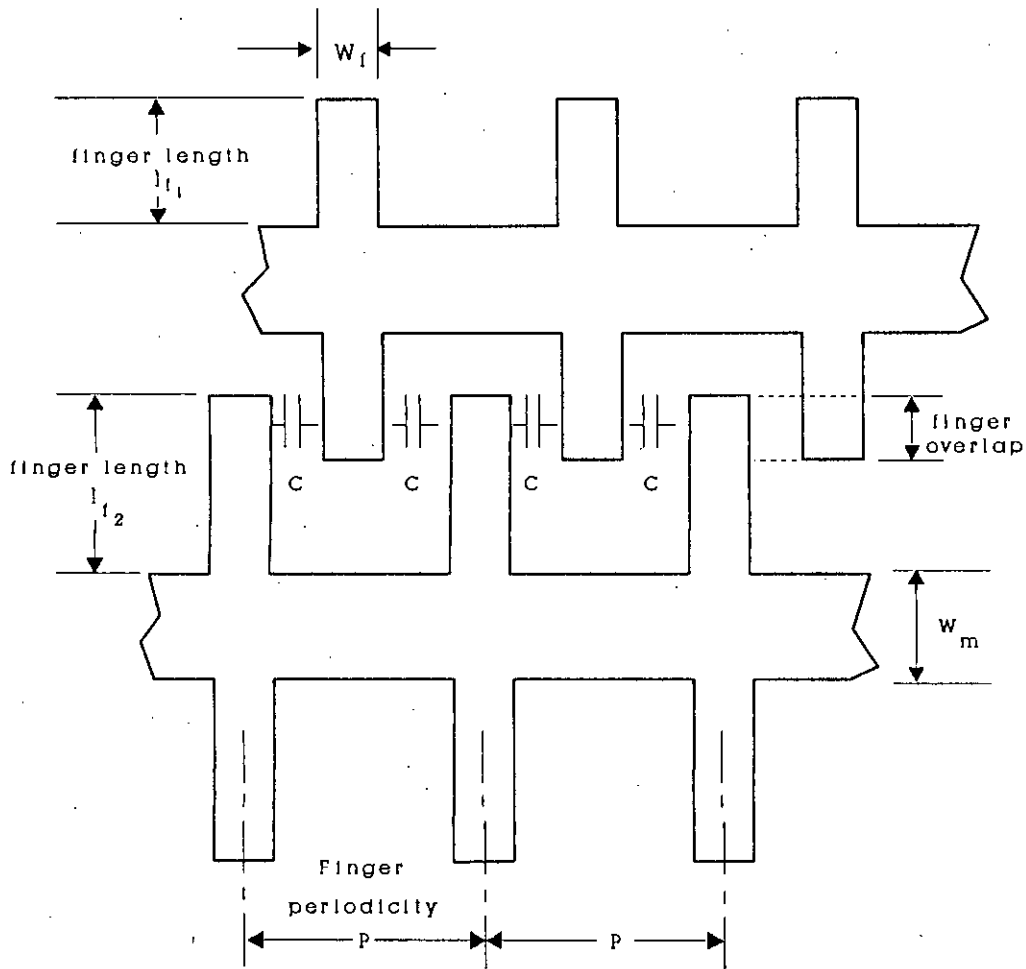


Figure 1.9 Capacitive coupling in a pair of coupled comblines is achieved through finger overlap.

long then the finger resonance causes difficulty in propagation. In order to avoid finger resonance, finger lengths should be less than $\lambda/4$ at highest the frequency of operation. For these reasons, while designing multiplexers using forward coupled microstrip combines, it is also very necessary to avoid operation near the stop-band frequency and also to keep the finger lengths sufficiently short.

1.4 Compline diplexer

The diplexer which uses the above mentioned comb or herringbone -lines is termed in this work as Compline Diplexer. Such a diplexer consists of two coupled combines. Each of these lines is periodically loaded with finger lines where the finger periodicity is small compared to a wavelength. The distance between the two comb lines is such that the fingers of both the lines overlap upto the required extent. In a diplexer, the combines are coupled through the overlapping finger lines as shown in figure 1.8 and figure 1.9. Such a coupling is capacitive and is achieved through the edges of the overlapping fingers. In order to avoid coupling between the tips of the fingers and the adjacent main line, the distance between the finger line tips and the next main line is kept larger than the gap between adjacent fingers. However, if tight coupling is used, the capacitance at the finger ends has to be taken into account.

The diplexer under consideration is a four port device. The wide band input signal is fed into only one port at the input side and the two output signals having different bands of frequencies are obtained from the two ports and thus diplexing is achieved. In such a compline diplexer the back terminal is terminated with matched terminating impedance because ideally there will be no power at this port. The amount of input power which will be transferred to the adjacent line will be determined mainly by the tightness of coupling achieved through the overlapping fingers.

1.5 Objective of this research

The objective of this research is to develop a design method for a microwave diplexer using coupled microstrip combines so that the resulting diplexer is small in size, compact in structure and easy to fabricate. It is also desirable to obtain a structure suitable for use in subsystems in the form of MIC (Microwave Integrated

Circuit) and if possible for MMIC (Monolithic Microwave Integrated Circuit). In this research forward coupling properties of a pair of coupled comb-lines will be used as the basis for developing the method of designing the diplexer. The entire research is actually dedicated to the process of formulating a design method to construct the diplexer under consideration. The goal is to find all the design parameters (i.e., physical properties and geometric dimensions) which may be used to manufacture a practical device.

1.6 Introduction to this work

The main objective of this work is to design a microwave diplexer using forward coupled microstrip comb-lines as the name of the thesis implies. The method used in this work for the design purpose has been briefly presented in the abstract. Introduction to microwave diplexers and multiplexers have been presented in this chapter. The microstrip comb- and herringbone- lines and their application in diplexers have also been presented. The objective of this research have been presented in this chapter.

In this research the equations required for computing the power and phase characteristics of a diplexer is derived from the generalized theory of n -coupled comb-lines. So a review of the theory of n -coupled comb-lines is required which is presented in chapter 2. Two major parameters in multiplexer design, the wave propagation matrix \underline{J} and the \underline{e} vector are introduced in this chapter. The equations relating the inductance and capacitance matrices, and the \underline{J} matrix are also presented. The process of obtaining the power and relative phase characteristics, and the line-parameters of an n -coupled comb-line system is described in chapter 2.

Chapter 3 is actually the special form of chapter 2, where the equations for diplexer are deduced from the equations of generalized n -coupled comb-lines presented in chapter 2. The process of obtaining the forward scattering matrix of a comb-line diplexer from its \underline{J} matrix is presented in chapter 3. The equations of coupled and uncoupled capacitance, inductance, characteristic impedance and phase velocity for an n -coupled system presented in chapter 2 are transformed into the equations for a diplexer in chapter 3. An important concept regarding scaling and shifting of \underline{J} matrix, which is required for obtaining realizable design values of a diplexer is presented in chapter 3.

The computer optimization procedure which is a major part of this work is presented in chapter 4. The method of optimization used in this work is described in details in this chapter. Selection of a starting \underline{e} vector and its optimization are also presented. The optimized \underline{e} vector thus obtained in this chapter is later used in designing the diplexer.

The complete procedure of obtaining the physical dimensions of a combline diplexer is presented in chapter 5.

In chapter 6 the design values of a herringbone- and a comb- line diplexer, i.e., the physical dimensions are presented. These design values may be used to fabricate a practical diplexer which is suitable for use in Microwave Integrated Circuits (MIC) as well as Microwave Monolithic Integrated Circuits (MMIC). The objective of this research is achieved with the conclusion of chapter 6.

In chapter 7 discussions and suggestions for possible future work are presented which may be used as the guidelines for any further research.

CHAPTER 2

Review of the theory of n -coupled comblines

2.1 Introduction

A generalized theory of n -coupled comblines has been presented in [5]. In order to develop a design method for a diplexer, this generalized theory will be taken as the basis. For this reason a result a brief review of the generalized theory of n -coupled comblines is presented in this chapter.

Starting with the voltage and current equations of an n -line coupled system the equation for the forward scattering matrix of such a system is presented in section 2.2. A matrix called \underline{J} matrix, which is termed as *wave-propagation matrix* is also introduced in section 2.3. It is also shown in this section that the *eigenvalues* of \underline{J} (i.e., the diagonal elements of $\underline{\beta}$ matrix) can be obtained by orthogonal transformation of \underline{J} matrix. In section 2.4 the relationship between the \underline{J} matrix and the capacitance and inductance matrices are shown. It is shown that for nearest neighbour interaction of microstrip combines the capacitance matrix \underline{C} is tridiagonal and the inductance matrix \underline{L} is diagonal. The equations for computing the forward scattering matrix of a coupled combline system are presented in section 2.5. If the \underline{J} matrix of the coupled combline system is known then one can obtain the forward scattering matrix by using these equations. The equations for obtaining the power and relative phase characteristics of the output ports of a coupled combline system are presented in section 2.6.

The equations for obtaining the elements of capacitance matrix \underline{C} and the elements of inductance matrix \underline{L} from the \underline{J} matrix are presented in section 2.7. The

equations for obtaining different *line parameters* of a coupled combline are also presented in section 2.7. In section 2.8 it is shown that a vector \underline{e} may be formed with the elements of \underline{J} matrix and the length of the coupled comblines. This \underline{e} vector will be used to specify a coupled combline system. The summary of this chapter is presented in section 2.9.

2.2 Theory of n -coupled lines

Consider an n -line coupled system having a coupled length of L_0 as shown in figure 2.1. It is assumed that the transmission lines of this system are lossless. The distributed self and mutual values of inductances and capacitances of such a coupled system may be represented by an *inductance matrix* \underline{L} , and a *capacitance matrix* \underline{C} respectively. In order to ensure that the energy stored in the system is positive, the inductance and the capacitance matrices are to be positive definite.

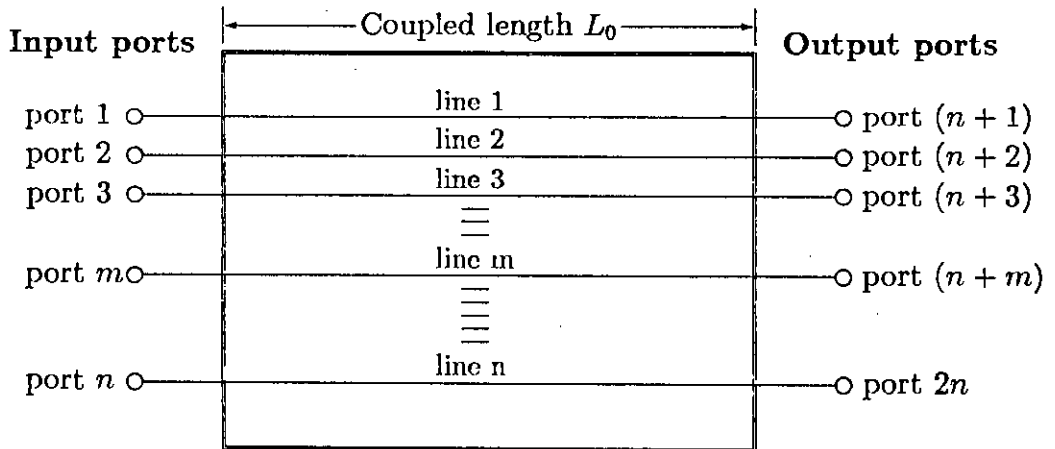


figure 2.1 An n -coupled line system

Thus for this system (shown in figure 2.1) the distributed line parameters are the per unit length self and mutual capacitances and the per unit length self and mutual inductances. The line voltages and currents of the coupled line system are

represented by the vectors \underline{v} and \underline{i} respectively. Following the wave equations of transmission lines it is now possible to write the voltage and current equations of this system as

$$\frac{\partial \underline{v}}{\partial z} = -\frac{\partial}{\partial t}(\underline{L} \underline{i}) \quad (2.1)$$

$$\frac{\partial \underline{i}}{\partial z} = -\frac{\partial}{\partial t}(\underline{C} \underline{v}) \quad (2.2)$$

Assuming $e^{j\omega t}$ time dependence the above two equations may be rewritten as

$$\frac{\partial \underline{v}}{\partial z} = -j \underline{X} \underline{i} \quad (2.3)$$

$$\frac{\partial \underline{i}}{\partial z} = -j \underline{B} \underline{v} \quad (2.4)$$

where,

$$\underline{X} = \omega \underline{L} \quad (2.5)$$

and,

$$\underline{B} = \omega \underline{C} \quad (2.6)$$

Here, \underline{X} and \underline{B} are symmetric matrices. For coplanar structure due to *nearest neighbour interaction* \underline{X} and \underline{B} are tridiagonal¹ matrices [5].

From equations (2.2.a) and (2.2.b) one obtains,

$$\frac{\partial^2 \underline{v}}{\partial z^2} + \underline{X} \underline{B} \underline{v} = 0 \quad (2.7)$$

$$\frac{\partial^2 \underline{i}}{\partial z^2} + \underline{B} \underline{X} \underline{i} = 0 \quad (2.8)$$

¹A matrix \underline{A} is *tridiagonal* if all of its elements except A_{ii} and $A_{i(i\pm 1)}$ are zero

The matrix $\underline{X} \underline{B}$ of equation (2.7) can be diagonalized by a transformation matrix \underline{U} such that $\underline{U}^{-1} \underline{X} \underline{B} \underline{U} = \underline{\beta}_i^2$ (diagonal) whereas the matrix $\underline{B} \underline{X}$ of equation (2.8) may be diagonalized by the transformation $\underline{U}^t \underline{B} \underline{X} (\underline{U}^t)^{-1} = \underline{\beta}_i^2$.

Using the operations for diagonalization of $\underline{X} \underline{B}$, equation (2.7) may be written as

$$\frac{\partial^2}{\partial z^2} (\underline{Z}_0^{-1/2} \underline{U}^{-1} \underline{v}) + \underline{Z}_0^{-1/2} \underline{U}^{-1} \underline{X} \underline{B} \underline{U} \underline{Z}_0^{1/2} (\underline{Z}_0^{-1/2} \underline{U}^{-1} \underline{v}) = 0 \quad (2.9)$$

Similarly equation (2.8) may be written as

$$\frac{\partial^2}{\partial z^2} (\underline{Z}_0^{1/2} \underline{U}^t \underline{i}) + \underline{Z}_0^{1/2} \underline{U}^t \underline{B} \underline{X} \underline{U}^{-1} \underline{Z}_0^{-1/2} (\underline{Z}_0^{1/2} \underline{U}^t \underline{i}) = 0 \quad (2.10)$$

Thus from equations (2.9) and (2.10) the diagonalized form of equations (2.7) and (2.8) may be written as [5]

$$\frac{\partial^2 \underline{v}_n}{\partial z^2} + \underline{\beta}_i^2 \underline{v}_n = 0 \quad (2.11)$$

$$\frac{\partial^2 \underline{i}_n}{\partial z^2} + \underline{\beta}_i^2 \underline{i}_n = 0 \quad (2.12)$$

In equation (2.11) \underline{v}_n represents the column vector containing the normal-mode voltages on different lines and in equation (2.12) \underline{i}_n represents the column vector containing the normal-mode currents. Here, the normalization by a matrix $\underline{Z}_0^{1/2}$ is used for the normal-mode voltages and currents such that

$$\underline{v}_n = \underline{Z}_0^{-1/2} \underline{U}^{-1} \underline{v} \quad (2.13)$$

$$\underline{i}_n = \underline{Z}_0^{1/2} \underline{U}^t \underline{i} \quad (2.14)$$

This is done so that the elements of \underline{v}_n and \underline{i}_n have the dimensions of square root of the power. The matrix \underline{Z}_0 is taken as the diagonal matrix containing the *characteristic impedances* of the line as its diagonal elements.

From equations (2.9) and (2.10) it may be observed that the matrices \underline{B} and \underline{X} may be written as

$$\underline{B} = \underline{U} \underline{Z}_0^{-1/2} \underline{\beta} \underline{Z}_0^{-1/2} \underline{U}^{-1} = \underline{U}^{t-1} \underline{Z}_0^{-1/2} \underline{\beta} \underline{Z}_0^{-1/2} \underline{U}^t \quad (2.15)$$

$$\underline{X} = \underline{U} \underline{Z}_0^{1/2} \underline{\beta} \underline{Z}_0^{1/2} \underline{U}^{-1} = \underline{U}^{t-1} \underline{Z}_0^{1/2} \underline{\beta} \underline{Z}_0^{1/2} \underline{U}^t \quad (2.16)$$

The general solution of equations (2.11) and (2.8) are given by

$$\underline{v}_{n_i} = \cos(\underline{\beta} L_0) \underline{v}_{n_o} + j \sin(\underline{\beta} L_0) \underline{i}_{n_o} \quad (2.17)$$

$$\underline{i}_{n_i} = \cos(\underline{\beta} L_0) \underline{i}_{n_o} + j \sin(\underline{\beta} L_0) \underline{v}_{n_o} \quad (2.18)$$

Here, L_0 is the coupled length.

The subscripts i and o of \underline{v}_n and \underline{i}_n in equations (2.17) and (2.18) represent the values at the *input* and *output* ports respectively.

The normal-mode voltage and currents at the ports are related by a mode terminating impedance matrix \underline{r} by [5]

$$\underline{v}_{n_o} = \underline{r} \underline{i}_{n_o} \quad (2.19)$$

$$\underline{Z}_0^{-1/2} \underline{U}^{-1} \underline{v}_o = \underline{r} \underline{Z}_0^{1/2} \underline{U}^t \underline{i}_o \quad (2.20)$$

Therefore,

$$\underline{v}_o = \underline{U} \underline{Z}_0^{1/2} \underline{r} \underline{Z}_0^{1/2} \underline{U}^t \underline{i}_o = \underline{Z}_t \underline{i}_o \quad (2.21)$$

where, $\underline{Z}_t = \underline{U} \underline{Z}_0^{1/2} \underline{r} \underline{Z}_0^{1/2} \underline{U}^t$.

The *termination impedance matrix* \underline{Z}_t specifies a network of impedances interlinking the output ports to one another and to ground and will in general not be diagonal. However, for non-mode converting terminations (n.m.c condition) the

matrix \underline{r} as well as \underline{Z}_t are diagonal [2]. If the mode termination impedance matrix \underline{r} is chosen to be diagonal then the normal-mode voltages and currents incident on the terminations are partly absorbed and partly reflected without any conversion from one mode into another.

Consider now a diagonal matrix, \underline{R}_t , where $\underline{R}_{t,i}$ (the diagonal elements of this matrix) are the resistive load terminations of the i th line to ground. The voltages and currents are then normalized with this termination impedance matrix \underline{R}_t . The *normalized voltage vector* $\underline{\phi}$ and the *normalized current vector* $\underline{\theta}$ are then written as $\underline{\phi} = \underline{R}_t^{-1/2} \underline{v}$ and $\underline{\theta} = \underline{R}_t^{1/2} \underline{i}$ respectively.

The above two equations may be restated as

$$\underline{\phi} = \underline{R}_t^{-1/2} \underline{U} \underline{Z}_0^{1/2} \underline{v}_n \quad (2.22)$$

$$\begin{aligned} &= \underline{R}_t^{-1/2} \underline{U} \underline{Z}_0^{1/2} \underline{r}^{1/2} \underline{r}^{-1/2} \underline{v}_n \\ &= \underline{Q}^t \underline{r}^{-1/2} \underline{v}_n \end{aligned} \quad (2.23)$$

$$\underline{\theta} = \underline{R}_t^{-1/2} \underline{U}^{t-1} \underline{Z}_0^{1/2} \underline{i}_n \quad (2.24)$$

$$\begin{aligned} &= \underline{R}_t^{-1/2} \underline{U} \underline{Z}_0^{1/2} \underline{r}^{1/2} \underline{r}^{-1/2} \underline{i}_n \\ &= \underline{Q}^t \underline{r}^{1/2} \underline{i}_n \end{aligned} \quad (2.25)$$

where,

$$\underline{Q}^t = \underline{R}_t^{-1/2} \underline{U} \underline{Z}_0^{1/2} \underline{r}^{1/2} = \underline{R}_t^{-1/2} \underline{U}^{t-1} \underline{Z}_0^{-1/2} \underline{r}^{-1/2} \quad (2.26)$$

Thus,

$$\underline{Q}^t = \underline{r}^{1/2} \underline{Z}_0^{1/2} \underline{U}^t \underline{R}_t^{-1/2} = \underline{r}^{-1/2} \underline{Z}_0^{-1/2} \underline{U}^{-1} \underline{R}_t^{-1/2} \quad (2.27)$$

From equation (2.26) and (2.27) it may be observed that the \underline{Q} matrix has the property of orthogonality, i.e., $\underline{Q}^t \underline{Q} = \underline{Q} \underline{Q}^t = \underline{I}$ (identity matrix).

The wave amplitude vectors at the input and output ports may be defined as,

$$\underline{a}_i = \frac{\phi_i + \theta_i}{2} \quad (2.28)$$

$$\underline{b}_i = \frac{\phi_i - \theta_i}{2} \quad (2.29)$$

$$\underline{a}_o = \frac{\phi_o - \theta_o}{2} \quad (2.30)$$

$$\underline{b}_o = \frac{\phi_o + \theta_o}{2} \quad (2.31)$$

Here the subscript i and o represent the values at the input and output ports respectively. In terms of this wave amplitude vectors, the total *scattering matrix* may be written in a partitioned form as,

$$\begin{bmatrix} \underline{b}_i \\ \underline{b}_o \end{bmatrix} = \begin{bmatrix} \underline{S}_{ii} & \underline{S}_{oi} \\ \underline{S}_{io} & \underline{S}_{oo} \end{bmatrix} \begin{bmatrix} \underline{a}_i \\ \underline{a}_o \end{bmatrix} \quad (2.32)$$

Here, due to symmetry $\underline{S}_{ii} = \underline{S}_{oo}$ and $\underline{S}_{io} = \underline{S}_{oi} = \underline{S}_{io}^t = \underline{S}_{oi}^t$.

From equation (2.32) one can write the wave amplitude vectors in terms of the forward scattering matrix \underline{S}_{io} as

$$\underline{b}_o = \underline{S}_{io} \underline{a}_i \quad (2.33)$$

Now, putting the values of \underline{a}_i and \underline{b}_o from equations (2.28) and (2.31) in equation (2.33) and one gets

$$\underline{S}_{oi} = \underline{Q}^t (\underline{F}\underline{E}\underline{F} - \underline{G}\underline{E}^{-1}\underline{G})^{-1}\underline{Q} \quad (2.34)$$

where,

$$\underline{F} = \frac{r^{1/2} + r^{-1/2}}{2} \quad (2.35)$$

and,

$$\underline{G} = \frac{\underline{r}^{1/2} - \underline{r}^{-1/2}}{2} \quad (2.36)$$

$$\underline{E} = \exp(j\underline{\beta}L_o) = \cos \underline{\beta}L_o + j \sin \underline{\beta}L_o \quad (2.37)$$

In a similar way the *reverse scattering matrix* may be written as follows.

$$\underline{S}_{ii} = \underline{Q}'(\underline{F}\underline{E}^{-1}\underline{G} - \underline{G}\underline{E}\underline{F})(\underline{F}\underline{E}\underline{F} - \underline{G}\underline{E}^{-1}\underline{G})^{-1}\underline{Q} \quad (2.38)$$

Equation (2.23) to (2.27) are the general relations for the scattering parameters of a n -line coupled system.

From equations (2.34) and (2.38) it is apparent that these will involve an enormous amount of computation for designing a coupler. A significant simplification of these equations is possible by applying the weak reflection approximation [5]. This will reduce the amount of computation to a great extent. The weak reflection approximation implies that the elements of the mode *reflection matrix* $\underline{\rho}$ are very small.

The mode termination matrix \underline{r} may be related to the mode reflection matrix $\underline{\rho}$, by [5]

$$\underline{r} = (\underline{I} + \underline{\rho})(\underline{I} - \underline{\rho})^{-1} \quad (2.39)$$

$$\text{Thus, } \underline{r}^{1/2} = (\underline{I} + \underline{\rho})^{1/2}(\underline{I} - \underline{\rho})^{-1/2} \quad (2.40)$$

$$\text{and, } \underline{r}^{-1/2} = (\underline{I} + \underline{\rho})^{-1/2}(\underline{I} - \underline{\rho})^{1/2} \quad (2.41)$$

If $\underline{r}^{-1/2}$ and $\underline{r}^{1/2}$ are expanded neglecting terms containing $\underline{\rho}^2$ and higher powers of $\underline{\rho}$, one obtains,

$$\underline{\tau}^{1/2} = \underline{I} + \underline{\rho} \quad (2.42)$$

$$\underline{\tau}^{-1/2} = \underline{I} - \underline{\rho} \quad (2.43)$$

so that,

$$\underline{F} = \underline{I} \quad (2.44)$$

$$\underline{G} = \underline{\rho} \quad (2.45)$$

This reduces equations (2.34) and (2.38) to

$$\underline{S}_{oi} = \underline{Q}^t \underline{E}^{-1} \underline{Q} \quad (2.46)$$

and,

$$\underline{S}_{ii} = \underline{Q}^t (\underline{E}^{-1} \underline{\rho} - \underline{\rho} \underline{E}) \underline{Q} \underline{S}_{oi} \quad (2.47)$$

Here it is necessary to define the normalized *admittance* and *impedance* matrices as

$$\underline{B}_n = \underline{R}_t^{1/2} \underline{B} \underline{R}_t^{1/2} \quad (2.48)$$

and,

$$\underline{X}_n = \underline{R}_t^{-1/2} \underline{X} \underline{R}_t^{-1/2} \quad (2.49)$$

where \underline{R}_t is the termination impedance matrix.

Using equations (2.15) and (2.16) it is possible to rewrite equations (2.48) and (2.49) as

$$\underline{B}_n = \underline{R}_t^{1/2} \underline{U}^t \underline{Z}_o^{-1/2} \underline{\beta} \underline{Z}_o^{-1/2} \underline{U} \underline{R}_t^{1/2} \quad (2.50)$$

and,

$$\underline{X}_n = \underline{R}_t^{-1/2} \underline{U} \underline{Z}_o^{1/2} \underline{\beta} \underline{Z}_o^{1/2} \underline{U}^{-1} \underline{R}_t^{-1/2} \quad (2.51)$$

Using equations (2.26) and (2.27) it is possible to rewrite equations (2.50) and (1.51) as

$$\underline{B}_n = \underline{Q}^t \underline{r}^{1/2} \underline{\beta} \underline{r}^{1/2} \underline{Q} \quad (2.52)$$

and,

$$\underline{X}_n = \underline{Q}^t \underline{r}^{-1/2} \underline{\beta} \underline{r}^{-1/2} \underline{Q} \quad (2.53)$$

2.3 The wave-propagation matrix \underline{J}

Consider that in an n -coupled line system only forward waves are propagating and scattering in the z direction and that the n -row *forward wave amplitude vector* is written as

$$a(z) = (1/2)(\underline{R}_t^{-1/2} \underline{v} + \underline{R}_t^{1/2} \underline{i}) \quad (2.54)$$

Thus using equations (2.5) - (2.8) it may be written that

$$\frac{d}{dz} a(z) = -j \underline{J} a(z) \quad (2.55)$$

where,

$$\underline{J} = \frac{\underline{B}_n + \underline{X}_n}{2} = \underline{Q}^t \underline{\beta} \underline{Q} \quad (2.56)$$

In equation (2.48) \underline{B}_n and \underline{X}_n matrices are the normalized admittance and inductance matrices as defined in equations (2.50), (2.51), (2.52) and (2.53).

Here the \underline{J} matrix may be called the *wave-propagation matrix*. From equation (2.56), one may observe that the \underline{J} matrix can be obtained from the capacitance and inductance matrices of the n -coupled line system. The values of \underline{B}_n and \underline{X}_n can be obtained from equations (2.5), (2.6), (2.50), (2.51), (2.52) and (2.53). For lossless lines the \underline{J} matrix is real and symmetric and for planar structure (with nearest neighbour interaction) this is a *tridiagonal* matrix.

The eigenvalues of the wave propagation matrix \underline{J} are the mode propagation constants β_i ($i = 1, 2, 3, \dots, N$) on the lines so that

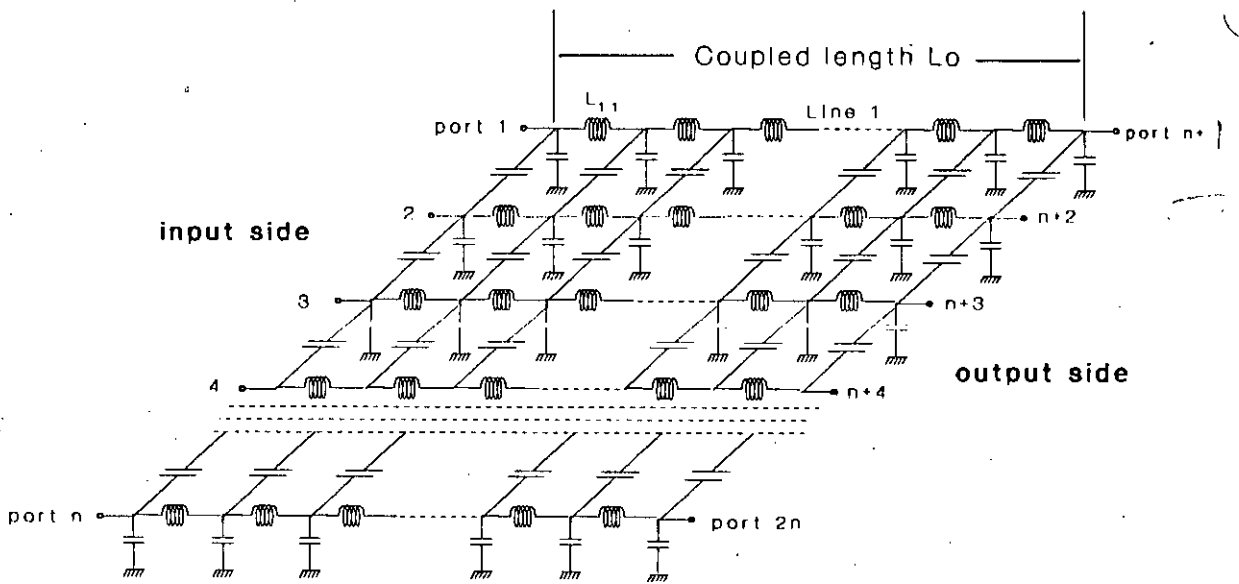


Figure 2.2 Model of an n -coupled combline system showing the distributed self capacitances, inductances and interline coupling capacitances. Here, only the nearest neighbour interaction is considered.

$$\underline{Q} \underline{J} \underline{Q}^t = \underline{\beta} \quad (2.57)$$

The matrix $\underline{\beta}$ [7] [19] is the diagonal matrix containing the mode propagation constants $\underline{\beta}_i$'s as the diagonal elements, and the \underline{Q} matrix [7] [19] [20] is the orthogonal modal matrix \underline{J} . For lossless lines, elements of orthogonal modal matrix \underline{Q} are real. The orthonormal row vectors of \underline{Q} are denoted as \underline{q}_i ($i = 1, 2, 3, \dots, N$) and the orthonormal column vectors of the same matrix as \underline{p}_j ($j = 1, 2, 3, \dots, N$). Here the \underline{q}_i vectors are the *eigenvectors* of the \underline{J} matrix.

2.4 Capacitance and inductance matrices of an n -coupled combline system

As shown in equation (2.56) the \underline{J} matrix may be rewritten as

$$\underline{J} = \frac{\underline{B}_n + \underline{X}_n}{2} \quad (2.58)$$

where, the normalized admittance and impedance matrices are

$$\underline{B}_n = \omega_L \underline{R}_i^{1/2} \underline{C} \underline{R}_i^{1/2} \quad (2.59)$$

$$\underline{X}_n = \omega_L \underline{R}_i^{-1/2} \underline{L} \underline{R}_i^{-1/2} \quad (2.60)$$

Here $\omega_L = 2\pi f_L$, and \underline{R}_i may be taken as a diagonal termination matrix with $\underline{R}_{i,i}$ as its diagonal element corresponding to the i th line. The inductance matrix \underline{L} is diagonal since the interline inductive coupling is negligible for a coupled combline system. The capacitance matrix \underline{C} is tridiagonal in case of nearest neighbour interaction. The diagonal elements of \underline{C} are the self-capacitances $C_{i,i}$ of the lines under coupled condition. An equivalent circuit of an n -line coupled system considering nearest neighbour interaction is shown in figure 2.2.

The distributed capacitance and inductance of a multiline coupled system may be represented by a *capacitance* and a *inductance matrix* respectively. Both the

capacitance and inductance matrices of an n -line multiplexer are represented by $n \times n$ square matrices which can be written in the most general form as

Capacitance matrix

$$\underline{C} = \begin{bmatrix} C_{11} & C_{12} & C_{13} & C_{14} & \cdots & C_{1(n-1)} & C_{1n} \\ C_{21} & C_{22} & C_{23} & C_{24} & \cdots & C_{2(n-1)} & C_{2n} \\ C_{31} & C_{32} & C_{33} & C_{34} & \cdots & C_{3(n-1)} & C_{3n} \\ C_{41} & C_{42} & C_{43} & C_{44} & \cdots & C_{4(n-1)} & C_{4n} \\ \vdots & \vdots & \vdots & \vdots & \ddots & \vdots & \vdots \\ C_{(n-1)1} & C_{(n-1)2} & C_{(n-1)3} & C_{(n-1)4} & \cdots & C_{(n-1)(n-1)} & C_{(n-1)n} \\ C_{n1} & C_{n2} & C_{n3} & C_{n4} & \cdots & C_{n(n-1)} & C_{nn} \end{bmatrix} \quad (2.61)$$

Inductance matrix

$$\underline{L} = \begin{bmatrix} L_{11} & L_{12} & L_{13} & L_{14} & \cdots & L_{1(n-1)} & L_{1n} \\ L_{21} & L_{22} & L_{23} & L_{24} & \cdots & L_{2(n-1)} & L_{2n} \\ L_{31} & L_{32} & L_{33} & L_{34} & \cdots & L_{3(n-1)} & L_{3n} \\ L_{41} & L_{42} & L_{43} & L_{44} & \cdots & L_{4(n-1)} & L_{4n} \\ \vdots & \vdots & \vdots & \vdots & \ddots & \vdots & \vdots \\ L_{(n-1)1} & L_{(n-1)2} & L_{(n-1)3} & L_{(n-1)4} & \cdots & L_{(n-1)(n-1)} & L_{(n-1)n} \\ L_{n1} & L_{n2} & L_{n3} & L_{n4} & \cdots & L_{n(n-1)} & L_{nn} \end{bmatrix} \quad (2.62)$$

In the case of a coupled microstrip combline system only nearest neighbour interaction will be considered. So for nearest neighbour interaction the above matrices may be written as

$$\underline{C} = \begin{bmatrix} C_{11} & C_{12} & 0 & 0 & 0 & \cdots & 0 & 0 \\ C_{21} & C_{22} & C_{23} & 0 & 0 & \cdots & 0 & 0 \\ 0 & C_{32} & C_{33} & C_{34} & 0 & \cdots & 0 & 0 \\ 0 & 0 & C_{43} & C_{44} & C_{45} & \cdots & 0 & 0 \\ \vdots & \vdots & \vdots & \vdots & \vdots & \ddots & \vdots & \vdots \\ 0 & 0 & \cdots & 0 & 0 & C_{(n-1)(n-2)} & C_{(n-1)(n-1)} & C_{(n-1)n} \\ 0 & 0 & \cdots & 0 & 0 & 0 & C_{n(n-1)} & C_{nn} \end{bmatrix} \quad (2.63)$$

and,

$$\underline{L} = \begin{bmatrix} L_{11} & L_{12} & 0 & 0 & 0 & \cdots & 0 & 0 \\ L_{21} & L_{22} & L_{23} & 0 & 0 & \cdots & 0 & 0 \\ 0 & L_{32} & L_{33} & L_{34} & 0 & \cdots & 0 & 0 \\ 0 & 0 & L_{43} & L_{44} & L_{45} & \cdots & 0 & 0 \\ \vdots & \vdots & \vdots & \vdots & \vdots & \ddots & \vdots & \vdots \\ 0 & 0 & \cdots & 0 & 0 & L_{(n-1)(n-2)} & L_{(n-1)(n-1)} & L_{(n-1)n} \\ 0 & 0 & \cdots & 0 & 0 & 0 & L_{n(n-1)} & L_{nn} \end{bmatrix} \quad (2.64)$$

In the matrices shown in equations (2.61) – (2.64) the diagonal elements represent the uncoupled self quantities, whereas the off-diagonal elements represent the interline coupling or mutual coupling quantities. For nearest neighbour interaction, only the coupling between adjacent lines are considered. As a result the generalized capacitance and inductance matrices shown in equations (2.61) and (2.62) become tridiagonal and take the form shown in equations (2.63) and (2.64) respectively. For coupled combines, since the coupling is predominantly capacitive, the inductance matrix is diagonal.

2.5 The forward scattering matrix of forward n -coupled microstrip combines

The equations required for designing a generalized n -channel multiplexer are presented in this section.

The relationship between input and output of an n -coupled line system is represented in terms of input and output wave amplitude vectors, and scattering matrix. The input wave amplitude vector \underline{a}_i and the output wave amplitude vector \underline{b}_o are related with the forward scattering matrix ($\underline{S}_{o,i}$) by [6] [7]

$$\underline{b}_o = \underline{S}_{o,i} \underline{a}_i \quad (2.65)$$

From equation (2.46) the relationship between the forward scattering matrix and the normal mode propagation matrix $\underline{\beta}$ (diagonal) may be written as [6] [7]

$$\underline{S}_{o,i} = \underline{Q}' [\exp\{j(f/f_0)L_0\underline{\beta}\}]^{-1} \underline{Q} \quad (2.66)$$

The matrix $\underline{\beta}$ used in equation (2.66) may be obtained from the tridiagonal wave propagation matrix \underline{J} , since the elements of the diagonal matrix $\underline{\beta}$ are the eigenvalues of \underline{J} . The \underline{Q} matrix is formed with the eigenvectors of the \underline{J} matrix. In the above equation f is the frequency of computation, f_0 is the frequency of

normalization and L_0 is the coupled length of the coupled lines. The column vectors of the \underline{Q} matrix in equation (2.66) are the eigenvectors of the symmetric wave propagation matrix \underline{J} . For lossless lines, the elements of the orthogonal modal matrix \underline{Q} are real.

From equation (2.66) it may be observed that if the \underline{J} matrix and the coupled combline system is known then one can compute the complex elements of the forward scattering matrix. For this purpose the first step is to compute the eigenvalues and the eigenvectors of the \underline{J} matrix. The next step is to form the β matrix with the eigenvalues of the \underline{J} matrix.

2.6 Power and relative phase characteristics of an n -coupled combline system

From the elements of the forward scattering matrix one can obtain the power characteristics of the coupled combline system. In the power characteristics it will be observed that the lower band edge frequency will be at $(f/f_0) = 1$.

Instead of computing the elements of the forward scattering matrix one can obtain the output wave amplitudes directly. This will give the power characteristics of the coupled line system.

Combining equations (2.65) and (2.66) one can write the output wave amplitude vector \underline{b}_o of a forward coupled microstrip combline in terms of the input wave amplitude vector \underline{a}_i as

$$\underline{b}_o = \underline{Q}^t \underline{E}^{-1} \underline{Q} \underline{a}_i \quad (2.67)$$

where,

$$\underline{E} = \exp\{j(f/f_0) L_0 \underline{\beta}\} \quad (2.68)$$

Taking unit excitation at the input port of the k th line and using equations (2.33) and (2.66), the output wave amplitude b_{oi} of the i th line can be computed.

Taking the unit excitation at the input port of the k th line and using equations (2.65) and (2.66), the output wave amplitude vector of i th line can be written as

$$b_{oi} = \underline{p}'_k \underline{E}^{-1} \underline{p}_i = b_{oiR} + j b_{oiI} \quad (2.69)$$

Here the subscript R and I are used for indicating *real* and *imaginary* part respectively.

The power at the output port of the i th line is then [7]

$$P_{oi} = b_{oi} b_{oi}^* = \underline{p}'_k \underline{E}^{-1} \underline{p}_i \underline{p}'_k \underline{E} \underline{p}_i \quad (2.70)$$

Assuming no loss within the device, the sum of power at the output ports at a single frequency must be equal to the input power P_{in} , which can be stated as [9]

$$\sum_{i=1}^n P_{oi} = P_{in} \quad (2.71)$$

The amplitude b_{oi} at the output port of the i th line and hence the power at all the output ports may now be obtained at any frequency by using equations (2.33) and (2.68). The normalized power characteristic in dB at any particular frequency f at i th port may then be obtained from the following equation.

$$\frac{P_{oi}}{P_{in}} = 10 \log(b_{oi} b_{oi}^*) \quad (2.72)$$

If the input power P_{in} in the above equation is taken as 1 then the normalized power at the i th output port may be written as

$$P_{oi} = 10 \log(b_{oi} b_{oi}^*) \quad (2.73)$$

The absolute phase of the i th line is

$$\Phi_{oi} = \tan^{-1}(b_{oiI}/b_{oiR}) \quad (2.74)$$

The relative phase of the i th line with respect to the k th line is

$$\Phi_{ri} = \Phi_{oi} - \Phi_{ok} = \tan^{-1} \left(\frac{b_{oiI}b_{okR} - b_{oiR}b_{okI}}{b_{oiR}b_{okR} + b_{oiI}b_{okI}} \right) \quad (2.75)$$

2.7 Obtaining the line parameters of an n -coupled combline system from the J matrix

Using equation (2.58) and writing the terms with respect to the i th line of an n -coupled combline system, one obtains

for the diagonal terms

$$2J_{ii} = \omega_L(R_{ti}C_{ii} + L_{ii}/R_{ti}) \quad (2.76)$$

and for off-diagonal terms

$$2J_{i(i+1)} = \omega_L R_{ti} C_{i(i+1)} \quad (2.77)$$

Equation (2.77) is valid only for coupled combline system since for this case there is no inductive type interline coupling.

From equation (2.76) it is observed that the difficulty here is to separate the inductance and capacitance values from the diagonal elements J_{ii} 's. Before trying to sort out this it is necessary to define the coupled and uncoupled conditions. It may be noted that in equation (2.76) the *self capacitance* term C_{ii} is the capacitance under coupled condition.

Therefore, the uncoupled self capacitance C_i of the i th line is [6]

$$C_i = C_{ii} - C_{(i-1)i} - C_{i(i+1)} \quad (2.78)$$

It should be noted here that [6],

$$C_{oi} = C_{io} = C_{(n+1)i} = C_{i(n+1)} = 0 \quad (2.79)$$

The process of finding capacitance under coupled condition is described in the following section.

Since there is no inductive coupling in a coupled combline system, the self inductance is the same for both coupled and uncoupled conditions. Using these quantities, the *uncoupled* and *coupled characteristic impedances* of the i th line can be obtained by using the following equations [7].

$$Z_{o_i}^u = \sqrt{L_{ii}/C_i} \quad (2.80)$$

$$Z_{o_i}^c = \sqrt{L_{ii}/C_{ii}} \quad (2.81)$$

The *uncoupled* and *coupled phase velocities* of the i th line are [7]

$$v_{p_i}^u = \frac{1}{\sqrt{L_{ii}C_i}} \quad (2.82)$$

$$v_{p_i}^c = \frac{1}{\sqrt{L_{ii}C_{ii}}} \quad (2.83)$$

The superscript c and u used in the above equations indicate the coupled and uncoupled conditions respectively. It may thus be observed that if the elements of the \underline{J} matrix are known then it is possible to find the values of C_i , C_{ii} and L_{ii} , and thus it is possible to compute $Z_{o_i}^u$, $Z_{o_i}^c$, $v_{p_i}^u$ and $v_{p_i}^c$.

For separating the inductance and capacitance values of equation (2.76) it is useful to have a quantity m_i corresponding to the i th line defined as

$$m_i = \frac{Z_{o_i}^c}{R_{t_i}} \quad (2.84)$$

so that in case of necessity the termination impedances of the i th line may be chosen to have a value other than the corresponding value of $Z_{o_i}^c$. Usually, for the matched

condition $Z_{o_i}^c = R_{t_i}$, i.e., $m_i = 1$. Now eliminating $Z_{o_i}^c$ from equations (2.81) and (2.64) one obtains

$$\sqrt{L_{ii}/C_{ii}} = m_i R_{t_i} \quad (2.85)$$

Putting the value of L_{ii} from equation (2.85) in equation (2.76), one gets

$$\frac{1 + m_i^2}{2} (\omega_L C_{ii} R_{t_i}) = J_{ii} \quad (2.86)$$

Again putting the value of C_{ii} from equation (2.85) into equation (2.76), one gets

$$\frac{\omega_L L_{ii}}{m_i^2 R_{t_i}} = \frac{2J_{ii}}{1 + m_i^2} \quad (2.87)$$

Equations (2.85) and (2.86) may be rewritten as

$$C_{ii} = \frac{2J_{ii}}{\omega_L R_{t_i} (1 + m_i^2)} \quad (2.88)$$

$$L_{ii} = \frac{m_i^2 R_{t_i}}{\omega_L} \left(\frac{2J_{ii}}{1 + m_i^2} \right) \quad (2.89)$$

From equation (2.75) the interline coupling capacitance $C_{i,(i+1)}$ may be written as

$$C_{i,(i+1)} = \frac{2J_{i,(i+1)}}{\omega_L R_{t_i}} \quad (2.90)$$

Thus specifying $Z_{o_i}^c$ and R_{t_i} , one can obtain C_{ii} , L_{ii} , C_i , $C_{i(i+1)}$, $C_{i(i-1)}$ from the \underline{J} matrix. With these values one can determine the line parameters, i.e., the $Z_{o_i}^u$, $v_{p_i}^c$ and $v_{p_i}^u$ of a coupled combline system.

Thus the line parameters (coupled and uncoupled impedances and the phase velocities) may be computed using equations (2.80) – (2.83) and equations (2.88) –

(2.89).

2.8 Defining the \underline{e} vector for an n -coupled combline system

For computation purpose it is very useful to have a set of parameters which can uniquely describe the behavior pattern of an n -coupled combline system. The \underline{e} is a column vector which is formed with the elements of the \underline{J} matrix and the coupled length of the system. For an n -coupled combline system the first n elements are the n diagonal elements of the \underline{J} matrix, the next $n - 1$ elements are the off-diagonal elements of the \underline{J} matrix and the last element is the coupled length of the system. So, the \underline{e} is a column vector having $2n$ number of elements as shown below.

$$\underline{e} = \begin{bmatrix} c_1 \\ c_2 \\ \vdots \\ c_i \\ \vdots \\ c_n \\ d_1 \\ d_2 \\ \vdots \\ d_{n+1} \\ L_0 \end{bmatrix} \quad (2.91)$$

In the above expression c_i 's are the diagonal elements and d_i 's are the off-diagonal elements of the tridiagonal matrix \underline{J} . The last element L_0 represents the coupled length (figure 2.1). A combline multiplexer with nearest neighbour interaction is thus uniquely identified by specifying this \underline{e} vector.

The relationship between the elements of \underline{e} vector and those of \underline{J} matrix may be shown as follows.

$$\left. \begin{aligned}
 c_1 &= J_{11} \\
 c_2 &= J_{22} \\
 c_3 &= J_{33} \\
 \vdots &= \vdots \\
 c_n &= J_{nn}
 \end{aligned} \right\} \quad (2.92)$$

and,

$$\left. \begin{aligned}
 d_1 &= J_{12} = J_{21} \\
 d_2 &= J_{23} = J_{32} \\
 d_3 &= J_{34} = J_{43} \\
 \vdots &= \vdots = \vdots \\
 d_{n-1} &= J_{(n-1)n} = J_{n(n-1)}
 \end{aligned} \right\} \quad (2.93)$$

2.9 Summary

In this chapter a brief review of the generalized theory of n -coupled combline system has been presented bearing in mind that equations for combline diplexers will be derived out of these equations.

The wave-propagation matrix \underline{J} has been introduced. The equations for the forward scattering matrix for coupled combline system has been presented. The equations for obtaining the power and relative phase characteristics have been presented. The equations for obtaining the parameters of a coupled combline system for the \underline{J} matrix has also been presented.

CHAPTER 3

Forward scattering matrix and line parameters of a combline diplexer

3.1 Introduction

In the last chapter the generalized theory of n -coupled microstrip comblines has been presented. Following the generalized equations of last chapter the equations for two coupled comblines system are derived. Thus for a two coupled system it will be seen that the wave-propagation matrix \underline{J} is a 2×2 matrix. Similarly the scattering matrix S_{oi} is also a 2×2 matrix. The input wave amplitude vector and the output wave amplitude vector are two-element column vectors. The equations for such a two coupled combline system may be considered to be the equations for a diplexer.

The equations for obtaining the forward scattering matrix of a combline diplexer from its wave-propagation matrix are presented in section 3.2. In section 3.3 the \underline{e} vector for a combline diplexer is written in terms of its wave-propagation matrix elements and the coupled length. Next in section 3.4 the techniques of scaling and shifting the wave-propagation matrix are presented. The equations for obtaining the line parameters of a combline diplexer are presented in section 3.5. The summary of this chapter is presented in section 3.6.

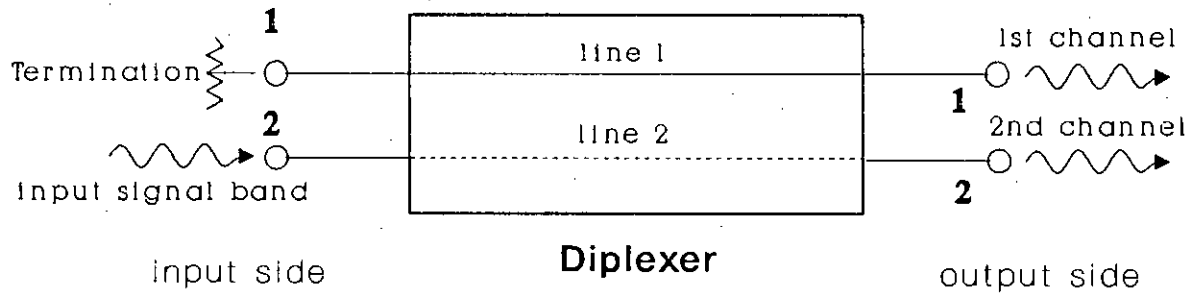


Figure 3.1 Block diagram of a diplexer.

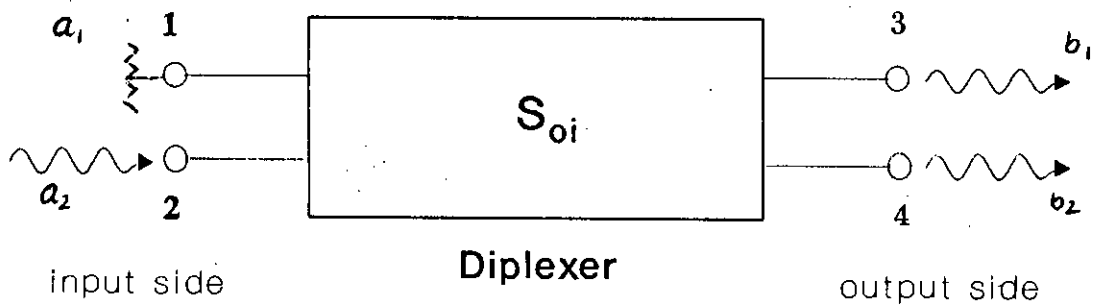


Figure 3.2 A diplexer represented by its forward scattering matrix S_{oi} .

3.2 Obtaining the forward scattering matrix of a combline diplexer from its wave-propagation matrix \underline{J}

In a diplexer the input signal of a certain frequency band is fed through one of the two input ports and the other port at the input side (known as the *back-port* is terminated by a matched coupled line impedance as shown in figure 3.1. The two bands of frequencies are obtained at the two different output ports of a diplexer.

The output wave amplitude vector \underline{b} and the input wave amplitude vector \underline{a} are related by the scattering matrix as shown in equation (2.33). In case of a diplexer (as shown in figure 3.2) this relationship may be written as

$$\begin{bmatrix} b_1 \\ b_2 \end{bmatrix} = \begin{bmatrix} S_{11} & S_{12} \\ S_{21} & S_{22} \end{bmatrix} \begin{bmatrix} a_1 \\ a_2 \end{bmatrix} \quad (3.1)$$

In the above equation the subscripts of a and b indicate the line number. The first and the second subscripts of S indicate the port numbers at the input and the output sides respectively. As mentioned earlier the wide band of input signal is fed into one of the two ports at the input side of a diplexer while the other port remains terminated with no signal input. So either a_1 or a_2 is equal to zero (which implies no signal at this port). If it is assumed that the input is fed through port 2 at the input side, then the backport (i.e., port 1), remains terminated (i.e., $a_1 = 0$). Under this condition equation (3.1) takes the following form.

$$\begin{bmatrix} b_1 \\ b_2 \end{bmatrix} = \begin{bmatrix} S_{11} & S_{12} \\ S_{21} & S_{22} \end{bmatrix} \begin{bmatrix} 0 \\ a_2 \end{bmatrix} = a_2 \begin{bmatrix} S_{12} \\ S_{22} \end{bmatrix} \quad (3.2)$$

From equation (2.68) it may be seen that

$$S_{oi} = \underline{Q}^t \underline{E}^{-1} \underline{Q}$$

where

$$\underline{E} = \exp[j(f/f_0)L_0\beta]$$

So in order to obtain the forward scattering matrix S_{oi} it is necessary to obtain the propagation constant β_1 and β_2 at the two lines. Thus equation (2.57) can be written as

$$\underline{Q} \underline{J} \underline{Q}^t = \underline{\beta} \quad (3.3)$$

For a diplexer equation (3.3) may be rewritten in terms of the matrix elements as

$$\begin{bmatrix} Q_{11} & Q_{12} \\ Q_{21} & Q_{22} \end{bmatrix} \begin{bmatrix} J_{11} & J_{12} \\ J_{21} & J_{22} \end{bmatrix} \begin{bmatrix} Q_{11} & Q_{12} \\ Q_{21} & Q_{22} \end{bmatrix}^t = \begin{bmatrix} \beta_1 & 0 \\ 0 & \beta_2 \end{bmatrix} \quad (3.4)$$

β_1 and β_2 in the above equation are the eigenvalues of \underline{J} matrix. These eigenvalues may be obtained by solving the following characteristic equation of the \underline{J} matrix.

$$|\beta \underline{I} - \underline{J}| = 0 \quad (3.5)$$

In the above equation \underline{I} is the identity matrix and β is the characteristic root of the \underline{J} matrix. In case of a diplexer equation (3.5) may be written as

$$\left| \beta \begin{bmatrix} 1 & 0 \\ 0 & 1 \end{bmatrix} - \begin{bmatrix} J_{11} & J_{12} \\ J_{21} & J_{22} \end{bmatrix} \right| = 0 \quad (3.6)$$

Simplifying the above equation one obtains

$$\beta^2 - \beta(J_{11} + J_{22}) + (J_{11}J_{22} - J_{12}J_{21}) = 0 \quad (3.7)$$

Equation (3.7) is a quadratic equation of β and solving this equation two characteristic roots (i.e., β_1 and β_2) are obtained. These two roots are the eigenvalues of \underline{J} matrix. From equation (3.7) one can obtain the equations for two eigenvalues as

$$\beta_1 = \frac{(J_{11} + J_{12}) + \sqrt{(J_{11} + J_{22})^2 + 4(J_{11}J_{22} + J_{12}J_{21})^2}}{2} \quad (3.8)$$

$$\beta_2 = \frac{(J_{11} + J_{12}) - \sqrt{(J_{11} + J_{22})^2 + 4(J_{11}J_{22} - J_{12}J_{21})^2}}{2} \quad (3.9)$$

For the diplexer under consideration the forward scattering matrix may be obtained from equation (2.56), which can be rewritten for a diplexer in the following form.

$$\begin{bmatrix} S_{11} & S_{12} \\ S_{21} & S_{22} \end{bmatrix} = \begin{bmatrix} Q_{11} & Q_{12} \\ Q_{21} & Q_{22} \end{bmatrix}^t \begin{bmatrix} e^{-j(J/f_0)L_0\beta_1} & 0 \\ 0 & e^{-j(J/f_0)L_0\beta_2} \end{bmatrix} \begin{bmatrix} Q_{11} & Q_{12} \\ Q_{21} & Q_{22} \end{bmatrix} \quad (3.10)$$

Thus using equations (3.8) and (3.9) it is possible to obtain the propagation constants on the two lines of a combline diplexer from its wave-propagation matrix. Next using equations (3.10), it is possible to obtain the elements of the forward scattering matrix of the diplexer. This means that one can then obtain the power characteristics of the diplexer.

3.3 The \underline{e} vector of a combline diplexer

Following section 2.8, it is possible to write the \underline{e} vector for a diplexer as a four-element column vector. So,

$$\underline{e} = \begin{bmatrix} c_1 \\ c_2 \\ d_1 \\ L_0 \end{bmatrix} \quad (3.11)$$

The first two elements c_1 and c_2 of the \underline{e} vector shown are the diagonal elements of the 2×2 wave-propagation matrix of diplexer. The third element d_1 is the off-diagonal element (since both the off-diagonal elements are same in this case). The fourth element L_0 represents the coupled length of the combline. So the elements of the \underline{e} vector can be written in terms of the elements of \underline{J} as

$$\left. \begin{aligned} c_1 &= J_{11} \\ c_2 &= J_{22} \\ d_1 &= J_{12} = J_{21} \end{aligned} \right\} \quad (3.12)$$

3.4 Scaling of \underline{J} matrix

The techniques of scaling the wave propagation matrix \underline{J} may be used for necessary adjustment of the combline parameters without changing the scattering matrix which actually represents the operating characteristics of the device. Scaling is necessary for obtaining the physical dimensions of the device within realizable ranges. The process of scaling does not affect the characteristics of a diplexer. Two types of scaling of \underline{J} matrix will be necessary. These two types of scaling are described in the following subsections.

3.4.1 Scaling by scalar multiplication of \underline{J} matrix

The first type of scaling can be done by multiplying the elements of the \underline{J} matrix by a scalar quantity (say x). This will multiply the interline coupling capacitances by x and shift the characteristics of the diplexer. So, in order to keep the characteristics unchanged the coupled length of the diplexer is divided by the same quantity x . As a result even after these two operations the characteristics of a diplexer remain unchanged [6]. In the following equation \underline{J}_{new} is the matrix after scaling the \underline{J} matrix by *scalar multiplication*.

$$\underline{J}_{new} = x \underline{J} = x \begin{bmatrix} J_{11} & J_{12} \\ J_{21} & J_{22} \end{bmatrix} = \begin{bmatrix} x J_{11} & x J_{12} \\ x J_{21} & x J_{22} \end{bmatrix} \quad (3.13)$$

$$\text{The new length, } L_0 = L'_0/x \quad (3.14)$$

where, L'_0 is the coupled length before the change.

It may be thus be observed that this operation is useful in increasing or reducing the interline coupling capacitances and also in changing the coupled length. Thus this operation is very useful in the design procedure.

3.4.2 Scaling by adding a constant value with all the diagonal elements of the \underline{J} matrix

This method is also known as *\underline{J} matrix shifting technique* [6]. If a constant amount of *phase constant* β_0 is added to or subtracted from each of the diagonal elements of the \underline{J} matrix then despite the changes in \underline{J} matrix the characteristics of the device remain unchanged. This operation may be represented by the following equation:

$$\underline{J}_{new} = \underline{J} + \beta_0 \underline{I} = \begin{bmatrix} J_{11} & J_{12} \\ J_{21} & J_{22} \end{bmatrix} + \begin{bmatrix} \beta_0 & 0 \\ 0 & \beta_0 \end{bmatrix} = \begin{bmatrix} J_{11} + \beta_0 & J_{12} \\ J_{21} & J_{22} + \beta_0 \end{bmatrix} \quad (3.15)$$

In the above equation though the \underline{J}_{new} and the \underline{J} matrices have different diagonal elements, they yield same scattering matrix.

This operation will be required to adjust the phase velocities of the combines of a diplexer.

3.5 Determination of the parameters of a forward coupled microstrip combline diplexer from its wave propagation matrix

Once the wave propagation matrix is known, the eigenvalues of the \underline{J} matrix can be computed using equations (3.8) and (3.9). The \underline{Q} matrix containing the eigenvectors can also be obtained by the usual matrix method. In order to obtain the line parameters of a forward coupled microstrip combline multiplexer it is necessary to obtain the inductance and the capacitance matrices from the wave propagation matrix. The techniques of obtaining the capacitance and inductance matrices and hence the line parameters are presented in this section.

The computations are done at the lower band edge frequency $\omega_L = 2\pi f_L$ of the diplexer. However, after computing the capacitance and inductance matrices, the wave propagation matrix \underline{J} (which means the mode propagation matrix β as

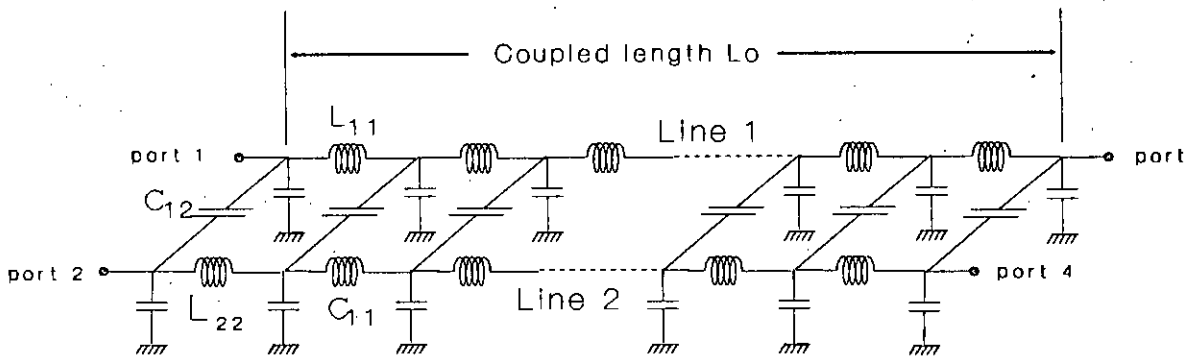


Figure 3.3 Model of an 2-line coupled combline system (diplexer) showing the distributed self capacitances, inductances and interline coupling capacitances. Here, only the nearest neighbour interaction is considered.

well) can be scaled in order to obtain realizable values of the line parameters. The process of scaling the \underline{J} matrix has already been discussed in section (3.4). It may be mentioned here once again that, the scaling operation leaves the scattering matrix S_{oi} (i.e. the power characteristics) unchanged.

In order to obtain the elements of the capacitance matrix \underline{C} and the inductance matrix \underline{L} in terms of the wave propagation matrix \underline{J} , it is necessary to recall here that, from its definition, the matrix \underline{J} may be written in the following form from equation (2.58).

$$\underline{J} = \frac{\underline{B}_n + \underline{X}_n}{2} \quad (3.16)$$

where $\underline{B}_n = \omega_i^{1/2} \underline{R}_i^{1/2} \underline{C} \underline{R}_i^{1/2}$ and $\underline{X}_n = \omega_l \underline{R}_l^{-1/2} \underline{L} \underline{R}_l^{-1/2}$ as shown in equations (2.59) and (2.60). In case of a combline diplexer the capacitance and inductance matrices shown in equations (2.61) and (2.63) reduce to the following form

Capacitance matrix

$$\underline{C} = \begin{bmatrix} C_{11} & C_{12} \\ C_{21} & C_{22} \end{bmatrix} \quad (3.17)$$

Inductance matrix

$$\underline{L} = \begin{bmatrix} L_{11} & L_{12} \\ L_{21} & L_{22} \end{bmatrix} \quad (3.18)$$

Here, $L_{12} = L_{21} = 0$ for a pair of coupled comblines. The equivalent circuit of a pair of coupled comblines may be represented as shown in figure 3.3.

The uncoupled capacitance of the two lines of a forward coupled microstrip diplexer can be computed from the equations (2.78) and (2.79) as shown below.

$$\left. \begin{aligned} C_1 &= C_{11} - C_{01} - C_{12} \\ &= C_{11} - C_{12} \end{aligned} \right\} \quad (3.19)$$

and

$$\left. \begin{aligned} C_2 &= C_{22} - C_{12} - C_{23} \\ &= C_{22} - C_{12} \end{aligned} \right\} \quad (3.20)$$

For a diplexer, the characteristic impedance under coupled and uncoupled conditions may be obtained from equations (2.80) and (2.81). The characteristic impedances of line-1 and line-2 are as follows.

Uncoupled characteristic impedance

$$\text{for line-1: } Z_{o_1}^u = \sqrt{L_{11}/C_1} \quad (3.21)$$

$$\text{for line-2: } Z_{o_2}^u = \sqrt{L_{22}/C_2} \quad (3.22)$$

Coupled characteristic impedance

$$\text{for line-1: } Z_{o_1}^c = \sqrt{L_{11}/C_{11}} \quad (3.23)$$

$$\text{for line-2: } Z_{o_2}^c = \sqrt{L_{22}/C_{22}} \quad (3.24)$$

The uncoupled and coupled phase velocities may be obtained from equations (2.82) and (2.83). For a diplexer the phase velocities of line-1 and line-2 can be written as

Uncoupled phase velocities

$$\text{for line-1: } v_{p_1}^u = 1/\sqrt{L_{11}C_1} \quad (3.25)$$

$$\text{for line-2: } v_{p_2}^u = 1/\sqrt{L_{22}C_2} \quad (3.26)$$

Coupled phase velocities

$$\text{for line-1: } v_{p_1}^c = 1/\sqrt{L_{11}C_{11}} \quad (3.27)$$

$$\text{for line-2: } v_{p_2}^c = 1/\sqrt{L_{22}C_{22}} \quad (3.28)$$

For a diplexer the ratios of coupled characteristic impedance and the terminating resistance may be obtained from equation (2.84) which are

$$m_1 = \frac{Z_{o1}^c}{R_{t1}} \quad \text{and} \quad m_2 = \frac{Z_{o2}^c}{R_{t2}} \quad (3.29)$$

From equation (2.88) the following equations may be written for a diplexer to obtain the coupled capacitances for line-1 and line-2 as shown below.

$$C_{11} = \frac{2}{\omega_L R_{t1} (1 + m_1^2)} (J_{11}) \quad (3.30)$$

$$C_{22} = \frac{2}{\omega_L R_{t2} (1 + m_2^2)} (J_{22}) \quad (3.31)$$

The equations for coupled inductances of a diplexer can be derived from equation (2.89) which are shown below.

$$L_{11} = \frac{m_1^2 R_{t1}}{\omega_L} \times \frac{2}{(1 + m_1^2)} (J_{11}) \quad (3.32)$$

$$L_{22} = \frac{m_2^2 R_{t2}}{\omega_L} \times \frac{2}{(1 + m_2^2)} (J_{22}) \quad (3.33)$$

From equation (2.90) the coupling capacitance between line-1 and line-2 (i.e., C_{12} or C_{21}) may be written as

$$C_{12} = C_{21} = \frac{2}{\omega_L R_{t1}} (J_{12}) \quad (3.34)$$

Thus specifying Z_{oi}^c and R_{ti} , one can obtain C_{ii} , L_{ii} , C_i , $C_{i(i+1)}$, $C_{i(i-1)}$ from the \underline{J} matrix. With these values one can determine the line parameters, i.e., the $Z_{\alpha_i}^u$, v_{pi}^c and v_{pi}^u of a forward coupled microstrip combline diplexer.

Thus the line parameters (coupled and uncoupled impedances and the phase velocities) may be computed using equations (3.19) – (3.22).

3.6 Summary

The equations presented in this chapter will be necessary for obtaining the power characteristics of a combline diplexer. For this, it is necessary to know the wave-propagation matrix \underline{J} of the diplexer. It has also been shown that if the \underline{J} matrix of a coupled diplexer is known then one can obtain the physical dimensions of the diplexer.

CHAPTER 4

Designing a combline diplexer by computer optimization

4.1 Introduction

In chapter 3 the equations and procedures for obtaining the forward scattering matrix, power characteristics and the line parameters from the wave-propagation matrix of a two coupled combline system have been presented. So, in order to get these, it is necessary to know the \underline{J} matrix and the coupled length of the system. The next requirement is to have a \underline{J} matrix and a value of the coupled length L_0 which will provide the desired characteristics of the diplexer. This means that an \underline{e} vector is necessary which will meet the requirements of the desired characteristics. Unfortunately, an analytical method of obtaining such an \underline{e} vector to get the desired characteristics could not yet be developed. So, this work will be done by computer optimization. The steps required for an optimization procedure are shown in figure 4.1.

In this chapter the technique of computer optimization of \underline{e} vector to achieve the desired diplexer characteristics is presented. The possible methods of optimization and the difficulties those are encountered in finding the maximum or minimum of a function are discussed briefly in section 4.2. The principles of two methods of optimization known as *Golden section search* and *Gradient method* are presented concisely in subsections 4.2.1 and 4.2.2 respectively. The aspects which should be taken under consideration while selecting or developing an optimization program

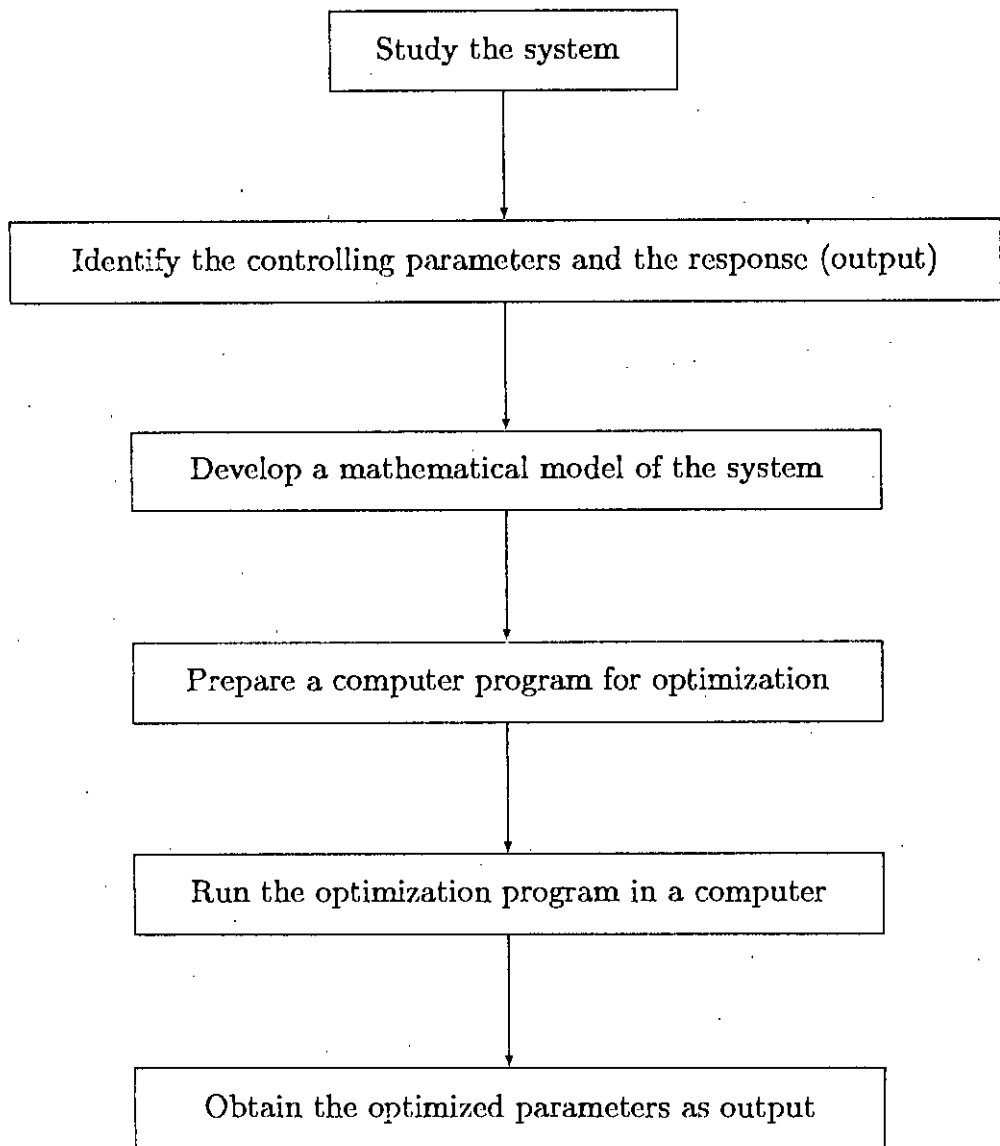


Figure 4.1 Steps required in an optimization procedure.

are presented in section 4.3. The criteria for selecting a particular optimization method are also presented in section 4.3. The optimization method used in this work is presented in section 4.4.

The effect of the elements of \underline{e} vector on the power against frequency characteristics of a diplexer are presented in section 4.5. Considerations regarding selecting a starting \underline{e} vector is presented in section 4.6. The necessity and procedure of optimizing the \underline{e} vector is discussed in section 4.7. The computation of error function is discussed in section 4.8. The optimization program used in this work is presented in section 4.9. Finally an example of optimization of \underline{e} vector is presented in section 4.10 with a sample set of data. The summary of this chapter is presented in section 4.11.

4.2 Possible methods of optimization

If there is a function f which depends on a number of independent variables, one can find the values of those variables for which f takes on a maximum or a minimum value by the process of optimization.

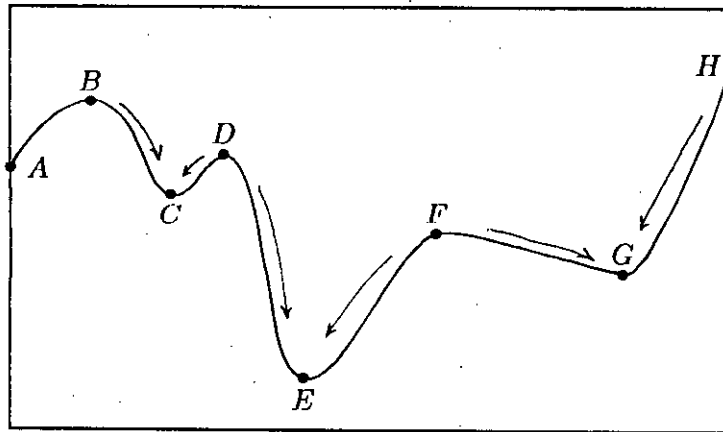


Figure 4.2 The function f shown in the range of AH has three local minimas at C , E and G . Here E is the global minima. The arrow signs indicates the tendency of the search to fall into the local minima.

An extremum (maximum or minimum point) can be either *global* (truly the highest or lowest function value) or *local* (the highest or lowest or lowest function value) or *local* (the highest or lowest in a finite neighbourhood and not on the boundary of that neighbourhood) [13]. Always the target is to obtain a global extremum. For very simple type of functions this can be achieved easily but for functions of complicated behaviour optimization work is very likely to get trapped in local extremum. Then the problem is to get out of the local extremum by improved search techniques. On the contrary, finding a local extremum is easy.

Let the function shown in figure 4.2 be considered for example. If the search for minima is started at any point between B and D , a routine will stuck at point C (the local minima) unless it extends its search beyond point D . Similarly if search is started at any point between F and H , a routine is likely to stuck at point G unless the search is extended beyond point F . So one standard procedure that is commonly used is to find local extrema starting from widely varying starting values of the independent variables, and then pick the most extreme of these (if they are not all the same which might occur in case of a function having unique extrema). In figure 4.2 if search is started from different points, the routine will find the global minima at E .

One-dimensional functions (where the response is the function of a single independent variable) can be handled more easily than the multi-dimensional functions (where the response is a function of a number of independent variables). A single-variable function can be plotted readily on a two dimensional plane from where the maxima or minima can be seen within a selected range. But in case of an n -variable function, an $(n+1)$ dimensional domain is required for plotting the function. So it is not possible to represented such a domain graphically. At best the two-dimensional functions may be plotted in a three dimensional space. It is also very difficult to

determine in case of an n -dimensional function, to determine the direction in which the search should be performed in the $(n + 1)$ dimensional domain to move toward the maxima or minima.

There are several methods for optimization of multi-variable functions. The commonly used methods are: Golden section search method, Least square method, Gradient method, Powell's method and variable metric method. All these methods have their merits and demerits. Two of these methods are briefly discussed in the following subsections. Any of these methods may be used for the optimization job required in this work. However, a different algorithm is used in this work for optimization considering different aspects of the \underline{g} vector under consideration.

4.2.1 Golden section search

A golden section search is designed to handle, in effect the worst possible case of function minimization. This process is similar to the bisection method of finding roots of function in one dimension [13]. The root is supposed to be bracketed¹ in one interval (a, b) . One then evaluates the function at an intermediate point x and obtains a new smaller bracketing interval, (a, x) or (x, b) . The process continues until the bracketing interval is acceptably small. It is optimal to choose x to be the midpoint of (a, b) so that decrease in the interval length is maximized.

A minimum is known to be bracketed only when there is a triplet of points, $a < b < c$, such that $f(b)$ is less than both $f(a)$ and $f(c)$. In this case it is known that the function (if it is nonsingular) has minimum in the interval (a, c) .

The analog of bisection is to choose a new point x , either between a and b or between b and c . Suppose, to be specific, the latter choice is made and $f(x)$ is evaluated. If $f(b) < f(x)$, then the new bracketing triplet of points is $a < b < x$; contrariwise, if $f(b) > f(x)$, then the new bracketing triplet is $b < x < c$. In all

¹A root of function is known to be bracketed by a pair of point, $a < b$, when the function has opposite sign at those points.

cases the middle point of the new triplet is the abscissa whose ordinate is the best minimum achieved so far.

4.2.2 Gradient methods

If y is a function of n number of variables (say, x_1, x_2, \dots, x_n) then the vector of first partial derivatives $(\Delta y/\Delta x_1, \Delta y/\Delta x_2, \dots, \Delta y/\Delta x_n) \equiv \nabla y$ is known as *gradient*. The vector gets its name because it points in the direction in which the response surface has the steepest slope. To see why this is so, an n -dimensional hypersphere of radius r , centered about the point \underline{x} . Points $\underline{x} + \Delta \underline{x}$ on this sphere satisfy

$$\sum_{j=1}^n (\Delta x_j)^2 = |\Delta \underline{x}|^2 = r^2 \quad (4.1)$$

The first order approximation of the objective function in the neighbourhood of \underline{x} gives the value of the objective function at various points on the sphere as

$$\Delta y = \nabla y \Delta \underline{x}' \quad (4.2)$$

The point on the hypersphere is sought where Δy is maximum. At this point the following Lagrangian must be stationary:

$$L = \nabla y \Delta \underline{x}' - \lambda [|\Delta \underline{x}|^2 - r^2] \quad (4.3)$$

Hence the maximizing perturbation $\Delta \underline{x}^*$ satisfies

$$\nabla L = \nabla y - 2\lambda \Delta \underline{x}^* = 0 \quad (4.4)$$

where

$$\Delta \underline{x}^* = (2\lambda)^{-1} \nabla y \quad (4.5)$$

Since λ , the Lagrange multiplier, is a constant, the geometric interpretation of equation (4.5) is that the optimum perturbation vector $\Delta \underline{x}^*$ points in the same direction as the gradient vector. The constraint equation (4.1) gives λ :

$$|\Delta \underline{x}^*|^2 = (2\lambda)^{-2} |\nabla y|^2 = r^2 \quad (4.6)$$

where

$$\lambda = \frac{|\nabla y|}{2r} \quad (4.7)$$

$$(4.8)$$

$$\Delta \underline{x}^* = \frac{r \nabla y}{|\nabla y|} \quad (4.9)$$

$$\Delta y^* = r |\nabla y|$$

The vector $\nabla y/|\nabla y|$ is called the *normalized gradient*.

The gradient method for seeking a maximum is to determine the gradient at point \underline{x}_0 . The set of points in the gradient direction is given by

$$\Delta \underline{x}_0 = \rho \nabla y(\underline{x}_0) \equiv \rho \nabla y_0 \quad (4.10)$$

Where ρ is a normalized hypersphere radius given by

$$\rho \equiv \frac{r}{|\nabla y|} \quad (4.11)$$

Positive values of the normalized radius ρ give locally increasing values of y , so the value of ρ maximizing Δy is found either by one-dimensional (Fibonacci) [21] search or, when possible by direct differentiation. The latter alternative involves substituting equation (4.10) into the objective function, differentiating with respect to ρ , setting the derivatives to zero, and solving for minimizing value ρ^* . Thus one finds ρ^* satisfying

$$\frac{\Delta y(\underline{x} + \rho \nabla y)}{\Delta \rho} \Big|_{\rho=\rho^*} = 0 \quad (4.12)$$

At new point \underline{x}_1 , one evaluates a new gradient and iterates the gradient climbing procedure. That is,

$$\underline{x}_1 = \underline{x}_0 + \rho_0^* \nabla y_0 \quad (4.13)$$

$$\Delta \underline{x}_1 = \rho_1^* \nabla y_1 \quad (4.14)$$

and so on.

4.3 Selection of optimization algorithm

There are a number of standard algorithms for optimization [13] [21]. Actually different types of optimization jobs may require different types of algorithms. So the selection of the most suitable algorithm is also of vital importance. There may be several optimization algorithms which will get a particular job done, but the best one should be chosen carefully. It becomes easier to select an optimization algorithm if the nature of the function under consideration is known beforehand.

It is desired that the computational procedures for optimization run quickly and use small memory while it is run in a computer. In other words it is desired to evaluate the particular function in question as few times as possible. As for example the optimization required for this research could be done with any of the multi-variable optimization procedures mentioned in section 4.2. But considering the fact that the function under consideration (i.e., the \underline{e} vector) is relatively simple and has only four independent variables, instead of using any standard optimization method a more simple and modified optimization algorithm is used in this work. This method of optimization is described in details in section 4.4. The algorithm developed in section 4.4 is simple, reasonably fast and suitable for this particular job.

4.4 Optimization algorithm used in this work

Though there are several optimization algorithms in practice as described in the last section, none of these techniques is completely followed in this work. For the optimization job in this work a different algorithm which suits the work under consideration has been adopted. The generalized form of the algorithm (i.e., with n number of independent variables) used in this work is presented in this section.

Let it be assumed that there are n number of controlling parameters or independent variables (say, x_1, x_2, \dots, x_n) on which the response or the output (P_{out}) depends.

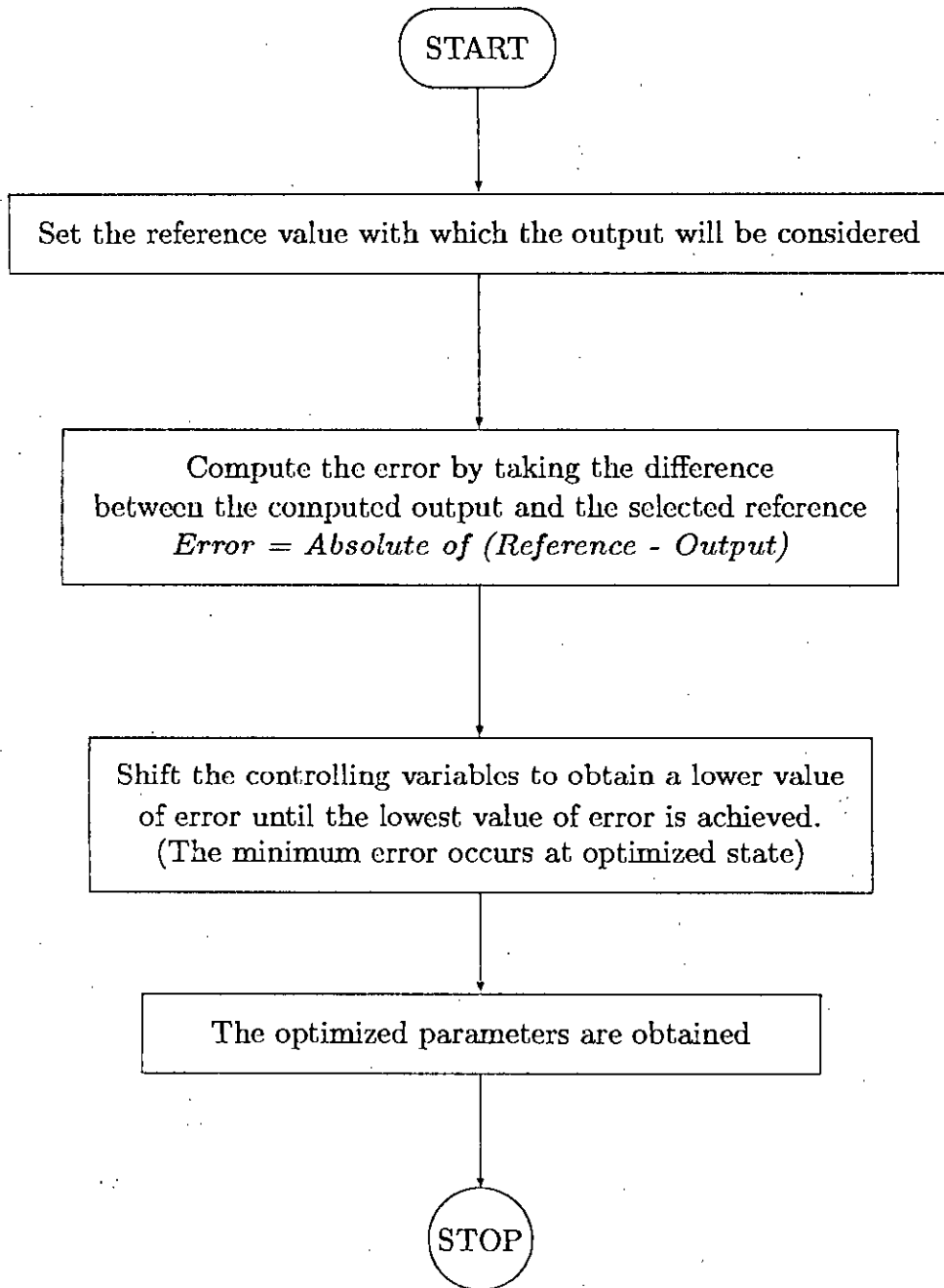


Figure 4.3 Major steps of the optimization algorithm used in this work.

In other words the output is a function of the n number of variables or independent variables, i.e., $P_{out} = f(x_1, x_2, \dots, x_n)$. Here a reference value (Y_{ref}) is chosen first with which the output is compared to give the amount of error or deviation.

At the beginning, a starting set of variables is chosen and with this known set of values the output (P_{out}) is computed. Now the difference between this computed output and the reference level is determined. This difference is considered as the deviation or the error. The job of optimization is to minimize this error to an optimum level. This is done by shifting the n number of variables. The shifting is done by gradually incrementing or decrementing the variables by a small quantity (say Δx).

Initially the first variable (x_1) is incremented by amount Δx keeping all other parameters unchanged. With this new value of x_1 (say x'_1 , where $x'_1 = x_1 + \Delta x$) the output is computed and the error is determined. If the error increases with x'_1 then x_1 is decremented by the same amount Δx to obtain the new x'_1 (where $x'_1 = x_1 - \Delta x$). If the error still increases with the decremented x_1 (i.e., x'_1), the original value of x_1 is retained. However, that value of x'_1 is accepted for which the error decreases and this x'_1 is used as x_1 in latter computations. Now the second parameter x_2 is similarly increased or decreased to obtain x'_2 (where, $x'_2 = x_2 + \Delta x$ if increased by Δx and $x'_2 = x_2 - \Delta x$ if decreased by Δx) or kept unchanged so that a smaller error is obtained. This x'_2 is accepted as the new x_2 and is used in latter computations.

In a similar fashion all other parameters are gradually changed to obtain smaller error. When all the variables are shifted once, the entire procedure is repeated once again and so on. If the process is continued, a condition occurs when the error reaches its minima and any further change of any of the controlling parameters gives a greater error. The set of controlling parameters which gives the minimum error is taken as the optimum set of parameters. The major steps of optimization algorithm used in this work is shown in Fig 4.3.

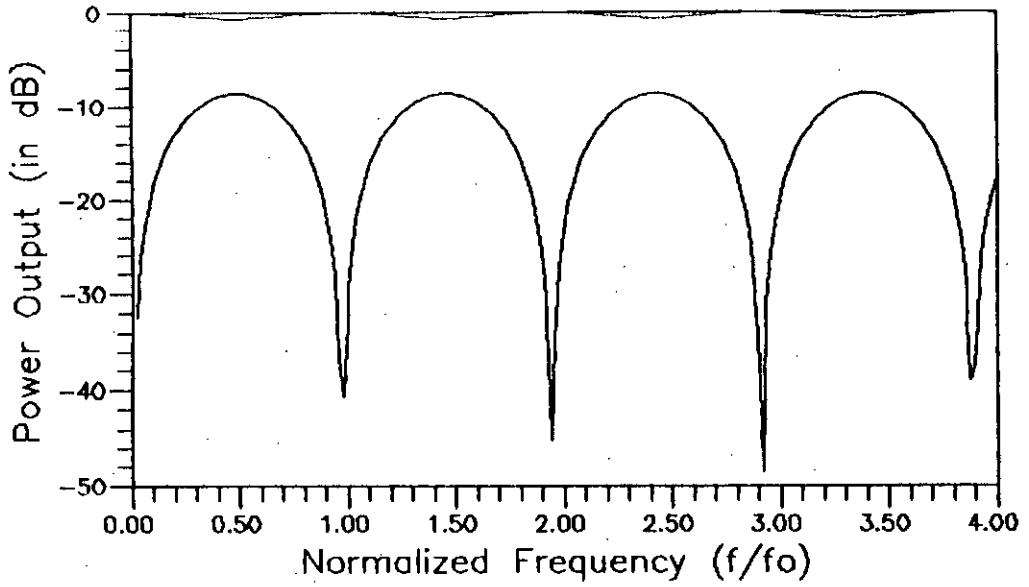
4.5 The effect of changing the elements of \underline{e} vector on the characteristics of a diplexer

The \underline{e} vector² of a diplexer contain four elements, first three of which (i.e., c_1 , c_2 and d_1) comes \underline{J} matrix and the fourth one (i.e., L_0) is the coupled length of the diplexer as mentioned in section 3.3. The power and phase characteristics are functions of \underline{e} vector. The characteristics of the curves may be modified by varying the elements of \underline{e} vector. Different elements of \underline{e} vector has different effects on the characteristics of a diplexer. To study and observe the effect of the elements of \underline{e} vector on the power against frequency characteristic a number of plots have been prepared (figure 4.4 – 4.23).

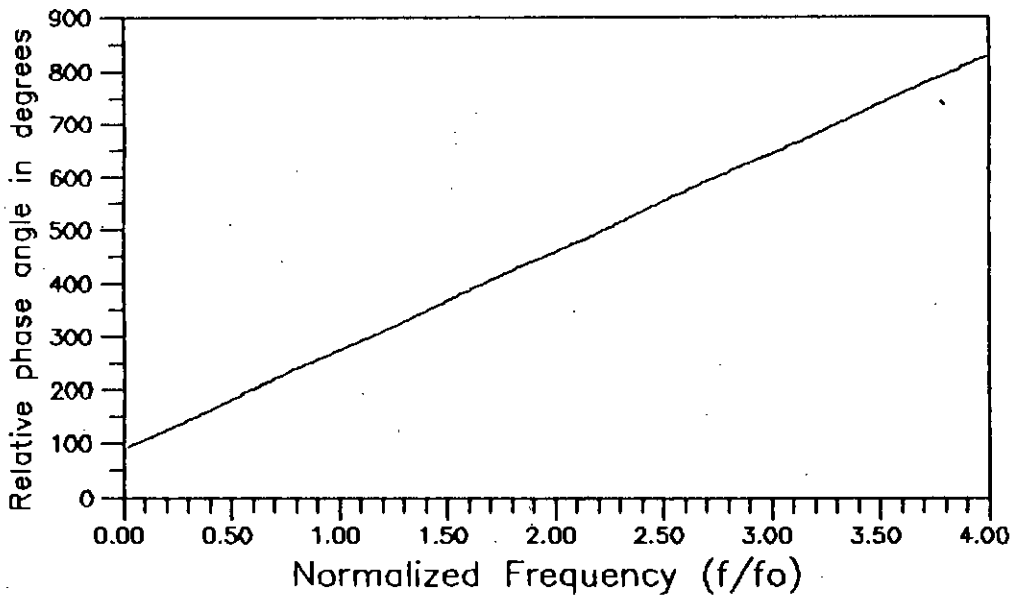
In Figs. 4.4 – 4.9 the power characteristics are plotted while decreasing the first element of \underline{e} vector (i.e., c_1) keeping other elements constant. It is seen the coupling between the lines increases as the difference between c_1 and c_2 decreases. When c_1 equals c_2 , maximum coupling between lines occur.

Similarly in Figs. 4.10 – 4.15 only the second element of \underline{e} (i.e., c_2) is varied. These plots also support the idea stated above. In Figs. 4.16 – 4.19 represent the power against frequency plots where only d_1 is varied keeping all other elements constant. It may be observed from these plots that the periodicity of reaching peak coupling decreases with increasing d_1 . Similarly only the coupled length L_0 is varied to obtain the plots shown in Figs. 4.20 – 4.23. It is observed that the characteristics can be shifted along the frequency scale by changing the coupled length L_0 . If the coupled length is increased, the frequency at which coupling reaches the required value can be lowered. This can better be understood by comparing the curves shown in Figs. 4.20 – 4.23. It can also inferred from these plots that in case of a diplexer the two channels may be brought closer or pushed away by respectively increasing or decreasing the coupled length of the diplexer.

²It may be recalled here that $\underline{e}^t = [c_1 \ c_2 \ d_1 \ L_0]$.

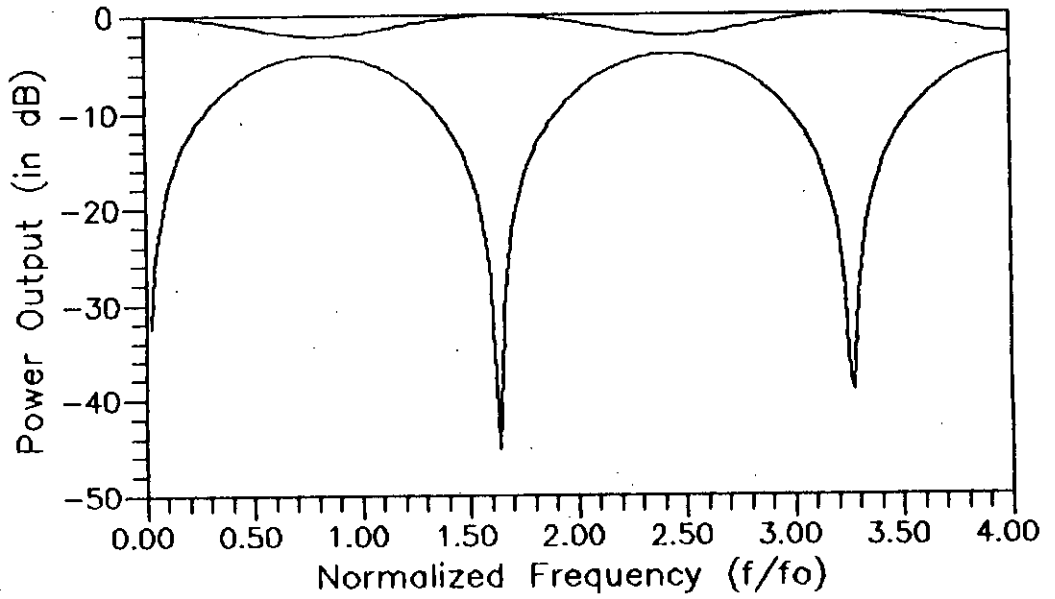


(a)

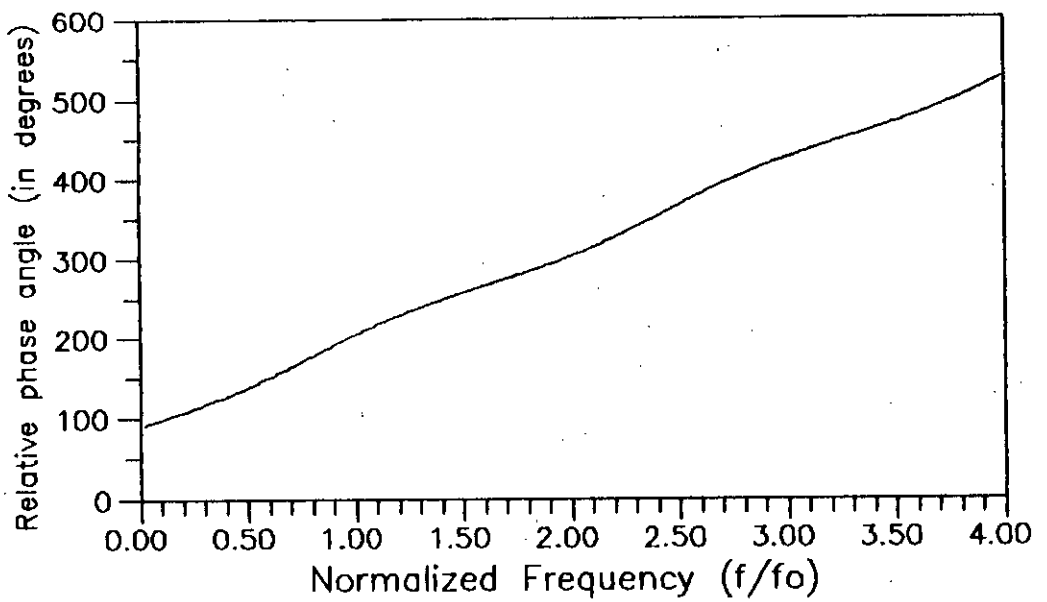


(b)

Figure 4.4 Characteristics of a diplexer: (a) power vs. frequency, and (b) relative phase vs. frequency plots with $\underline{e}^t = [1.5 \ 0.5 \ -0.2 \ 6.0]$.

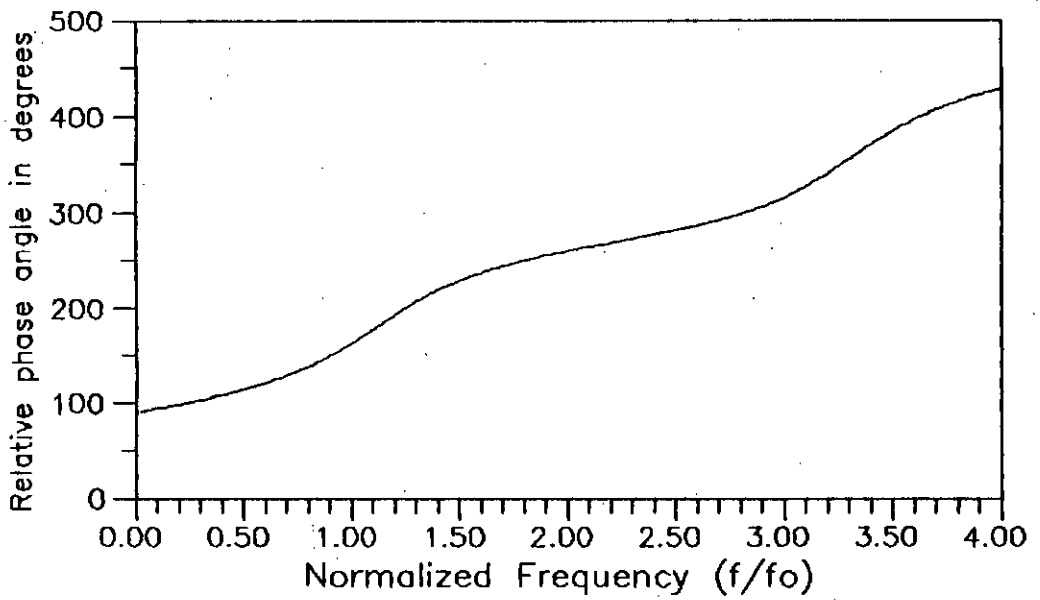
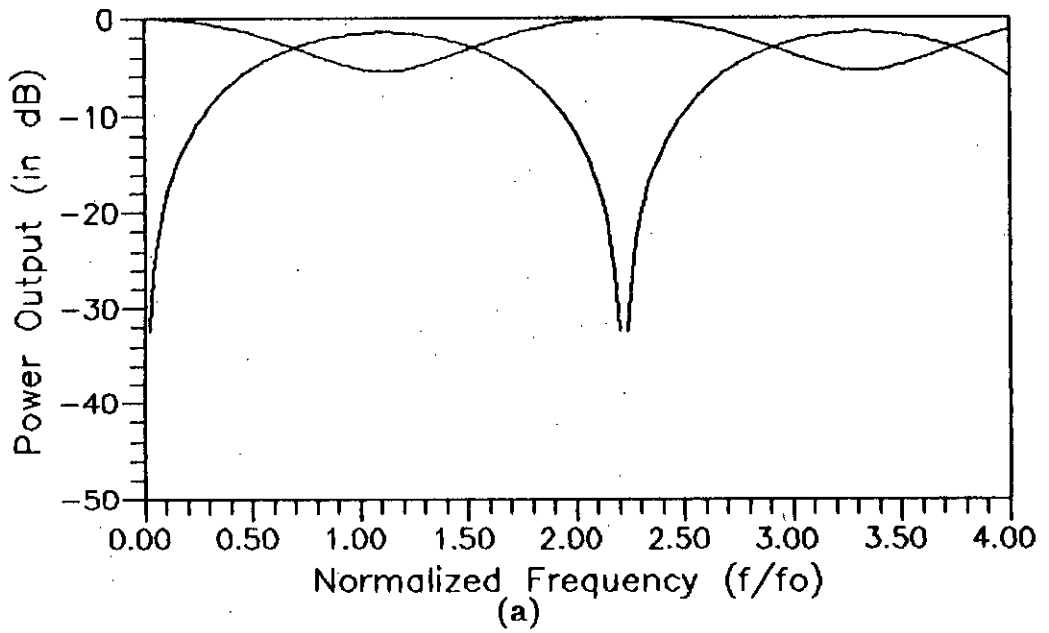


(a)



(b)

Figure 4.5 Characteristics of a diplexer: (a) *power vs. frequency*, and (b) *relative phase vs. frequency* plots with $\underline{e}^t = [1.0 \ 0.5 \ -0.2 \ 6.0]$.



(b)

Figure 4.6 Characteristics of a diplexer: (a) *power vs. frequency*, and (b) *relative phase vs. frequency* plots with $\mathbf{e}^t = [0.75 \ 0.5 \ -0.2 \ 6.0]$.

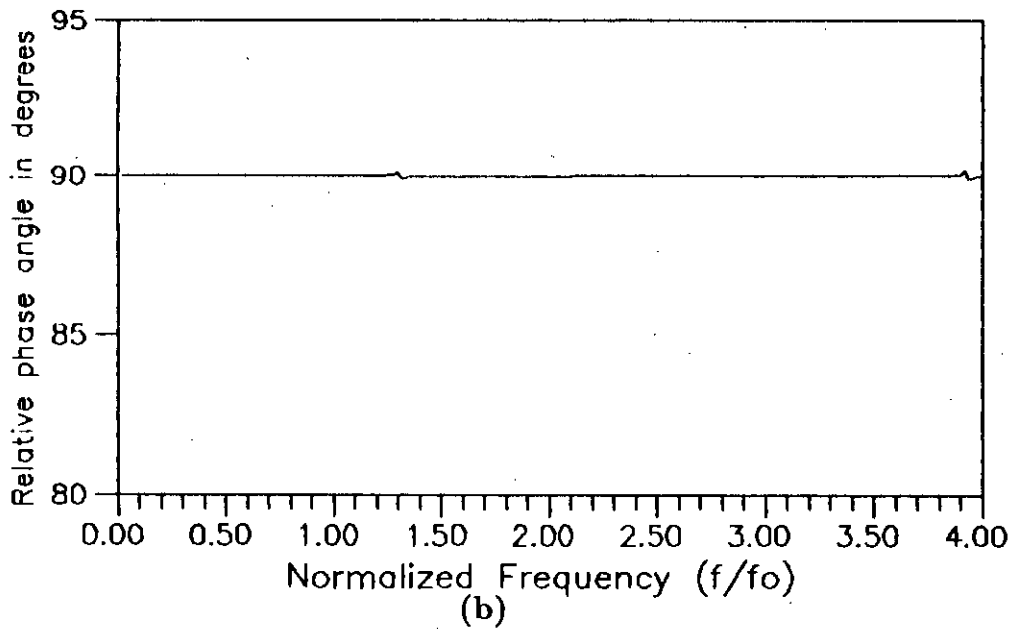
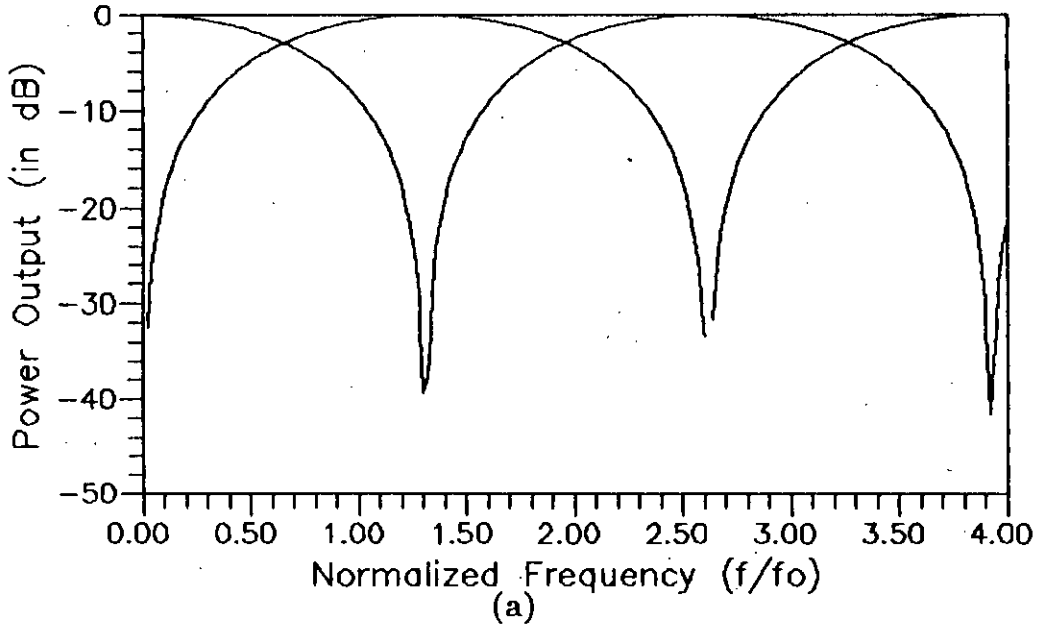


Figure 4.7 Characteristics of a diplexer: (a) *power vs. frequency*, and (b) *relative phase vs. frequency* plots with $e^t = [0.5 \ 0.5 \ -0.2 \ 6.0]$.

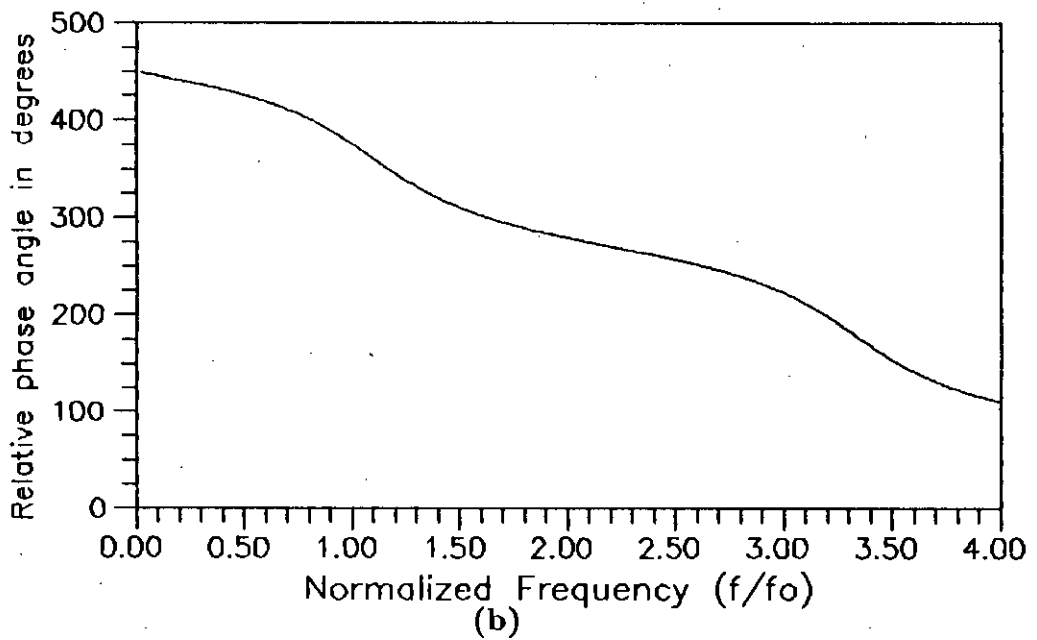
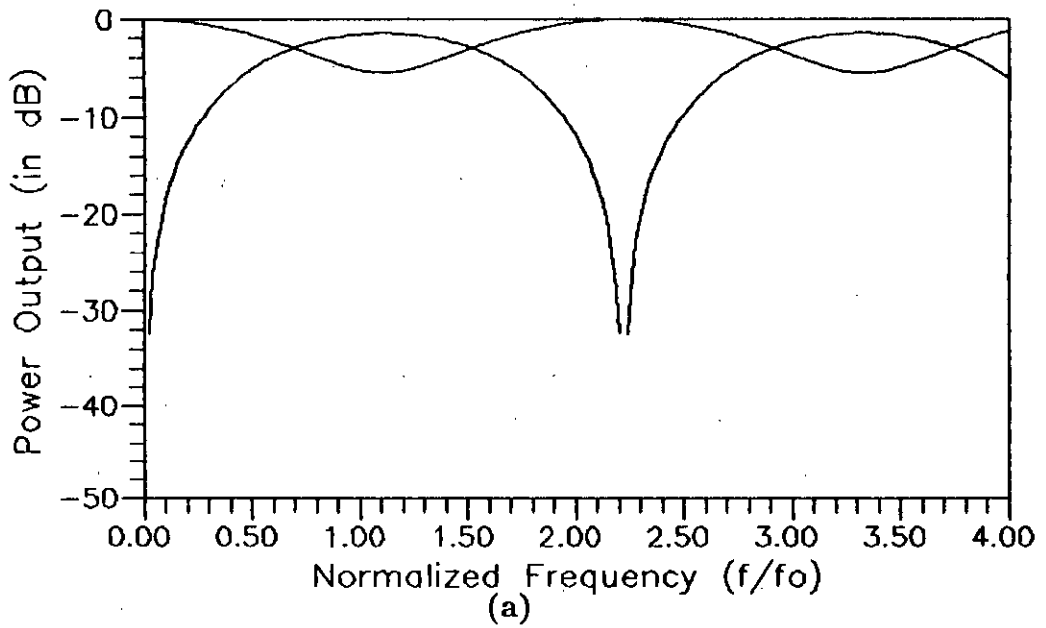


Figure 4.8 Characteristics of a diplexer: (a) *power vs. frequency*, and (b) *relative phase vs. frequency* plots with $\underline{e}^t = [0.25 \ 0.5 \ -0.2 \ 6.0]$.

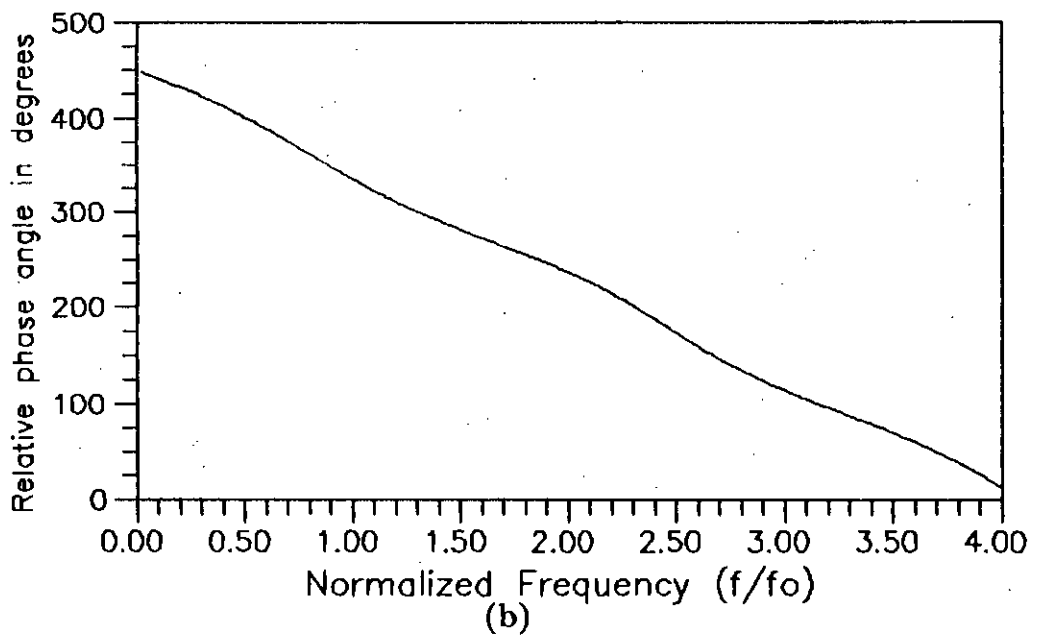
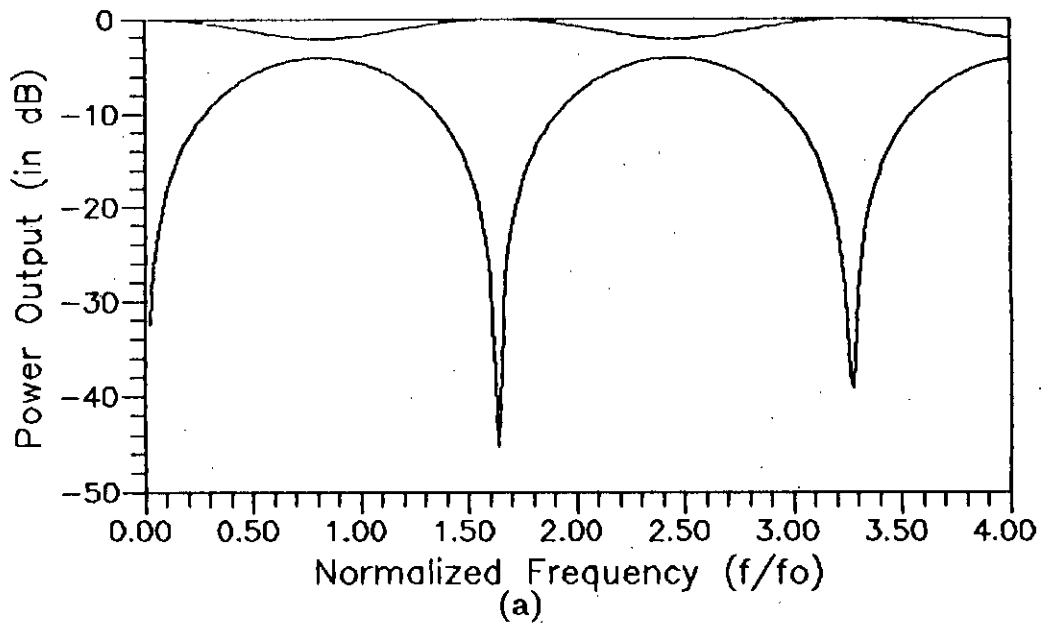


Figure 4.9 Characteristics of a diplexer: (a) *power vs. frequency*, and (b) *relative phase vs. frequency* plots with $\underline{e}^t = [0 \ 0.5 \ -0.2 \ 6.0]$.

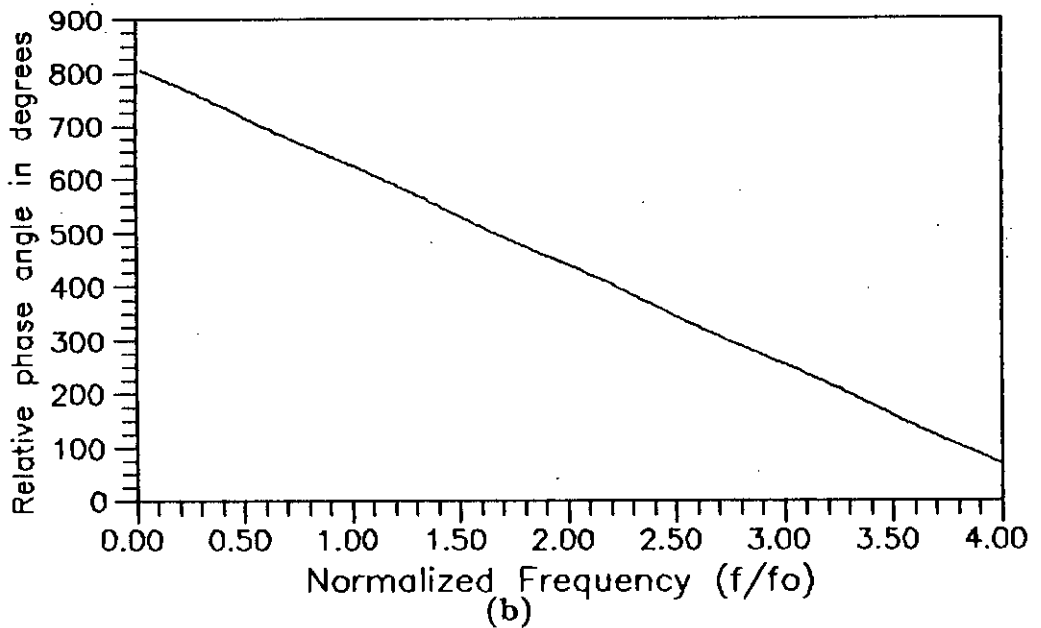
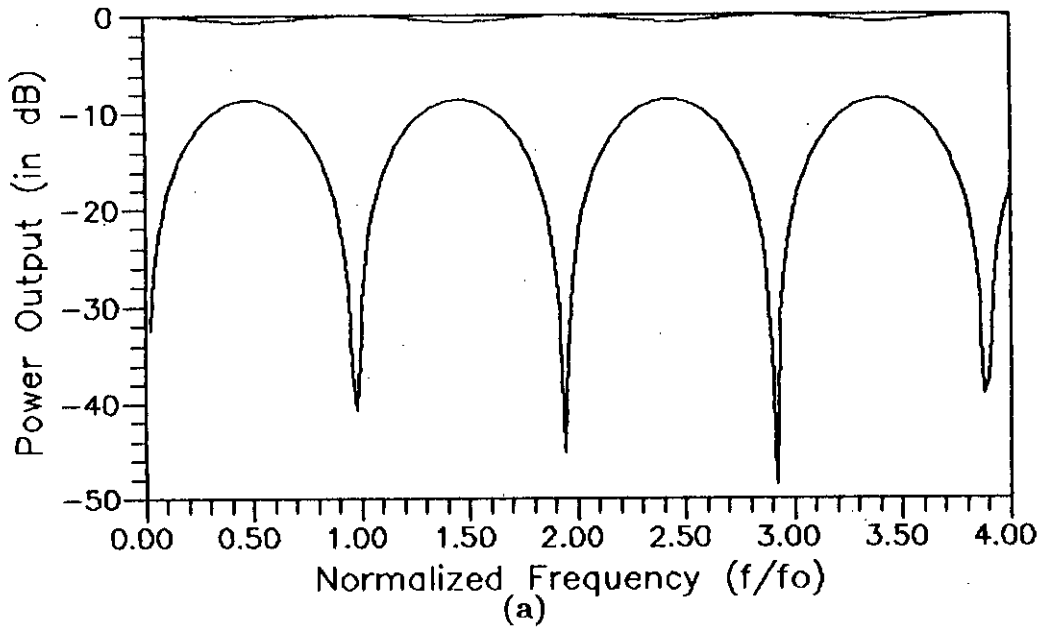


Figure 4.10 Characteristics of a diplexer: (a) power vs. frequency, and (b) relative phase vs. frequency plots with $\underline{e}^t = [0.5 \ 1.5 \ -0.2 \ 6.0]$.

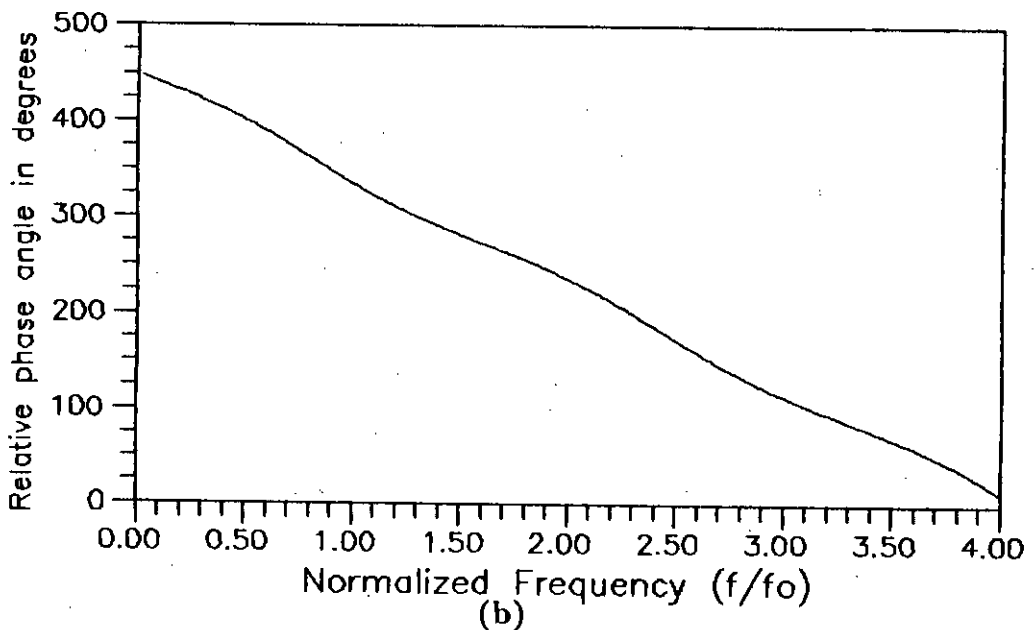
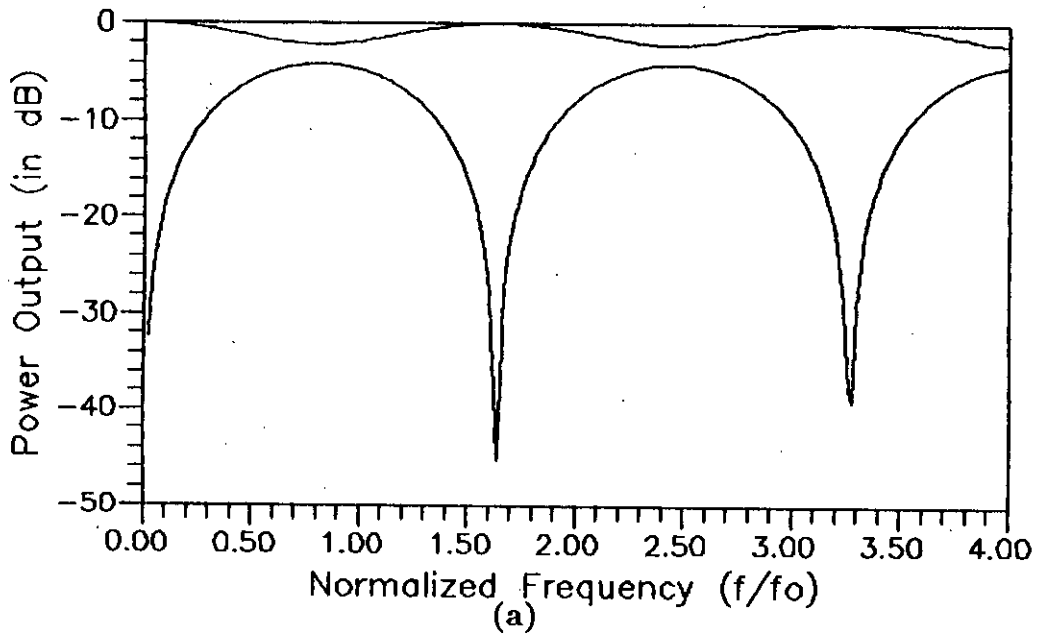


Figure 4.11 Characteristics of a diplexer: (a) power vs. frequency, and (b) relative phase vs. frequency plots with $e^t = [0.5 \ 1.0 \ -0.2 \ 6.0]$.

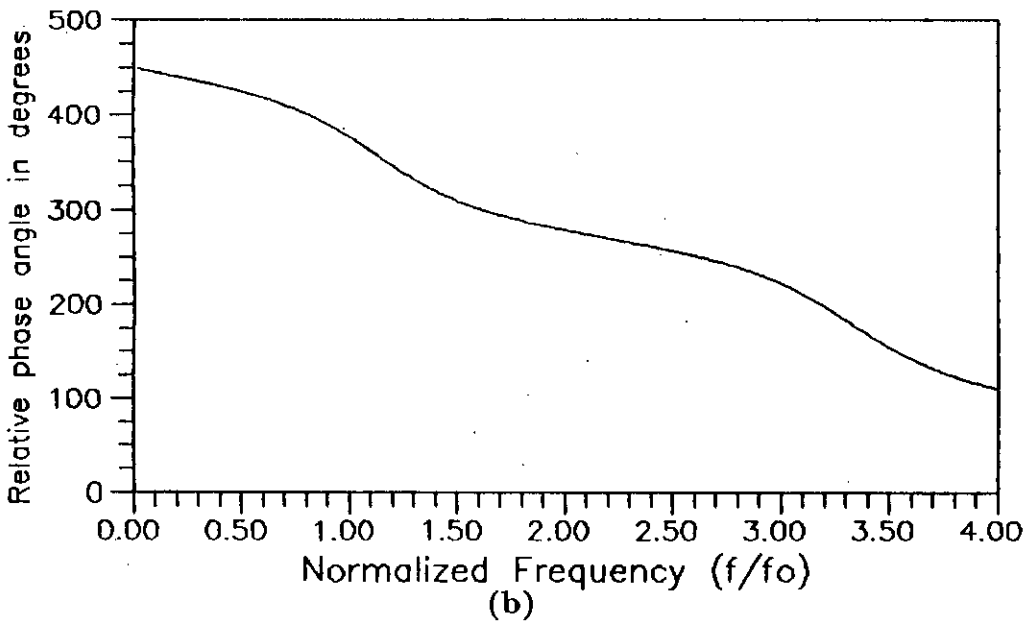
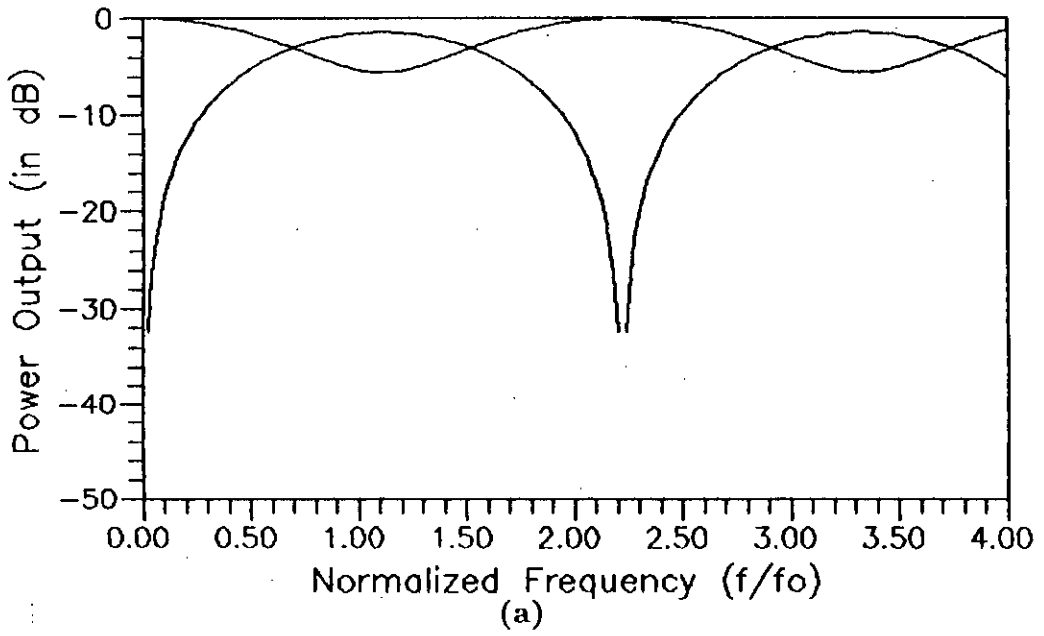


Figure 4.12 Characteristics of a diplexer: (a) *power vs. frequency*, and (b) *relative phase vs. frequency* plots with $\underline{e}^t = [0.5 \ 0.75 \ -0.2 \ 6.0]$.

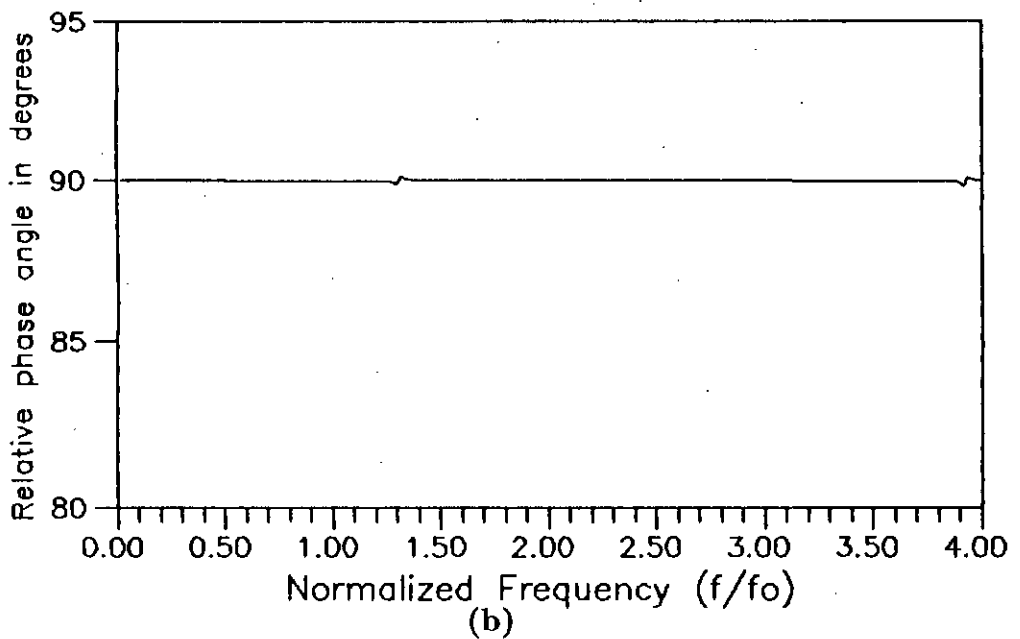
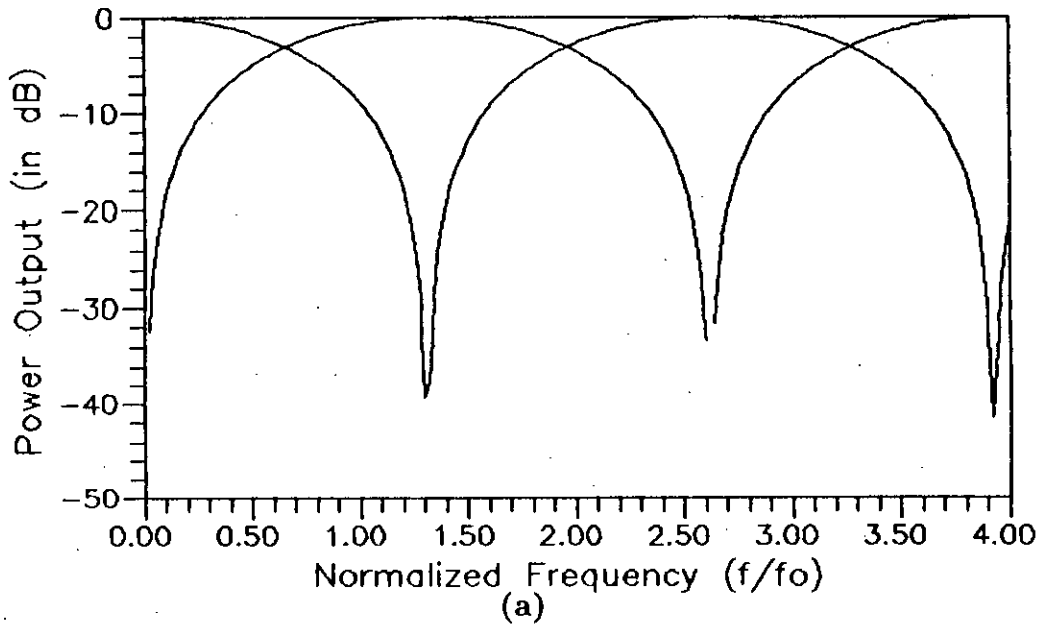
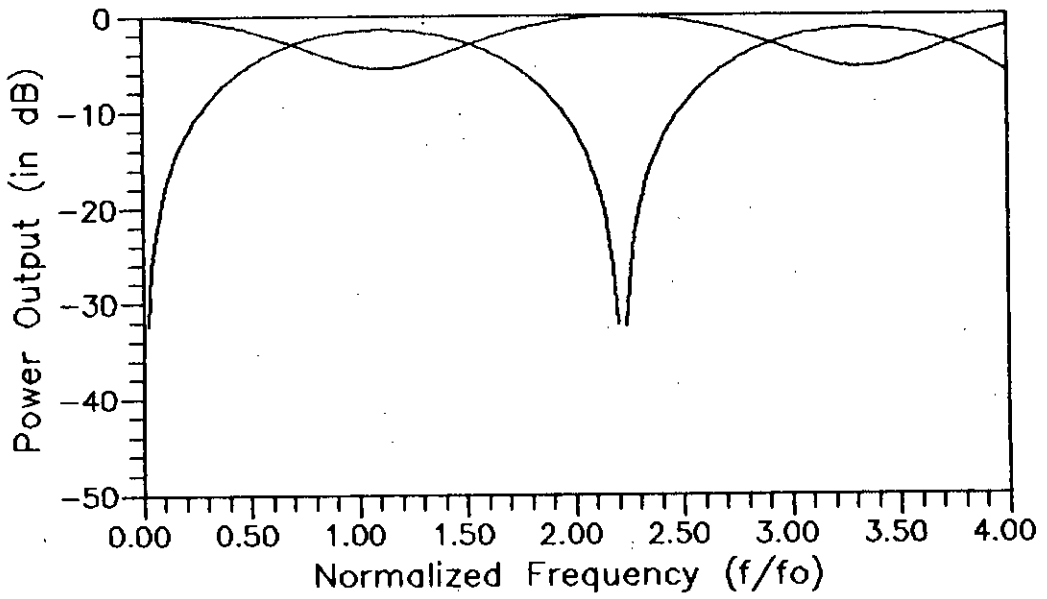
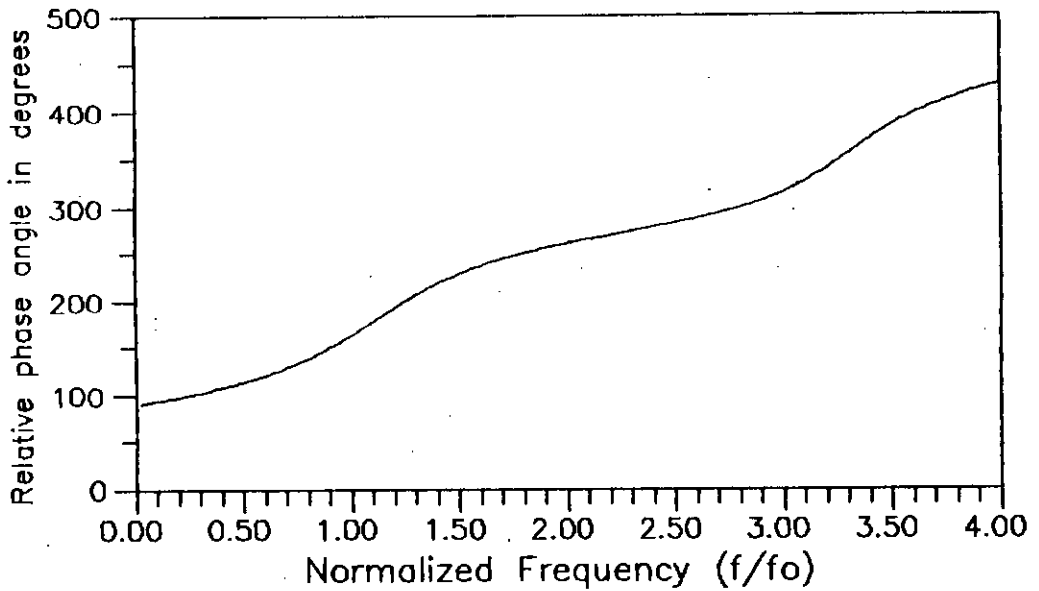


Figure 4.13 Characteristics of a diplexer: (a) *power vs. frequency*, and (b) *relative phase vs. frequency* plots with $\underline{e}^t = [0.5 \ 0.5 \ -0.2 \ 6.0]$.



(a)



(b)

Figure 4.14 Characteristics of a diplexer: (a) *power vs. frequency*, and (b) *relative phase vs. frequency* plots with $\underline{e}^t = [0.5 \ 0.25 \ -0.2 \ 6.0]$.

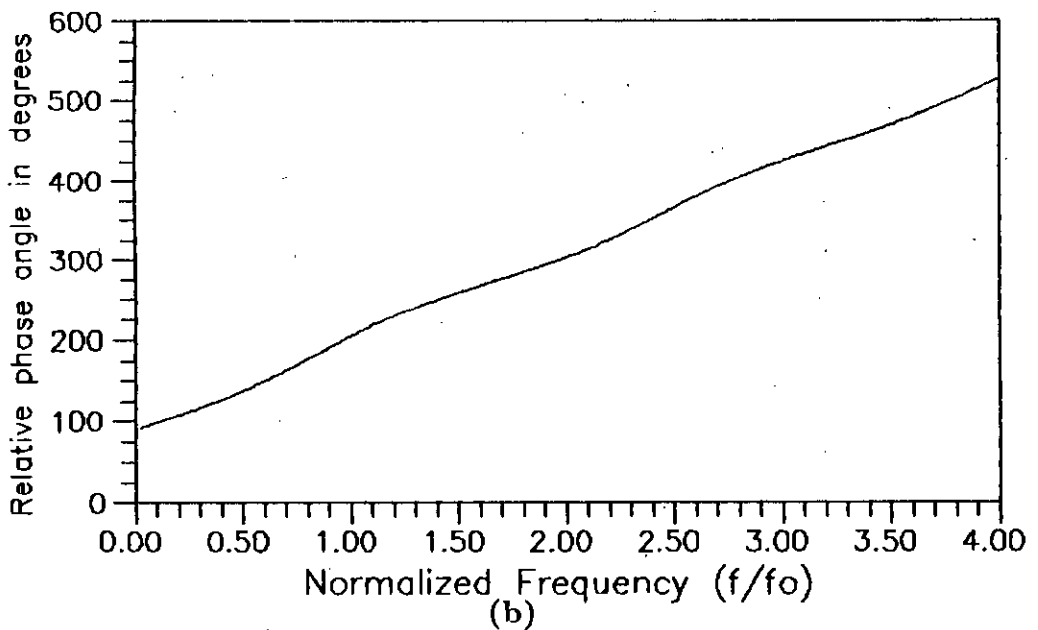
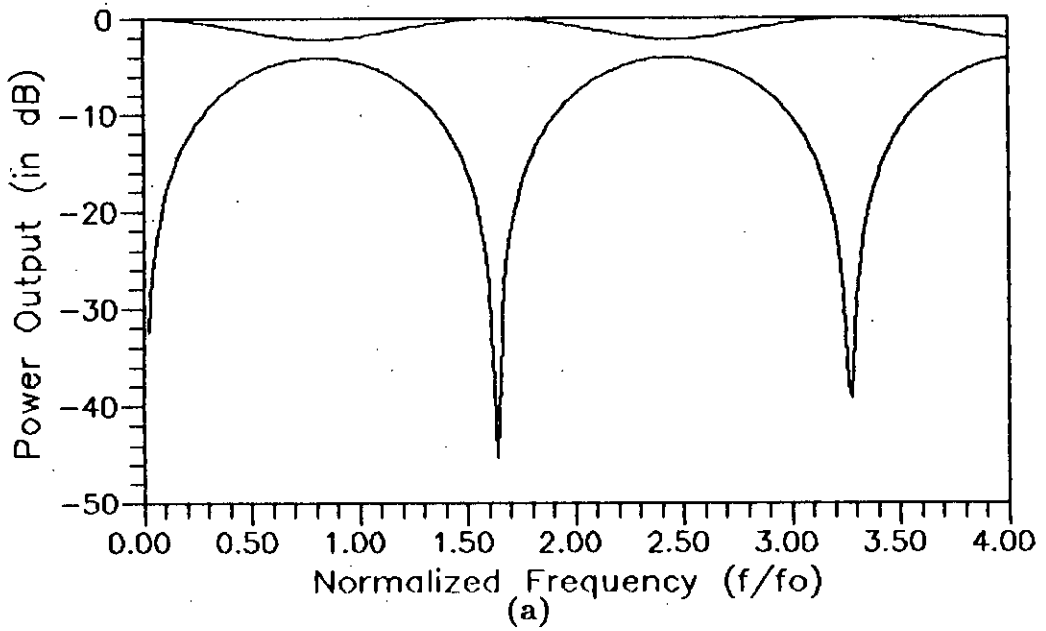


Figure 4.15 Characteristics of a diplexer: (a) *power vs. frequency*, and (b) *relative phase vs. frequency* plots with $\underline{e}^t = [0.5 \ 0 \ -0.2 \ 6.0]$.

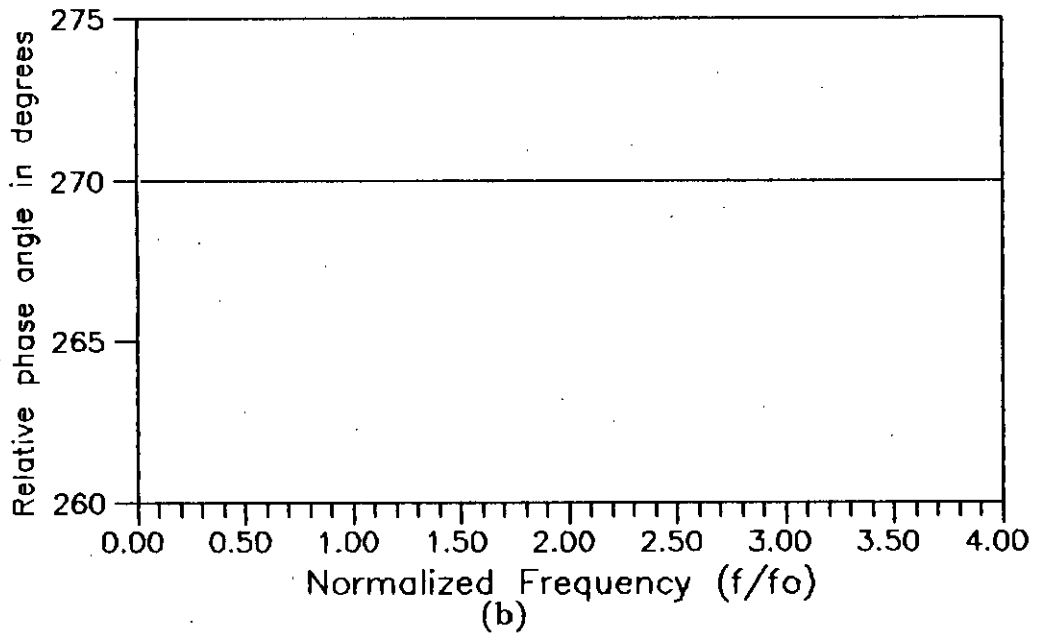
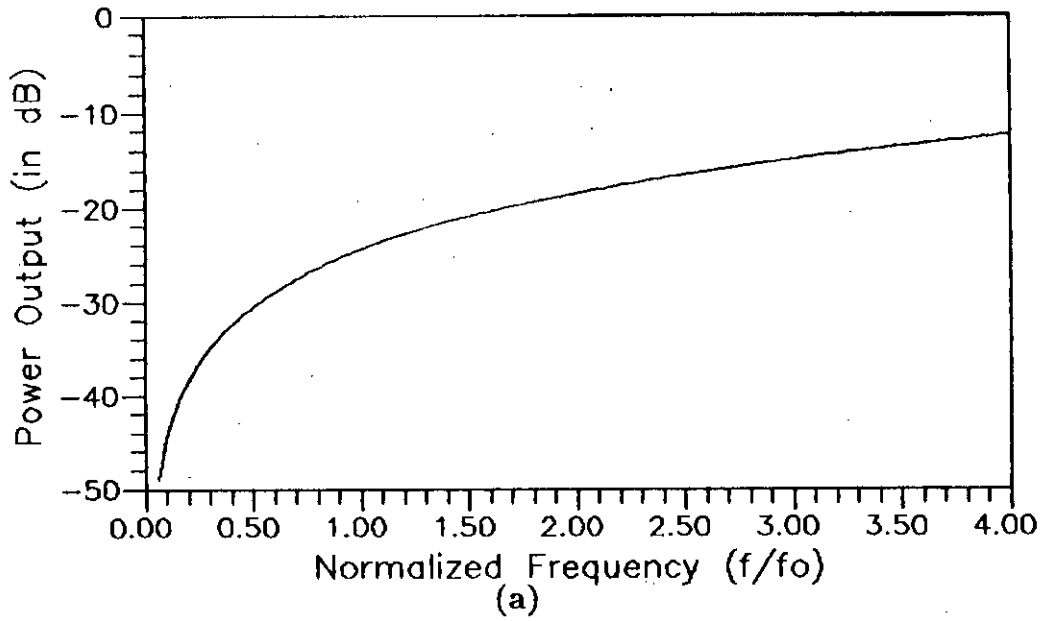


Figure 4.16 Characteristics of a diplexer: (a) *power vs. frequency*, and (b) *relative phase vs. frequency* plots with $\underline{e}^t = [0.5 \ 0 \ -0.01 \ 6.0]$.

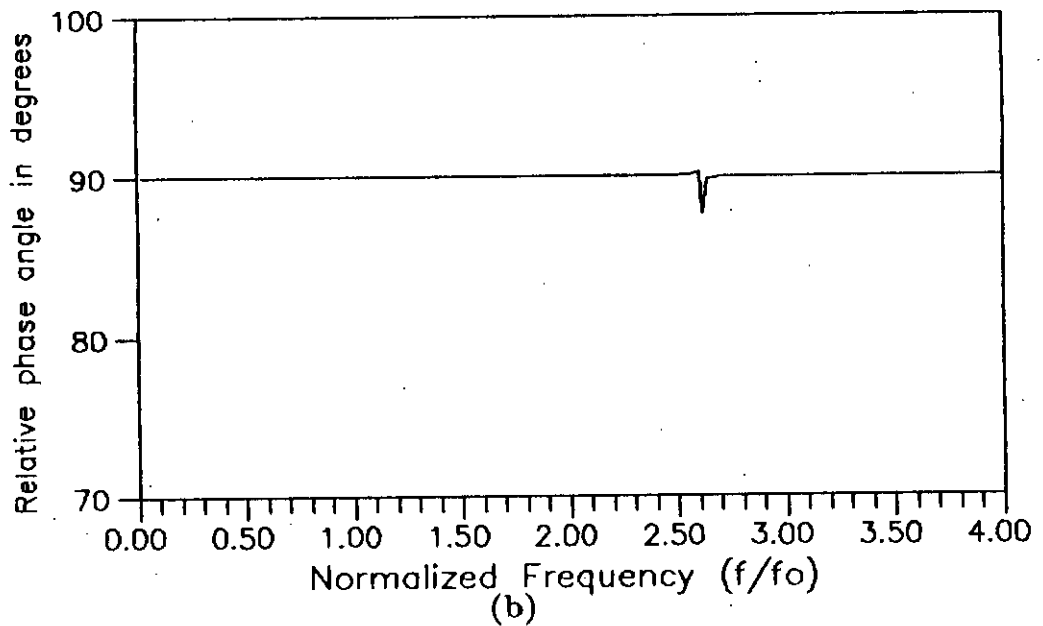
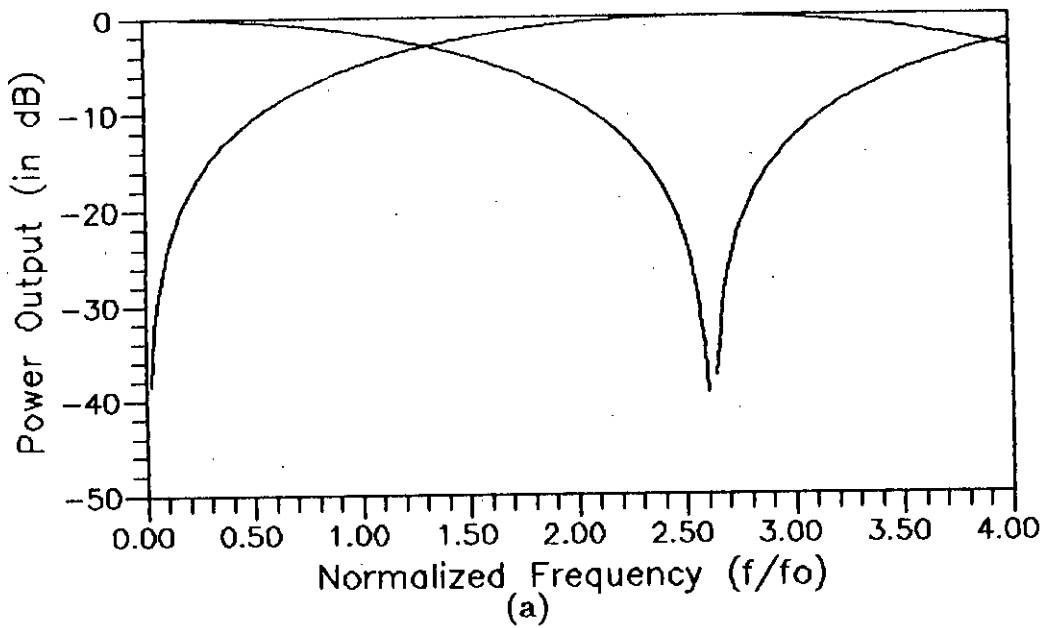


Figure 4.17 Characteristics of a diplexer: (a) *power vs. frequency*, and (b) *relative phase vs. frequency* plots with $\underline{e}^t = [0.5 \ 0 \ -0.1 \ 6.0]$.

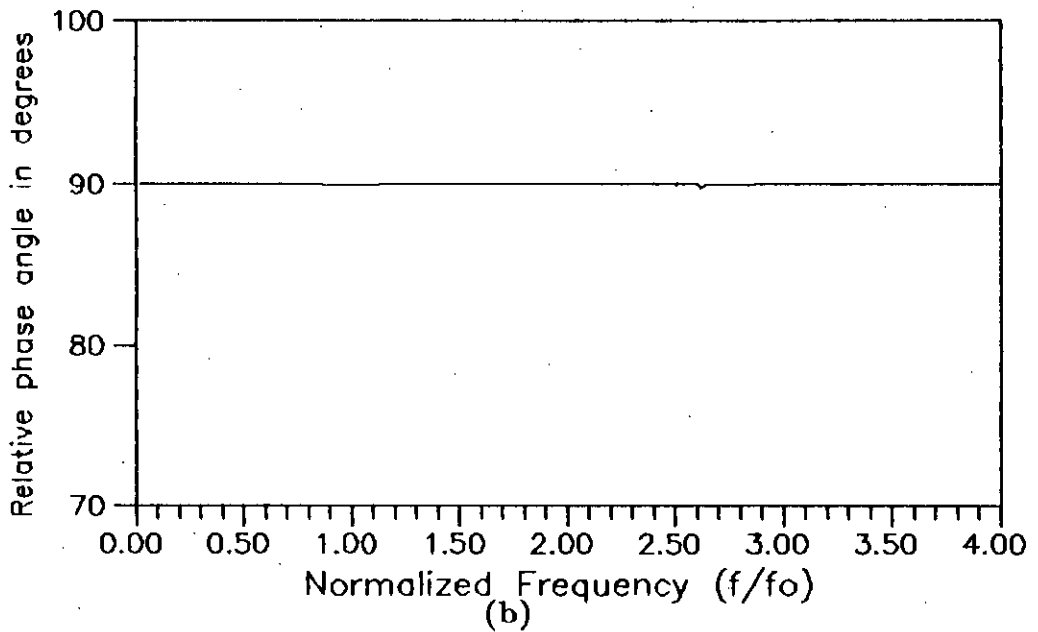
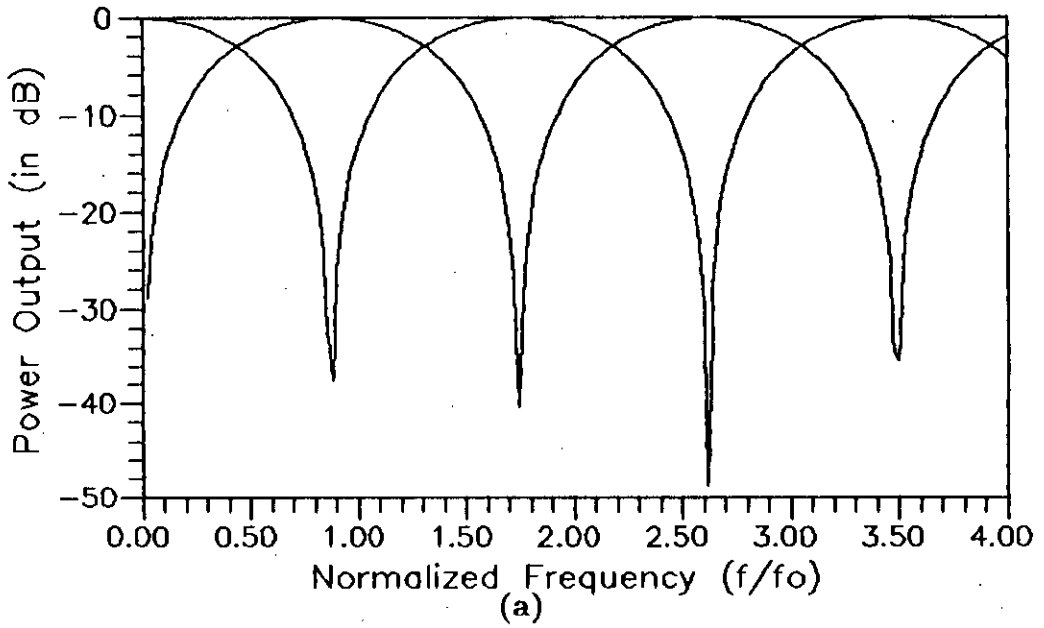


Figure 4.18 Characteristics of a diplexer: (a) *power vs. frequency*, and (b) *relative phase vs. frequency* plots with $\underline{e}^t = [0.5 \ 0 \ -0.3 \ 6.0]$.

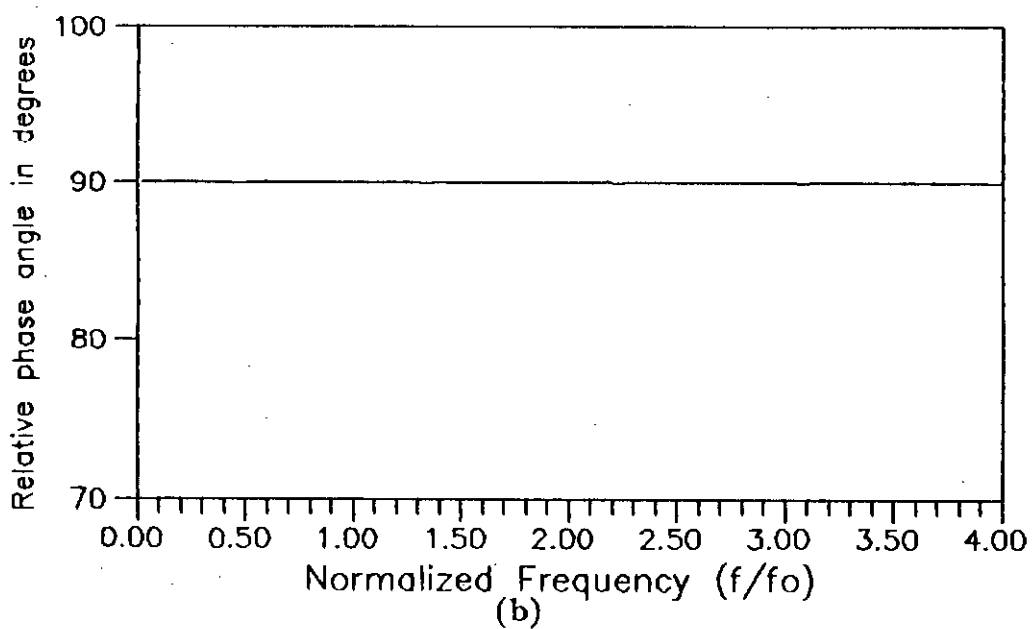
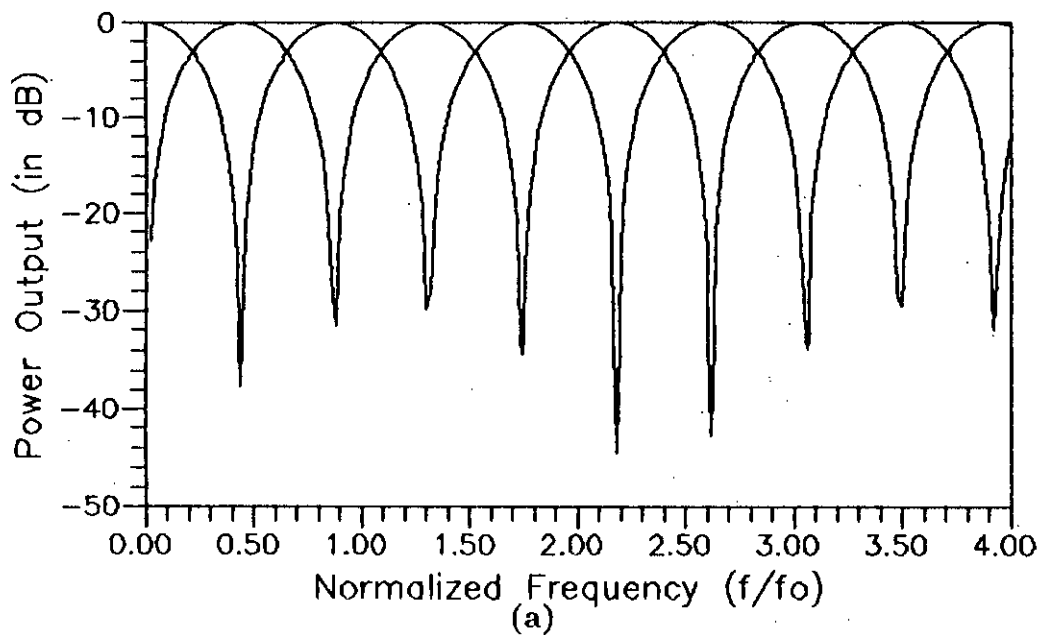


Figure 4.19 Characteristics of a diplexer: (a) power vs. frequency, and (b) relative phase vs. frequency plots with $\underline{e}^t = [0.5 \ 0 \ -0.6 \ 6.0]$.

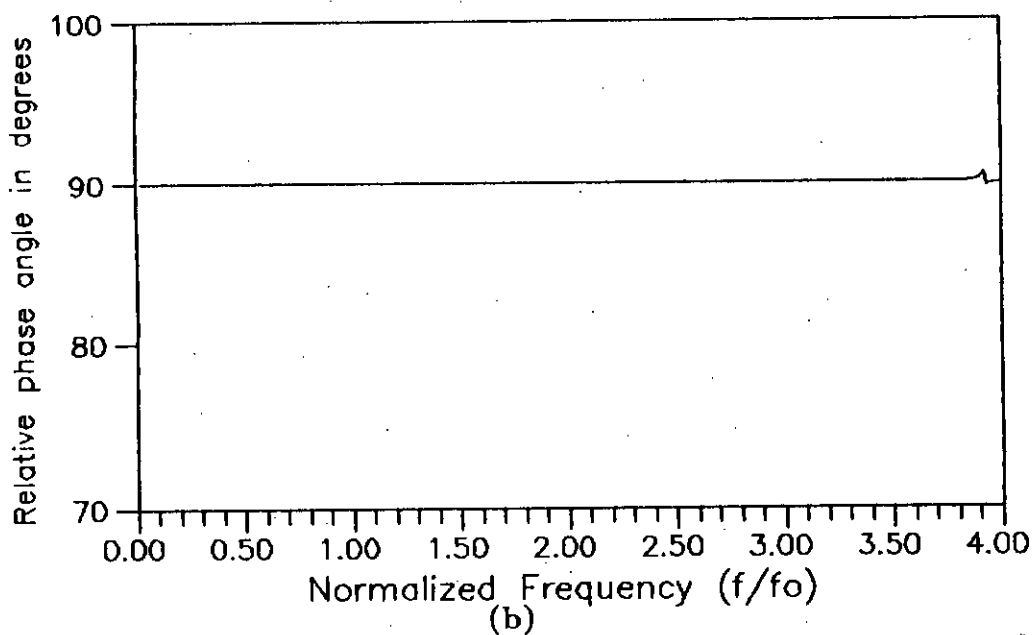
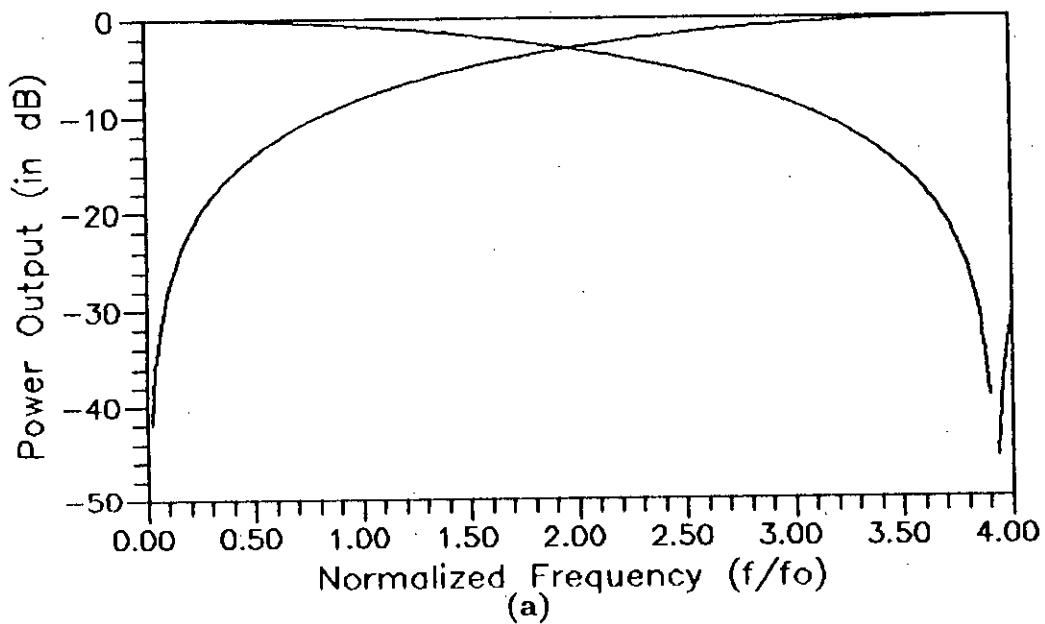


Figure 4.20 Characteristics of a diplexer: (a) *power vs. frequency*, and (b) *relative phase vs. frequency* plots with $\underline{e}^t = [0.5 \ 0 \ -0.2 \ 2.0]$.

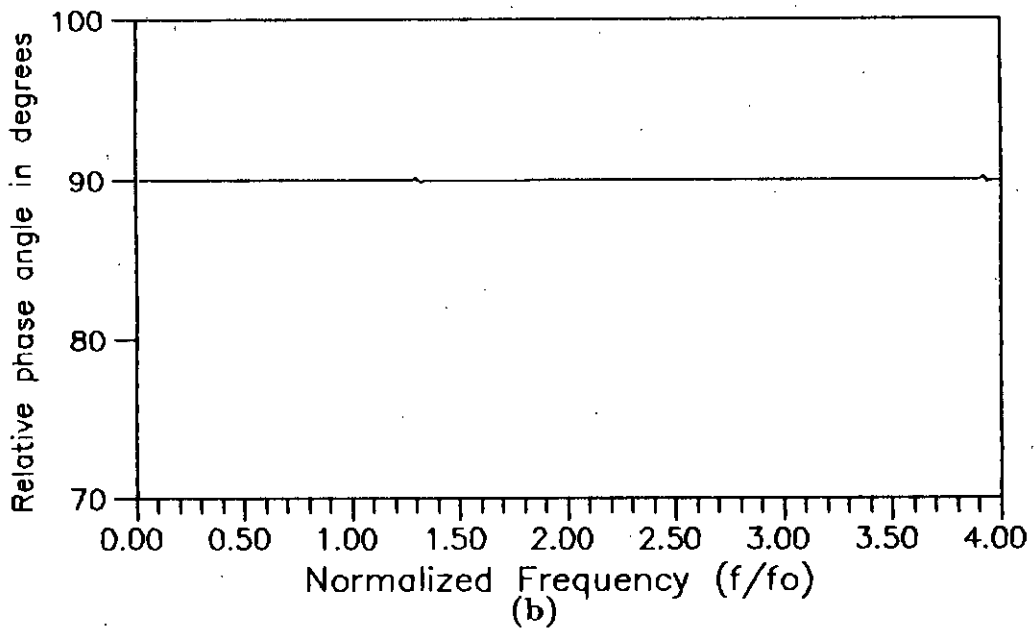
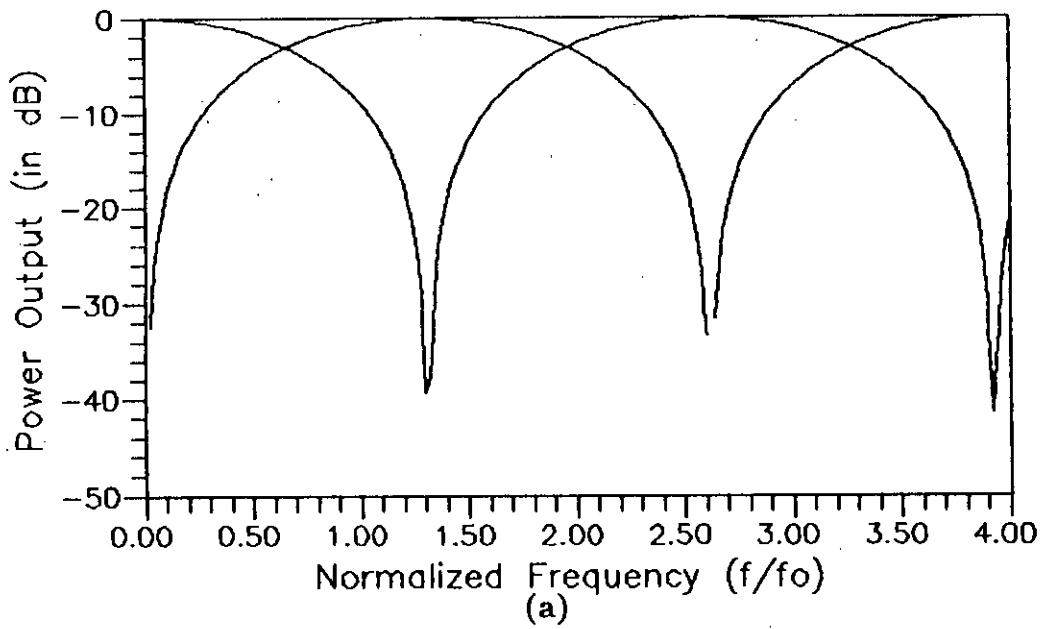


Figure 4.21 Characteristics of a diplexer: (a) *power vs. frequency*, and (b) *relative phase vs. frequency* plots with $\underline{e}^t = [0.5 \ 0 \ -0.2 \ 6.0]$.

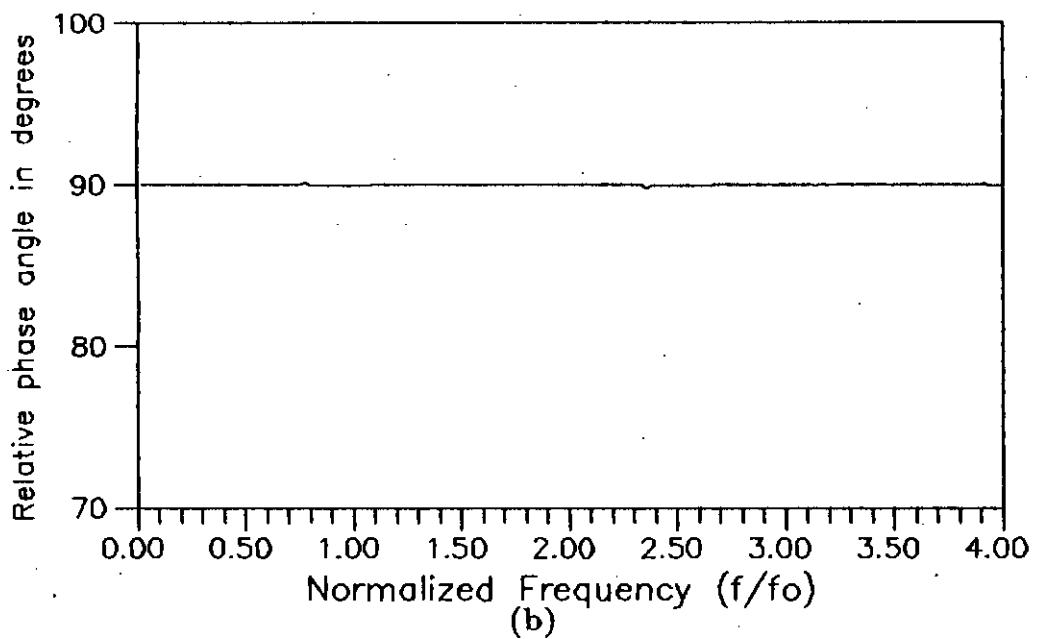
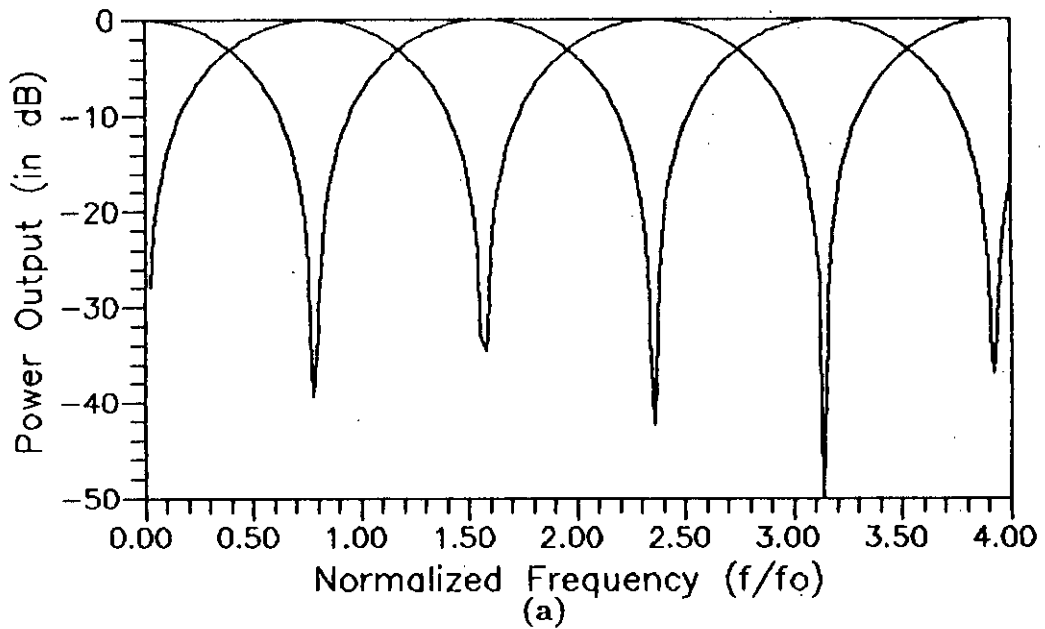


Figure 4.22 Characteristics of a diplexer: (a) power vs. frequency, and (b) relative phase vs. frequency plots with $e^t = [0.5 \ 0 \ -0.2 \ 10.0]$.

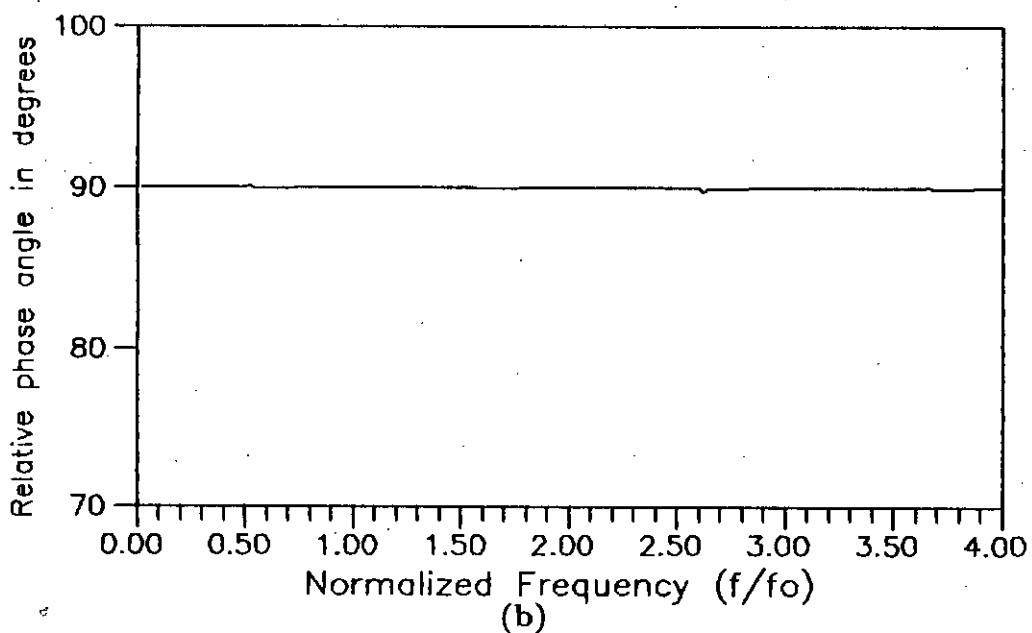
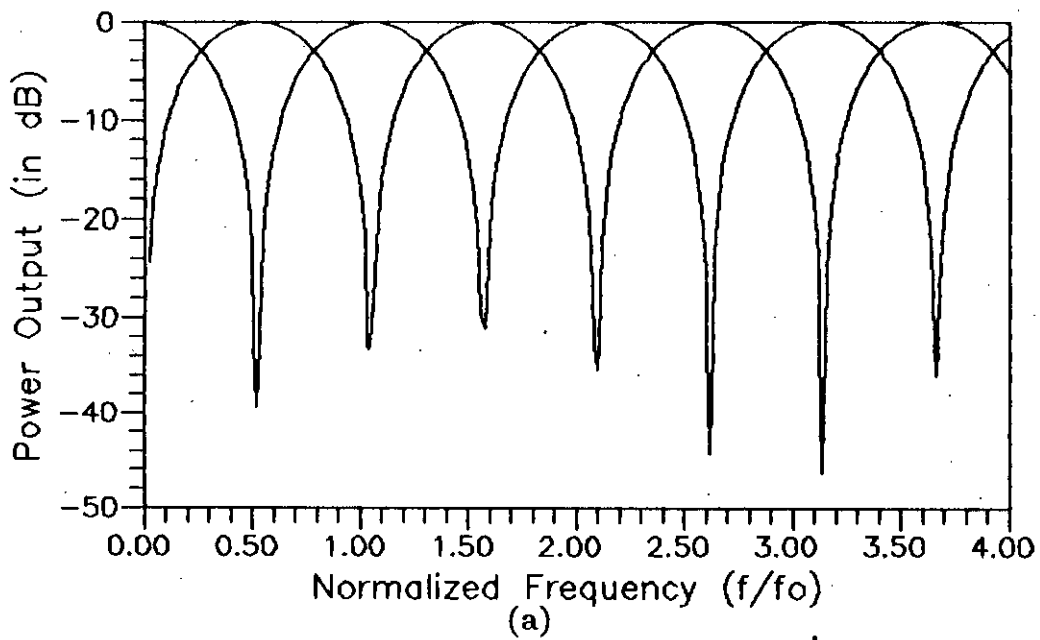


Figure 4.23 Characteristics of a diplexer: (a) *power vs. frequency*, and (b) *relative phase vs. frequency* plots with $\underline{e}^t = [0.5 \ 0 \ -0.2 \ 15.0]$.

4.6 Starting value of the \underline{e} vector

In every algorithms for optimization it is a vital problem to choose a starting point. The search for minimum or maximum is started from this point. If the starting point is chosen badly, not only the search takes longer time, but in case of a complex function the search may also stuck in a valley or pothole. So, it is very important to select a good starting point.

At the beginning of optimization a starting \underline{e} vector is required for initial computation of power. Selection of a suitable starting \underline{e} vector makes it easier to find the optimized \underline{e} vector reliably and quickly. The starting \underline{e} vector can not be taken arbitrarily. It should be chosen so that the coupling of peak power between two lines of the diplexer occurs in the vicinity of the two selected frequency bands. So, while selecting a starting \underline{e} vector the power characteristics of a diplexer should be plotted with several sets of \underline{e} vectors and the one which fits closest to the requirement should be chosen.

While selecting a starting \underline{e} vector the relationship of the power characteristics with the elements of \underline{e} vector should be understood. The effect of the elements of \underline{e} vector on the power against frequency characteristics discussed in section 4.5 gives an idea where the starting point may be selected. The idea about selecting a starting \underline{e} vector for this work is obtained from a work on the design of microwave forward directional couplers [6]. After making few modifications of the \underline{e} vector used in reference [6] on the basis of the concept developed in section 4.5 a starting \underline{e} vector is chosen so that the power characteristics fit the two operating bands of the diplexer.

In this work the diplexer under consideration is desired to operate in the frequency bands of (1 – 1.3) and (2 – 2.3) GHz. Here two starting \underline{e} vectors are chosen for optimization. The 1st \underline{e} vector is chosen from the plots given in Figs. 4.4 – 4.23 which is the \underline{e} vector of figure 4.6.

The 1st starting \underline{e} vector: $\underline{e}^t = [0.75 \ 0.5 \ -0.2 \ 6.0]$.

The 2nd starting \underline{e} vector is chosen on the basis of the data given in reference [6].

The 2nd starting \underline{e} vector: $\underline{e}^t = [0.646 \ 0.5523 \ -0.2 \ 6.7]$.

The optimization program is individually operated with both of these starting \underline{e} vectors. It will be seen that the optimization program will optimize both the \underline{e} vectors to the same minimum error level (section 4.10).

4.7 Optimization of the \underline{e} vector

The characteristics of the diplexer under consideration depends on the elements of the \underline{e} vector. In this work the \underline{e} vector contains four elements. In other words the \underline{e} vector is a four-variable function. The characteristics of the diplexer may be controlled by changing the values of the elements of the \underline{e} vector. So to obtain the desired power characteristics in two different frequency bands, the function that requires to be optimized is the \underline{e} vector.

The method used for optimization in this work has been described in section 4.4. For a diplexer the \underline{e} vector is a four-variable function and all the four variables are required to be changed to obtain maximum power in two desired band of frequencies. Before starting optimization, two bands of frequencies (within which optimization is performed) and a reference power level (with which output power is compared) are selected.

The starting \underline{e} vector used in this work is given in section 4.6. After selecting the starting \underline{e} vector power is computed in the two selected frequency bands and this computed power is subtracted from the reference power level to obtain the *error function* as described in section 4.8. The goal of the optimization in this work is to minimize this error function so that maximum coupling of power can be achieved in the selected frequency bands. To minimize this error function the method of

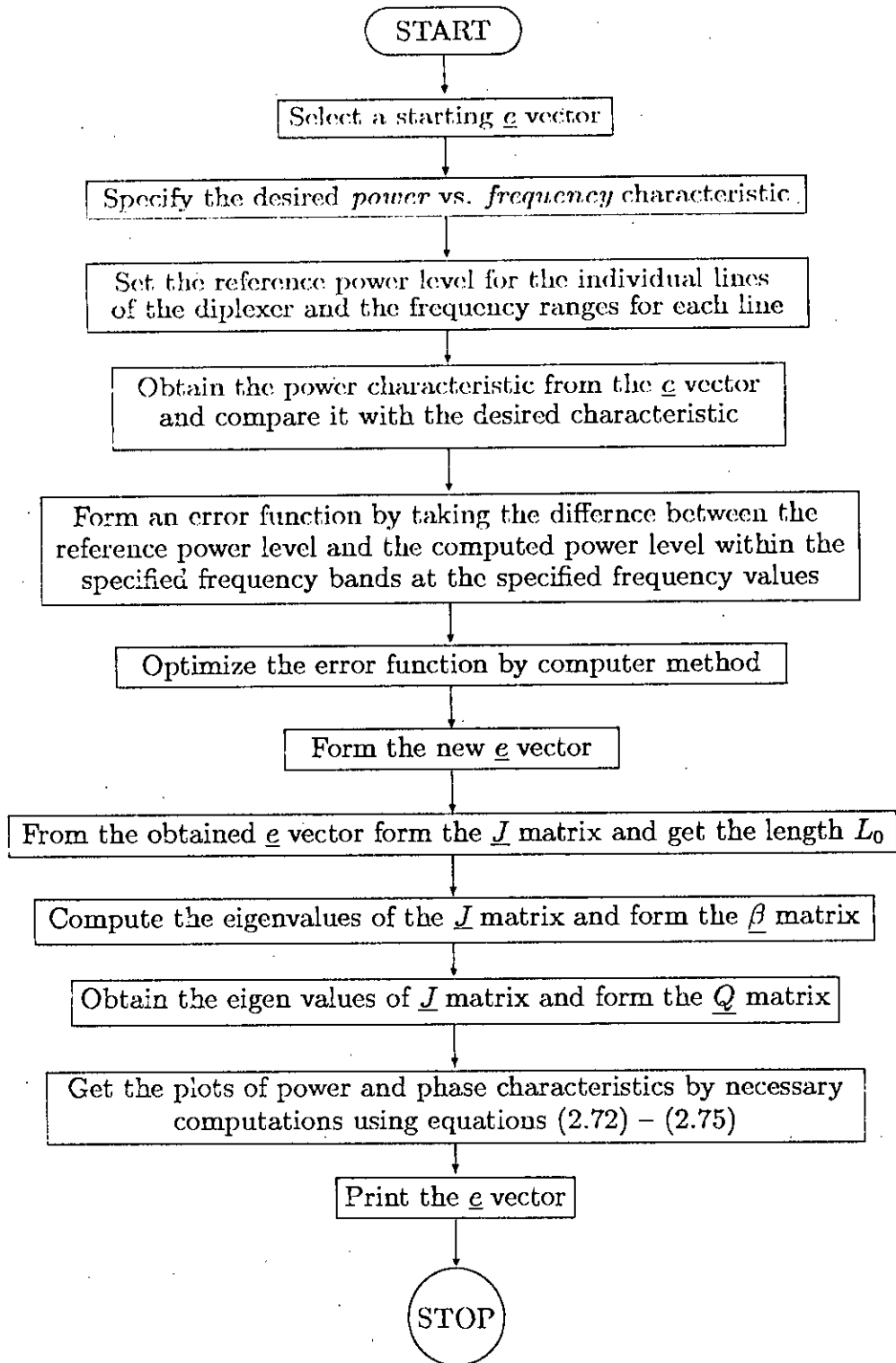


Figure 4.25 Flow-chart showing the sequence of computations for obtaining an optimized $\underline{\epsilon}$ vector of the required diplexer.

optimization described in section 4.4 is followed.

The optimization of \underline{e} vector is a major step in designing the diplexer under consideration. After optimizing the \underline{e} vector, the methods of scaling and shifting the \underline{J} matrix (described in section 3.4) are applied to get realizable physical dimensions of the diplexer. The sequence of computations required for obtaining an optimized \underline{e} vector is shown in the flow-diagram of Fig 4.25. The optimized \underline{e} vector thus obtained is latter used for computing the physical dimensions of the required diplexer.

4.8 Computation of the error function

It may be seen from figure 4.3 that before beginning optimization a reference level is selected so that the deviation of the response from this reference level can be computed. In an optimization procedure, computation of this deviation or error is very important. The total error computed within desired limits is known as *error function*. The process of computing the error function of a diplexer is discussed in this section.

The general process of computing an error function of any function $f(x)$ is shown in figure 4.26. In case of a diplexer, two operating bands of frequencies – one for channel-1 and the other for channel-2 are selected within which the diplexer is desired to operate (figure 4.27). For channel-1 let the lower and the upper frequency boundary be f_1 and f_2 . Similarly let the lower and upper frequency boundary be respectively f_3 and f_4 . The area enclosed by the reference line and the power-curve between frequency range f_1 and f_2 is computed to find the error in channel-1 (say, ER_1). Similarly error for channel-2 (say, ER_2) is also computed by finding the enclosed area between the reference line and the power curve of channel-2 within the boundary f_3 and f_4 . The total error is obtained by adding ER_1 and ER_2 .

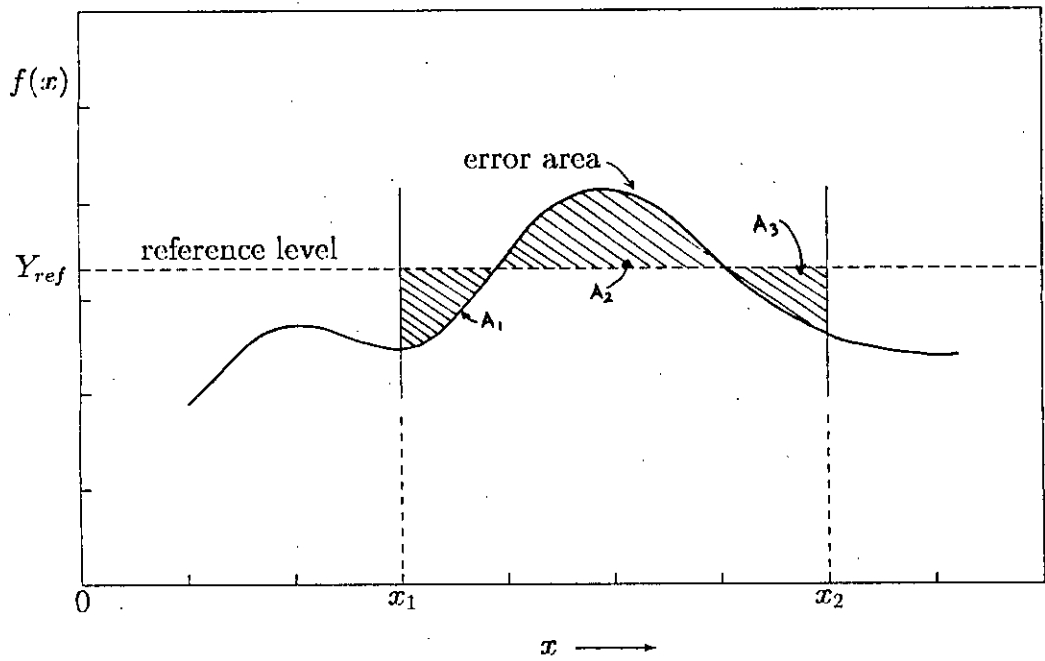


Figure 4.26 Computing the *error function* of a general function $f(x)$ by finding the error area (indicated by hatched lines). The total error is equal to the sum of total area, i.e., $\text{error} = (A_1 + A_2 + A_3) = \int_{x_1}^{x_2} |Y_{ref} - f(x)| dx$.

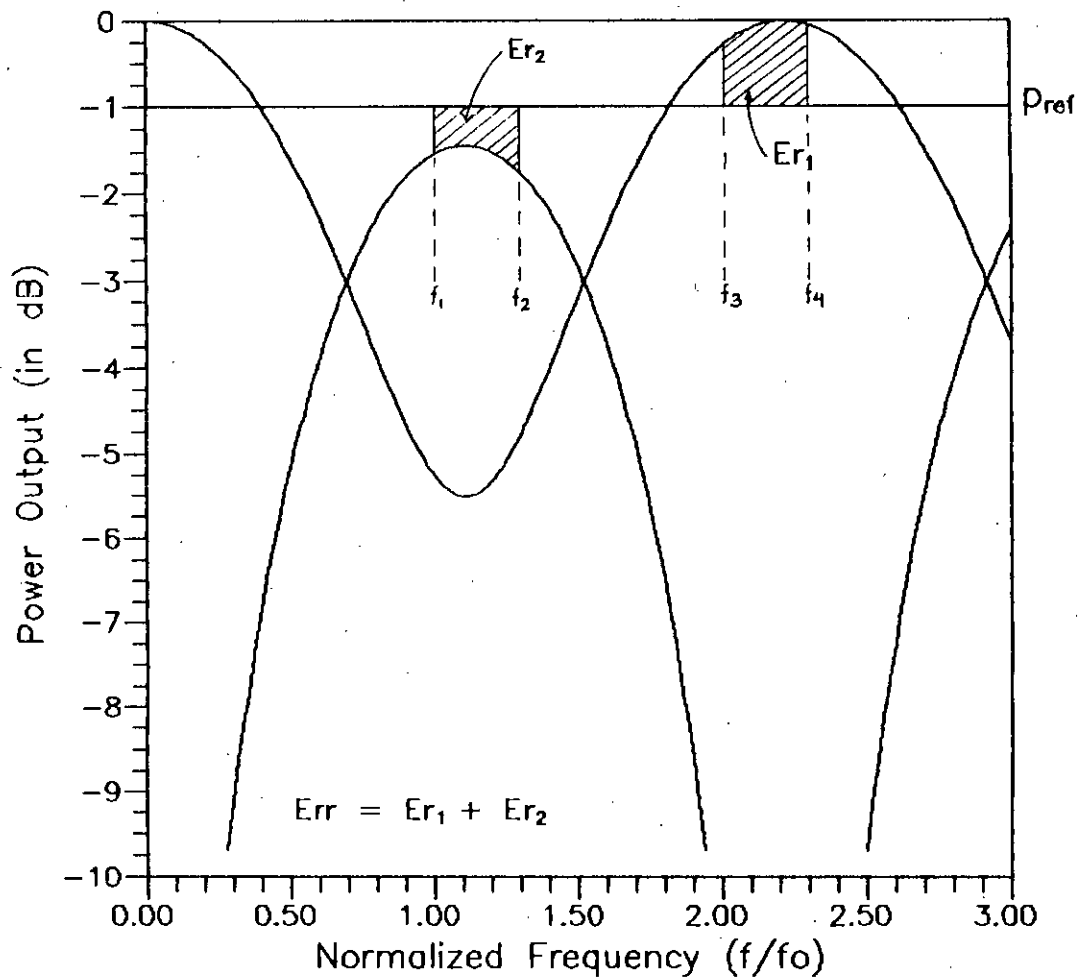


Figure 4.27 Error function of a diplexer is computed by adding the error area enclosed by the the power curve, reference line, and the lower and upper band edge rfrequencies. The error area are indicated by the hatched lines. The total error $Err = Er_1 + Er_2$.

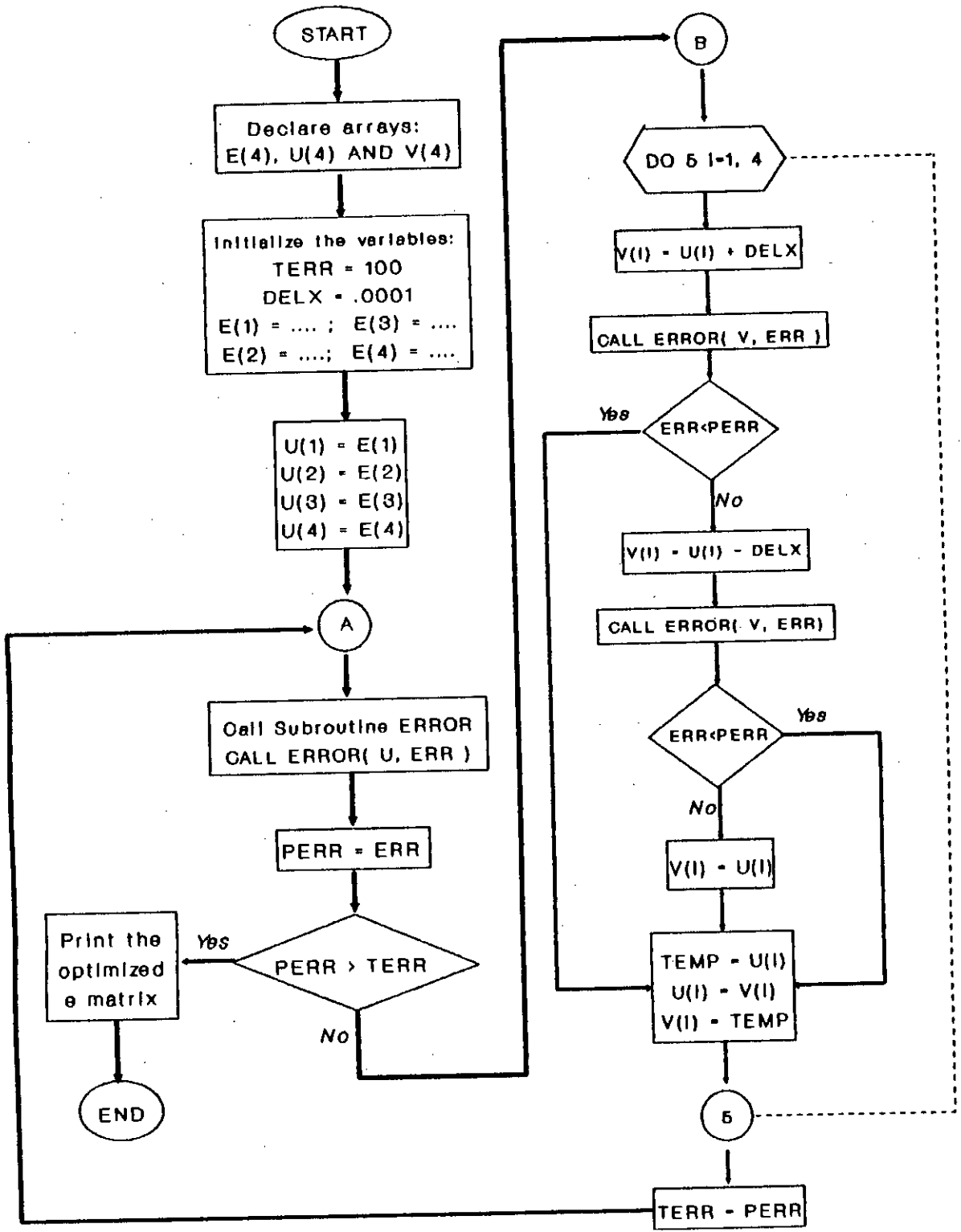


Figure 4.28 Flow-chart of the optimization program OPT.FOR.

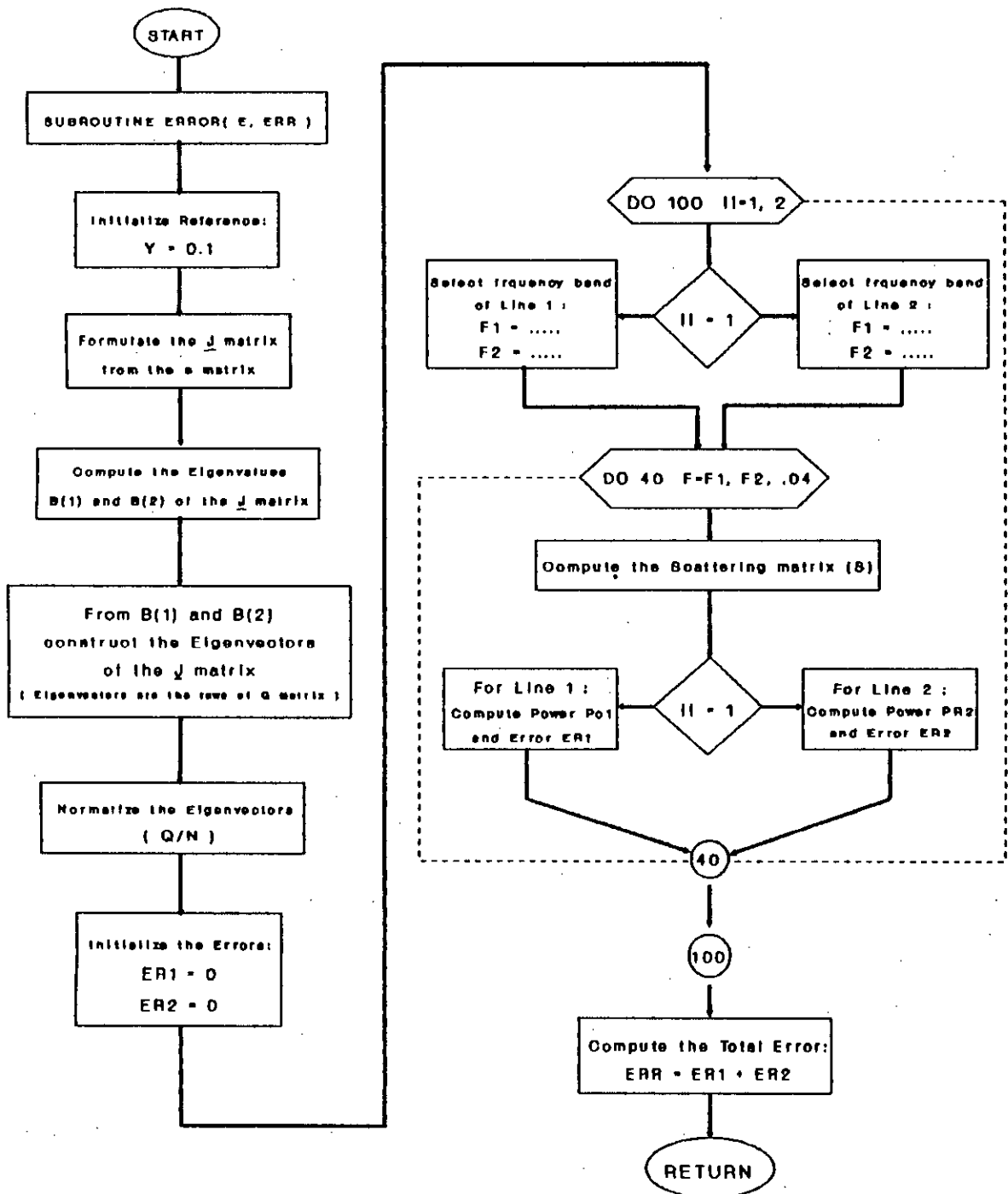


Figure 4.29 Flowchart of the subroutine ERROR.

The errors can be computed by following equations. Error of channel-1 is:

$$ER_1 = \int_{f_1}^{f_2} |Y_{ref} - P_{1out}| df \quad (4.15)$$

Error of channel-2 is:

$$ER_2 = \int_{f_1}^{f_2} |Y_{ref} - P_{2out}| df \quad (4.16)$$

So the net error is obtained by adding the error areas of the two individual channels.

$$\text{The total error, } ERR = ER_1 + ER_2 \quad (4.17)$$

This error is a function of \underline{e} vector and so the error can be minimized by manipulating the \underline{e} vector. The error is computed numerically with computer programs as a part of the main optimization program.

4.9 The Optimization program

The process of minimizing the error function described in the previous section is done with the help of a computer program which is developed for optimizing the diplexer characteristics. The program takes the known parameters of a diplexer (mentioned in section 5.10) and a starting \underline{e} vector as input and gives the optimized \underline{e} vector as output. This optimized \underline{e} vector gives the minimum error for a specified bands of frequencies and a chosen reference level.

The flow-chart of the main optimization program is shown in figure 4.28. The main program uses a subroutine named ERROR. This subroutine actually does the major portion of the job. The main program passes an \underline{e} vector to the subroutine ERROR. With this \underline{e} vector the subroutine computes eigenvalues, eigenvectors, scattering matrix and the output power. The output power thus obtained is then compared with the reference power level to find the error. The error area between

the computed power and the reference power level is obtained by the process of numerical integration. The flow diagram of the subroutine is shown in figure 4.29.

According to the steps shown in the flow charts (figures 4.28 – 4.29) a program (OPT.FOR) has been developed in FORTRAN. The listing of the program is given in the appendix-B. In the process of optimizing the \underline{e} vector, one has to repeatedly compute the power at different frequencies. The program for finding the power and phase characteristics of a diplexer is presented in appendix A. The number of iterations the program performs depends on the value of Δx (mentioned in section 4.4). The smaller the value of Δx the higher will be the number of iterations. If a very small value of Δx is taken, the number of iterations will be very high and the program will take longer time to run. Again if a large value of Δx is taken the accuracy of the search will be reduced.

In program OPT.FOR (given in appendix-B) there is an option to choose the value of Δx . There are also several other options for selecting the starting \underline{e} vector. Using this program one can reach same minimum point starting with different \underline{e} vectors.

4.10 Examples of optimization

The optimization program actually modifies the \underline{e} vector so that the minimum error (i.e., the maximum output) is obtained. The program starts with a set of pre-defined variables and a starting \underline{e} vector. In this section the optimization program is run with a set of sample data to see how the optimization program gradually changes the elements of the \underline{e} vector and minimize the error. when the minimum error is achieved, the program gives the optimized \underline{e} vector and terminates.

Here the optimization program is run with two different starting \underline{e} vectors as discussed in section 4.6.

The 1st starting \underline{e} vector: $\underline{e}^t = [0.75 \ 0.5 \ -0.2 \ 6.0]$

Table 4.1.a Data generated during the optimization of \underline{e} vector starting with $e^t = [.75 \ .5 \ -.2 \ 6.0]$. The \underline{e} vector, error and output power during the first 34 iterations are shown in this Table. The program used for generating these data is OPT.FOR given in appendix B.

Iteration	The \underline{e} Vector				Error	Power
1	0.750000	0.500000	-.200000	6.000000	14.449820	-1.708293
2	0.749250	0.500750	-.200750	6.000750	14.253240	-1.691223
3	0.748500	0.501500	-.201500	6.001500	14.059370	-1.674690
4	0.747750	0.502250	-.202250	6.002250	13.868180	-1.658703
5	0.747000	0.503000	-.203000	6.003000	13.679770	-1.643268
6	0.746250	0.503750	-.203750	6.003750	13.494120	-1.628390
7	0.745500	0.504500	-.204500	6.004500	13.311300	-1.614071
8	0.744750	0.505250	-.205250	6.005250	13.131360	-1.600330
9	0.744000	0.506000	-.206000	6.006001	12.954300	-1.587157
10	0.743250	0.506750	-.206750	6.006751	12.780180	-1.574572
11	0.742501	0.507500	-.207500	6.007501	12.609110	-1.562578
12	0.741751	0.508250	-.208250	6.008251	12.441050	-1.551184
13	0.741001	0.509000	-.209000	6.009001	12.276090	-1.540396
14	0.740251	0.509750	-.209750	6.009751	12.114280	-1.530226
15	0.739501	0.510500	-.210500	6.010501	11.955660	-1.520672
16	0.738751	0.511250	-.211250	6.009751	11.799890	-1.509810
17	0.738001	0.512000	-.212000	6.009002	11.647000	-1.499504
18	0.737251	0.512750	-.212750	6.008252	11.496990	-1.489765
19	0.736501	0.513500	-.213500	6.007503	11.349930	-1.480591
20	0.735751	0.514250	-.214250	6.006753	11.205830	-1.471997
21	0.735001	0.515000	-.215000	6.006003	11.064720	-1.463980
22	0.734251	0.515750	-.215750	6.005254	10.926650	-1.456555
23	0.733501	0.516500	-.216500	6.004504	10.791710	-1.449722
24	0.732751	0.517250	-.217250	6.003755	10.659860	-1.443487
25	0.732001	0.518000	-.218000	6.003005	10.531190	-1.437857
26	0.731251	0.518750	-.218750	6.002255	10.405720	-1.432848
27	0.730501	0.519500	-.219500	6.001506	10.283530	-1.428453
28	0.729751	0.520250	-.220250	6.000756	10.164630	-1.424685
29	0.729002	0.521000	-.221000	6.000007	10.049080	-1.421553
30	0.728252	0.521750	-.221750	5.999257	9.936935	-1.419065
31	0.727502	0.522500	-.221750	5.998507	9.829186	-1.394055
32	0.726752	0.523250	-.222500	5.997758	9.720054	-1.392208
33	0.726002	0.524000	-.222500	5.997008	9.613948	-1.367518
34	0.725252	0.524750	-.222500	5.996259	9.509856	-1.343156

Table 4.1.b Continuation of Table 4.1.a. The \underline{e} vector, error and output power during iterations 35 to 68 are shown in this Table.

Iteration	The \underline{e} Vector				Error	Power
35	0.724502	0.525500	-.223250	5.995509	9.403306	-1.341944
36	0.723752	0.526250	-.223250	5.994760	9.300788	-1.317894
37	0.723002	0.527000	-.224000	5.994010	9.197314	-1.317337
38	0.722252	0.527750	-.224000	5.993260	9.096290	-1.293594
39	0.721502	0.528500	-.224000	5.992511	8.997247	-1.270161
40	0.720752	0.529250	-.224750	5.991761	8.896376	-1.270260
41	0.720002	0.530000	-.224750	5.991012	8.798774	-1.247128
42	0.719252	0.530750	-.224750	5.990262	8.703100	-1.224312
43	0.718502	0.531500	-.225500	5.989512	8.604842	-1.225060
44	0.717752	0.532250	-.225500	5.988763	8.510522	-1.202534
45	0.717002	0.533000	-.226250	5.988013	8.415428	-1.203954
46	0.716252	0.533750	-.226250	5.987264	8.322452	-1.181725
47	0.715503	0.534500	-.226250	5.986514	8.231359	-1.159794
48	0.714753	0.535250	-.227000	5.985765	8.138912	-1.161884
49	0.714003	0.536000	-.227000	5.985015	8.049064	-1.140235
50	0.713253	0.536750	-.227000	5.984265	7.961027	-1.118890
51	0.712503	0.537500	-.227750	5.983516	7.871284	-1.121654
52	0.711753	0.538250	-.227750	5.982766	7.784455	-1.100585
53	0.711003	0.539000	-.227750	5.982017	7.699413	-1.079807
54	0.710253	0.539750	-.228500	5.981267	7.612387	-1.083258
55	0.709503	0.540500	-.228500	5.980517	7.528485	-1.062751
56	0.708753	0.541250	-.228500	5.979768	7.446300	-1.042537
57	0.708003	0.542000	-.229250	5.979018	7.362011	-1.046672
58	0.707253	0.542750	-.229250	5.978269	7.280935	-1.026727
59	0.706503	0.543500	-.229250	5.977519	7.201535	-1.007061
60	0.705753	0.544250	-.230000	5.976769	7.120069	-1.011902
61	0.705003	0.545000	-.230000	5.976020	7.041708	-0.992497
62	0.704253	0.545750	-.230000	5.975270	6.964968	-0.973375
63	0.703503	0.546500	-.230750	5.974521	6.886380	-0.978929
64	0.702753	0.547250	-.230750	5.973771	6.810631	-0.960064
65	0.702003	0.548000	-.230750	5.973022	6.736487	-0.941468
66	0.701254	0.548750	-.231500	5.972272	6.660838	-0.947750
67	0.700504	0.549500	-.231500	5.971522	6.587619	-0.929407
68	0.699754	0.550250	-.231500	5.970773	6.515970	-0.911339

Table 4.1.c Continuation of Table 4.1.b. The \underline{g} vector, error and output power during iterations 69 to 102 are shown in this Table.

Iteration	The \underline{g} Vector				Error	Power
69	0.699004	0.551000	-.232250	5.970023	6.443338	-0.918351
70	0.698254	0.551750	-.232250	5.969274	6.372583	-0.900533
71	0.697504	0.552500	-.232250	5.968524	6.303306	-0.882969
72	0.696754	0.553250	-.232250	5.967774	6.235543	-0.865677
73	0.696004	0.554000	-.233000	5.967025	6.165396	-0.873428
74	0.695254	0.554750	-.233000	5.966275	6.098450	-0.856380
75	0.694504	0.555500	-.233000	5.965526	6.032965	-0.839580
76	0.693754	0.556250	-.233750	5.964776	5.966002	-0.848104
77	0.693004	0.557000	-.233750	5.964026	5.901299	-0.831543
78	0.692254	0.557750	-.233750	5.963277	5.838034	-0.815246
79	0.691504	0.558500	-.233750	5.962527	5.776150	-0.799195
80	0.690754	0.559250	-.234500	5.961778	5.711857	-0.808486
81	0.690004	0.560000	-.234500	5.961028	5.650692	-0.792664
82	0.689254	0.560750	-.234500	5.960279	5.590909	-0.777101
83	0.688504	0.561500	-.235250	5.959529	5.530080	-0.787194
84	0.687755	0.562250	-.235250	5.958779	5.470989	-0.771860
85	0.687005	0.563000	-.235250	5.958030	5.413227	-0.756765
86	0.686255	0.563750	-.235250	5.957280	5.356777	-0.741919
87	0.685505	0.564500	-.236000	5.956531	5.298855	-0.752816
88	0.684755	0.565250	-.236000	5.955781	5.243055	-0.738193
89	0.684005	0.566000	-.236000	5.955031	5.188528	-0.723808
90	0.683255	0.566750	-.236000	5.954282	5.135260	-0.709663
91	0.682505	0.567500	-.236750	5.953532	5.080456	-0.721395
92	0.681755	0.568250	-.236750	5.952783	5.027787	-0.707471
93	0.681005	0.569000	-.236750	5.952033	4.976375	-0.693779
94	0.680255	0.569750	-.236750	5.951283	4.926170	-0.680324
95	0.679505	0.570500	-.237500	5.950534	4.874645	-0.692920
96	0.678755	0.571250	-.237500	5.949784	4.824988	-0.679681
97	0.678005	0.572001	-.237500	5.949035	4.776551	-0.666669
98	0.677255	0.572751	-.237500	5.948285	4.729271	-0.653890
99	0.676505	0.573501	-.238250	5.947536	4.681220	-0.667372
100	0.675755	0.574251	-.238250	5.946786	4.634486	-0.654807
101	0.675005	0.575001	-.238250	5.946036	4.588884	-0.642460
102	0.674255	0.575751	-.238250	5.945287	4.544425	-0.630344

Table 4.1.d Continuation of Table 4.1.c. The \underline{e} vector, error and output power during iterations 103 to 136 are shown in this Table.

Iteration	The \underline{e} Vector				Error	Power
103	0.673506	0.576501	-.238250	5.944537	4.501055	-0.618440
104	0.672756	0.577251	-.239000	5.943788	4.456142	-0.632850
105	0.672006	0.578001	-.239000	5.943038	4.413315	-0.621163
106	0.671256	0.578751	-.239000	5.942288	4.371535	-0.609695
107	0.670506	0.579501	-.239000	5.941539	4.330829	-0.598440
108	0.669756	0.580251	-.239000	5.940789	4.291186	-0.587400
109	0.669006	0.581001	-.239750	5.940040	4.249744	-0.602766
110	0.668256	0.581751	-.239750	5.939290	4.210601	-0.591947
111	0.667506	0.582501	-.239750	5.938540	4.172468	-0.581326
112	0.666756	0.583251	-.239750	5.937791	4.135364	-0.570924
113	0.666006	0.584001	-.239750	5.937041	4.099251	-0.560723
114	0.665256	0.584751	-.240500	5.936292	4.061625	-0.577107
115	0.664506	0.585501	-.240500	5.935542	4.026000	-0.567121
116	0.663756	0.586251	-.240500	5.934793	3.991361	-0.557343
117	0.663006	0.587001	-.240500	5.934043	3.957667	-0.547765
118	0.662256	0.587751	-.240500	5.933293	3.924945	-0.538395
119	0.661506	0.588501	-.241250	5.932544	3.891541	-0.555839
120	0.660756	0.589251	-.241250	5.931794	3.859289	-0.546683
121	0.660007	0.590001	-.241250	5.931045	3.827999	-0.537724
122	0.659257	0.590751	-.241250	5.930295	3.797626	-0.528972
123	0.658507	0.591501	-.241250	5.929545	3.768147	-0.520405
124	0.657757	0.592251	-.241250	5.928796	3.739554	-0.512039
125	0.657007	0.593001	-.242000	5.929546	3.710941	-0.532937
126	0.656257	0.593751	-.242000	5.928796	3.682755	-0.524777
127	0.655507	0.594501	-.242000	5.928047	3.655450	-0.516806
128	0.654757	0.595251	-.242000	5.927297	3.629022	-0.509031
129	0.654007	0.596001	-.242000	5.926548	3.603455	-0.501442
130	0.653257	0.596751	-.242000	5.925798	3.578724	-0.494050
131	0.652507	0.597501	-.242000	5.925798	3.554798	-0.487951
132	0.651757	0.598251	-.242000	5.926548	3.531520	-0.483135
133	0.651007	0.599001	-.242000	5.927298	3.508932	-0.478484
134	0.650257	0.599751	-.242750	5.928048	3.486198	-0.501037
135	0.649507	0.600501	-.242750	5.927299	3.464145	-0.494376
136	0.648757	0.601251	-.242750	5.926549	3.442928	-0.487907

Table 4.1.e Continuation of Table 4.1.d. The \underline{e} vector, error and output power during iterations 137 to 169 are shown in this Table.

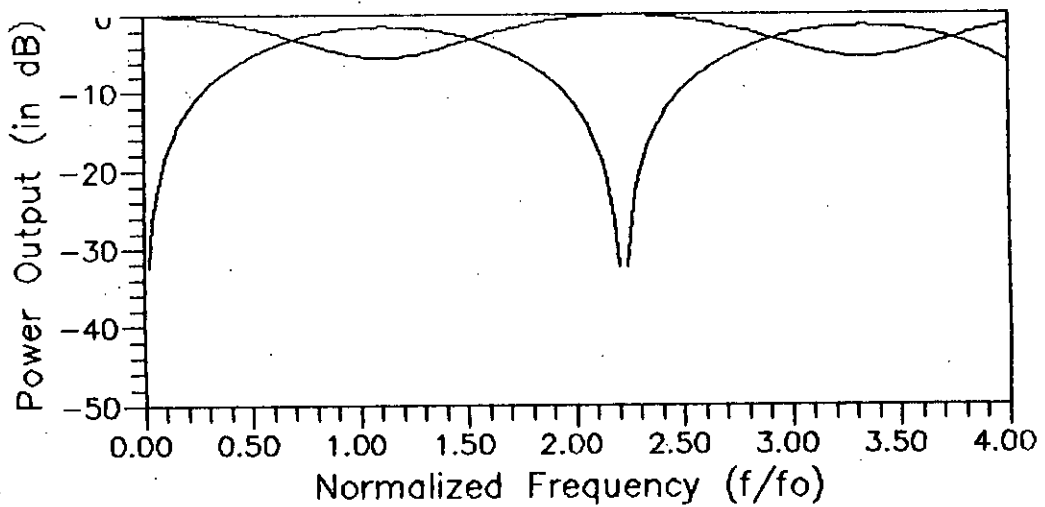
Iteration	The \underline{e} Vector				Error	Power
137	0.648007	0.602001	-.242750	5.925799	3.422480	-0.481611
138	0.647257	0.602751	-.242750	5.925050	3.402849	-0.475511
139	0.646508	0.603501	-.242750	5.924300	3.383993	-0.469586
140	0.645758	0.604251	-.242750	5.925050	3.365861	-0.466081
141	0.645008	0.605001	-.242750	5.925800	3.348366	-0.462737
142	0.644258	0.605751	-.242750	5.926550	3.331514	-0.459558
143	0.643508	0.606501	-.242750	5.927300	3.315322	-0.456541
144	0.642758	0.607251	-.242750	5.928051	3.299761	-0.453687
145	0.642008	0.608001	-.242750	5.928801	3.284868	-0.450997
146	0.641258	0.608751	-.242750	5.929551	3.270588	-0.448471
147	0.640508	0.609501	-.242750	5.930301	3.256956	-0.446104
148	0.639758	0.610251	-.242750	5.931051	3.243969	-0.443904
149	0.639008	0.611001	-.242750	5.931801	3.231612	-0.441863
150	0.638258	0.611751	-.242750	5.932551	3.219903	-0.439993
151	0.637508	0.612501	-.242750	5.933301	3.208827	-0.438276
152	0.636758	0.613251	-.242750	5.934051	3.198373	-0.436731
153	0.636008	0.614001	-.242750	5.934801	3.188558	-0.435340
154	0.635258	0.614751	-.242750	5.935551	3.179389	-0.434123
155	0.634508	0.615501	-.242750	5.936301	3.170848	-0.433060
156	0.633758	0.616251	-.242750	5.937051	3.162949	-0.432164
157	0.633008	0.617001	-.242750	5.937801	3.155675	-0.431433
158	0.632259	0.617751	-.242750	5.938551	3.149057	-0.430867
159	0.631509	0.618501	-.242750	5.939301	3.143058	-0.430461
160	0.630759	0.619251	-.242750	5.940052	3.137714	-0.430225
161	0.630009	0.620001	-.242750	5.940802	3.132992	-0.430145
162	0.629259	0.620751	-.242750	5.941552	3.128932	-0.430241
163	0.628509	0.621501	-.242750	5.942302	3.125516	-0.430493
164	0.627759	0.622251	-.242750	5.943052	3.122738	-0.430917
165	0.627009	0.623001	-.242750	5.943802	3.120504	-0.431502
166	0.626259	0.623751	-.242750	5.944552	3.119148	-0.432262
167	0.625509	0.624501	-.242750	5.945302	3.118315	-0.433177
168	0.624759	0.625251	-.242750	5.946052	3.118159	-0.434266
169	0.625509	0.624501	-.242750	5.946802	3.118227	-0.435413

Table 4.2.a Data generated during the optimization of \underline{e} vector strating with $\underline{e}^t = [.646 \ .5523 \ -.2 \ 6.7]$. The \underline{e} vector, error and output power during the first 32 iterations are shown in this Table. The program used for generating these data is OPT.FOR given is appendix B.

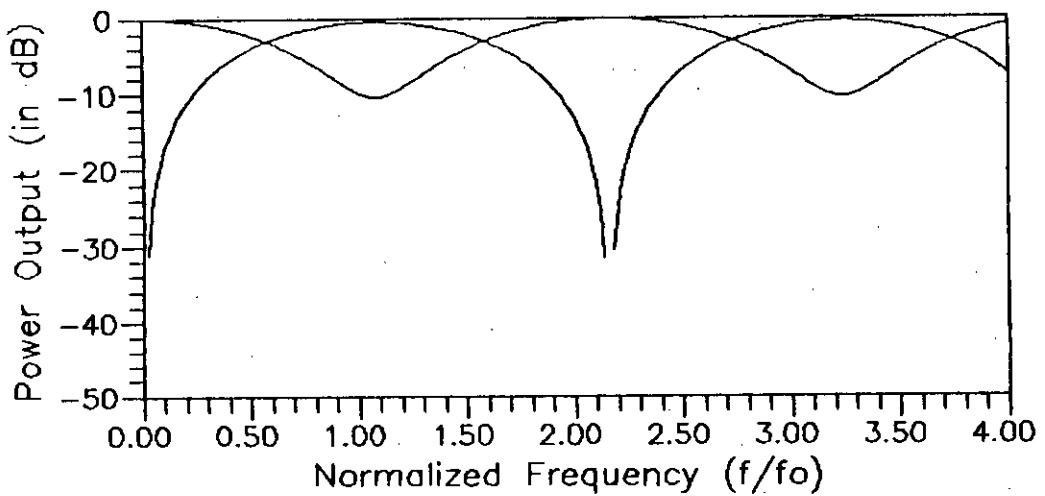
Iteration	The \underline{e} Vector				Error	Power
1	0.646000	0.552300	-.200000	6.700000	5.832225	-.3911839
2	0.645250	0.553050	-.200750	6.700750	5.663136	-.3909530
3	0.644500	0.553800	-.201500	6.701500	5.500857	-.3918845
4	0.643750	0.554550	-.202250	6.702250	5.345592	-.3940239
5	0.643000	0.555300	-.203000	6.703000	5.197395	-.3973585
6	0.642250	0.556050	-.203750	6.703750	5.056554	-.4019512
7	0.641500	0.556800	-.204500	6.704500	4.923080	-.4077820
8	0.640750	0.557550	-.205250	6.705250	4.797157	-.4148880
9	0.640000	0.558300	-.206000	6.706000	4.678905	-.4232783
10	0.639251	0.559050	-.206750	6.706750	4.568480	-.4329824
11	0.638501	0.559800	-.207500	6.707500	4.466009	-.4440151
12	0.637751	0.560550	-.208250	6.708251	4.371676	-.4564109
13	0.637001	0.561300	-.209000	6.709001	4.285531	-.4701633
14	0.636251	0.562050	-.209750	6.709751	4.207781	-.4853130
15	0.635501	0.562800	-.210500	6.710501	4.138458	-.5018558
16	0.634751	0.563550	-.211250	6.711251	4.077835	-.5198447
17	0.634001	0.564300	-.212000	6.712001	4.025918	-.5392691
18	0.633251	0.565050	-.212750	6.712751	3.982950	-.5601779
19	0.632501	0.565800	-.212750	6.712001	3.944899	-.5496509
20	0.631751	0.566550	-.212750	6.711252	3.908041	-.5393825
21	0.631001	0.567300	-.212750	6.710502	3.872311	-.5293548
22	0.630251	0.568050	-.213500	6.710502	3.836251	-.5507790
23	0.629501	0.568800	-.213500	6.709753	3.801111	-.5410233
24	0.628751	0.569550	-.213500	6.709003	3.767175	-.5315312
25	0.628001	0.570300	-.213500	6.708253	3.734313	-.5222754
26	0.627251	0.571050	-.213500	6.707504	3.702611	-.5132771
27	0.626501	0.571800	-.213500	6.706754	3.671924	-.5045031
28	0.625751	0.572550	-.213500	6.707504	3.642289	-.4979462
29	0.625002	0.573300	-.213500	6.708254	3.613492	-.4915891
30	0.624252	0.574050	-.214250	6.709004	3.584456	-.5159311
31	0.623502	0.574800	-.214250	6.708255	3.556311	-.5078856
32	0.622752	0.575550	-.214250	6.707505	3.529308	-.5000985

Table 4.2.b Continuation of Table 4.2.a. The \underline{e} vector, error and output power during iterations 33 to 64 are shown in this Table.

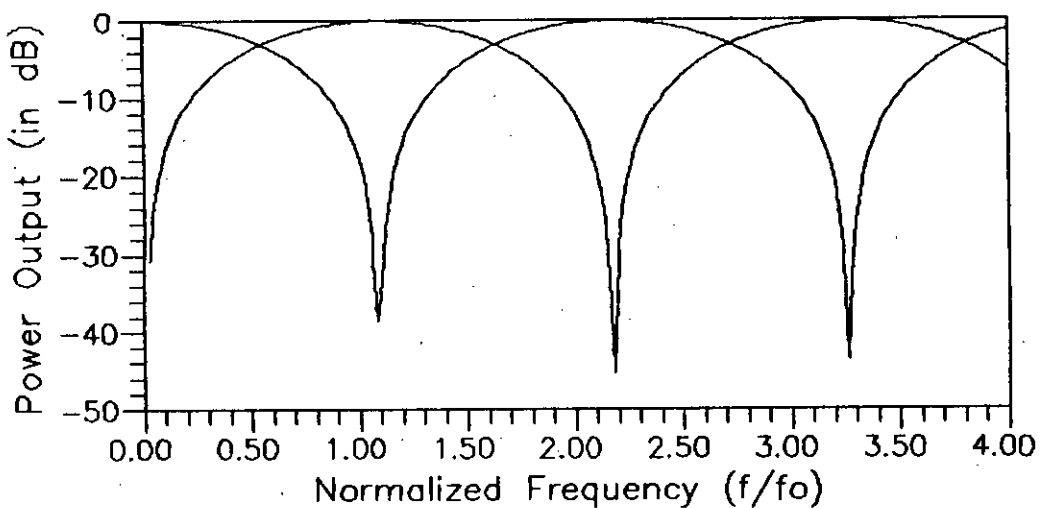
Iteration	The \underline{e} Vector				Error	Power
33	0.622002	0.576300	-.214250	6.706756	3.503250	-.4925289
34	0.621252	0.577050	-.214250	6.706006	3.478305	-.4852131
35	0.620502	0.577800	-.214250	6.705256	3.454278	-.4781103
36	0.619752	0.578550	-.214250	6.706007	3.431240	-.4732231
37	0.619002	0.579300	-.214250	6.706757	3.408993	-.4685342
38	0.618252	0.580050	-.214250	6.707507	3.387689	-.4640794
39	0.617502	0.580800	-.214250	6.708257	3.367134	-.4598124
40	0.616752	0.581550	-.214250	6.709007	3.347465	-.4557664
41	0.616002	0.582300	-.214250	6.709757	3.328597	-.4519233
42	0.615252	0.583050	-.215000	6.710507	3.310136	-.4791320
43	0.614502	0.583800	-.215000	6.709757	3.292274	-.4736434
44	0.613752	0.584550	-.215000	6.709008	3.275362	-.4683832
45	0.613002	0.585300	-.215000	6.708258	3.259342	-.4633376
46	0.612252	0.586050	-.215000	6.707509	3.244322	-.4585327
47	0.611503	0.586800	-.215000	6.706759	3.230165	-.4539355
48	0.610753	0.587550	-.215000	6.706009	3.216992	-.4495786
49	0.610003	0.588300	-.215000	6.706009	3.204624	-.4464163
50	0.609253	0.589050	-.215000	6.706759	3.193117	-.4444728
51	0.608503	0.589800	-.215000	6.707510	3.182378	-.4427229
52	0.607753	0.590550	-.215000	6.708260	3.172549	-.4412043
53	0.607003	0.591300	-.215000	6.709010	3.163484	-.4398776
54	0.606253	0.592050	-.215000	6.709760	3.155229	-.4387655
55	0.605503	0.592800	-.215000	6.710510	3.147792	-.4378600
56	0.604753	0.593550	-.215000	6.711260	3.141224	-.4371758
57	0.604003	0.594300	-.215000	6.712010	3.135412	-.4366846
58	0.603253	0.595050	-.215000	6.712760	3.130510	-.4364278
59	0.602503	0.595800	-.215000	6.713510	3.126345	-.4363621
60	0.601753	0.596550	-.215000	6.714260	3.123073	-.4365215
61	0.601003	0.597300	-.215000	6.715010	3.120583	-.4368815
62	0.600253	0.598050	-.215000	6.715760	3.118971	-.4374675
63	0.599503	0.598800	-.215000	6.716510	3.118147	-.4382511
64	0.598753	0.599550	-.215000	6.716510	3.118198	-.4382659



(a)



(b)



(c)

Figure 4.30 Output power vs. frequency characteristics of a diplexer with: a) starting \underline{e} vector from table 4.1.a, $\underline{e}^t = [.75 \ .5 \ -.2 \ 6.0]$, b) an intermediate \underline{e} vector obtained in 69th iteration, $\underline{e}^t = [.69904 \ .551 \ -.23225 \ 5.970023]$, c) optimized \underline{e} vector, $\underline{e}^t = [.625509 \ .624501 \ -.23225 \ 5.970023]$

and 2nd second starting \underline{e} vector: $\underline{e}^t = [0.646 \quad 0.5523 \quad -0.2 \quad 6.7]$

The following set of values are also assumed:

Small change, $\text{delx } (\Delta x) = .00075$

The normalized frequency band of *channel 1* :

$$f_1 = 1.0 \text{ to } f_2 = 1.3 \text{ GHz}$$

The normalized frequency band of *channel 2* :

$$f_3 = 2.0 \text{ to } f_4 = 2.3 \text{ GHz}$$

First the optimization program OPT.FOR is run with the 1st starting \underline{e} vector. When the program is run, with the above set of values it continues to modify the \underline{e} vector and minimize the error through iterations as can be seen from the output of the optimization program. The gradual change of the \underline{e} vector with decreasing error is shown in tables 4.1.a - 4.1.e. It may be seen from these tables that the optimization program requires 169 iterations to reach the minimum error level. The optimized \underline{e} obtained with the 1st starting \underline{e} vector is:

$$\text{Optimized } \underline{e}^t = [.648757 \quad .601251 \quad -.24275 \quad 5.926549]$$

Again the optimization program is run with the 2nd starting \underline{e} vector. The data generated during optimization is shown in tables 4.2.a - 4.2.b. The power against frequency characteristics of the diplexer with the starting \underline{e} vector, an intermediate \underline{e} vector and the optimized \underline{e} vector is shown in figure 4.30. It is seen from the tables that the optimization program requires 64 iterations to reach the same minimum error level as obtained with the first starting \underline{e} vector. The program requires less number of iterations because the 2nd starting \underline{e} vector was closer to the optimized \underline{e} vector than that of the 1st starting \underline{e} vector which can readily be verified from the tables 4.1.a - 4.2.b and figure 4.30. As may be seen from table 4.2.b the optimized \underline{e} obtained with the 2nd starting \underline{e} vector is:

$$\text{Optimized } \underline{e}^t = [.648757 \quad .601251 \quad -.24275 \quad 5.926549]$$

Before starting the optimization of an \underline{e} vector it is necessary to select the

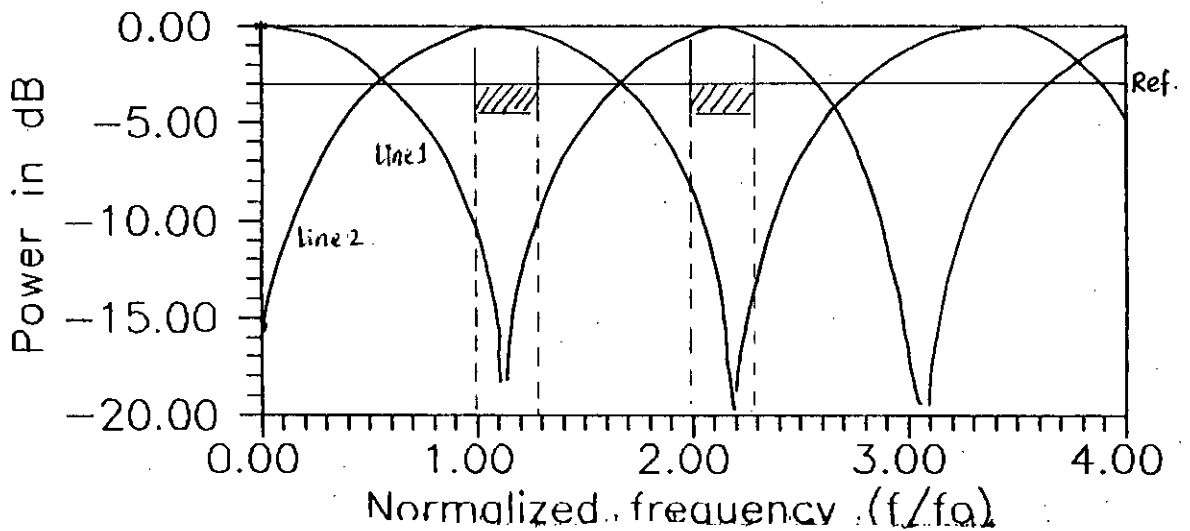
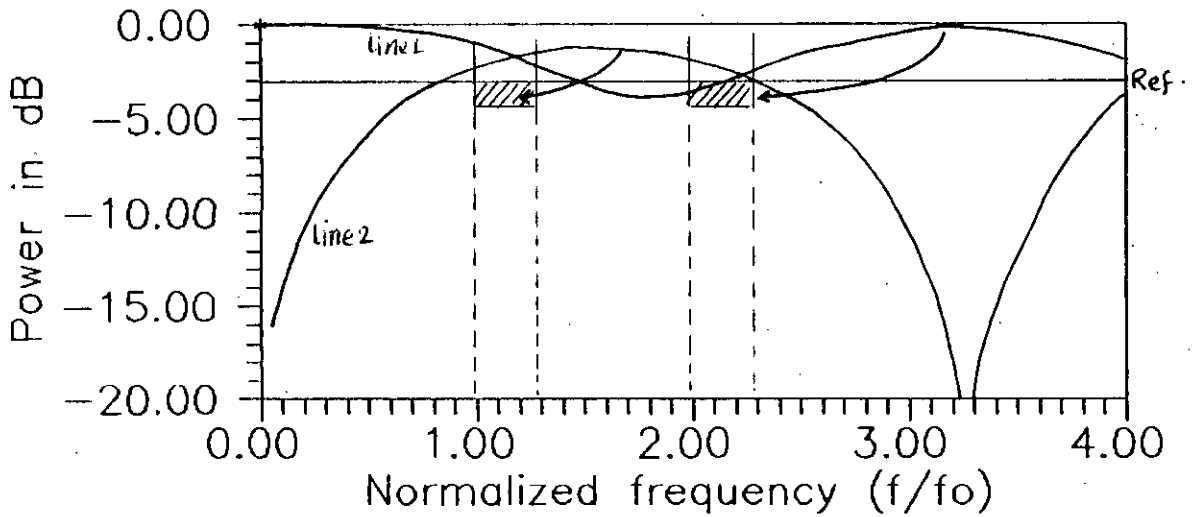
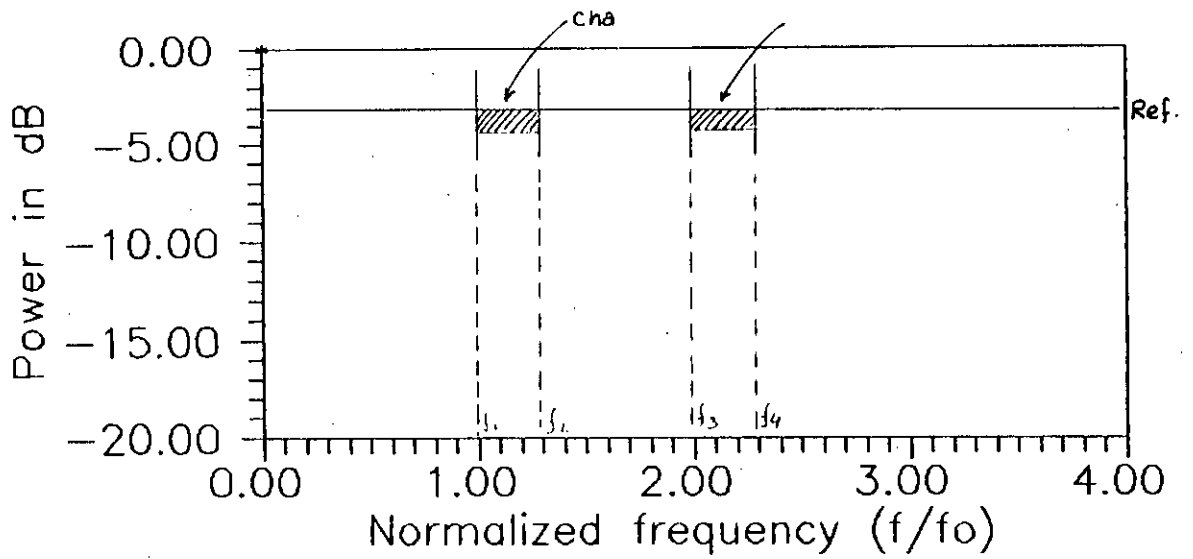


Figure 4.31 Plots showing how the characteristic is brought in the desired bands with minimum error. (a) The selected bands of operation. (b) Characteristic with an arbitrary starting \underline{g} vector. (c) Characteristic with optimized \underline{g} vector.

two channels of the desired diplexer. It is considered that for the desired example diplexer, each channel shall have a band width of 0.3 GHz. For this case we choose the optimizing band for the first output channel within 1 – 1.3 GHz and for the second output channel within 2 – 2.3 GHz. A reference power level is also selected for these two outputs. It is assumed that the reference power level of both the channels is 0.1 dB. The selected channels and the reference power level are shown in figure 4.31.a.

In the next step a power against frequency plot of the coupled combline system is obtained with a starting \underline{e} vector which is shown in figure 4.31.b. It may be seen from figure 4.yy that the maximum distributed power on the lines do not occur in the selected channels. To make the diplexer work in the desired channels the power characteristic curves should be dragged toward the selected channels as indicated by the arrow sign (figure 4.31.b). It is also desired to obtain minimum deviation from the reference power level i.e., minimum loss in the selected bands.

With the help of the computer optimization procedure the characteristics of the diplexer are brought within the desired frequency ranges by shifting the \underline{e} vector. The power characteristic of the diplexer with an optimized \underline{e} vector is shown in figure 4.31.c. It might be desirable to bring the channels closer to make the diplexer a contiguous channel type diplexer. But it has been observed that the behaviour of this type of coupled lines does not permit to have a contiguous channel type diplexer.

4.11 summary

Some possible methods of optimization have been discussed. The optimization algorithm used in this work has been presented. The influence of \underline{e} vector on the power against frequency characteristics has been presented with a number of plots. The flow-chart of the optimization program OPT.FOR, used for the optimization

in this work, has been presented. The method of optimizing the \underline{g} vector has been described and examples of optimization of \underline{g} vector have also been presented in this chapter. A design example of a diplexer have been considered and the \underline{g} of this diplexer obtained after computer optimization have been used to obtain the characteristics of the diplexer. The optimized \underline{g} vector obtained for this example will used as the basis for obtaining the physical dimensions of a diplexer.

CHAPTER 5

Obtaining the physical dimensions of a combline diplexer

5.1 Introduction

In the last chapter the technique of obtaining an optimized \underline{g} vector which provides the desired characteristics of a diplexer is presented. Once an \underline{g} vector is obtained, the next step is to obtain the line parameters of the combline diplexer by using the equations of section 3.5. One can then obtain the physical dimensions of a combline diplexer on the basis of the obtained line parameters. Since the diplexers under discussion are made of comblines, a model for a solitary combline is needed and the equations for obtaining the line dimensions from the line parameters are needed. This chapter starts with such a presentation.

The microstrip T-junction equivalent circuit and the equivalent circuit of a solitary combline using the microstrip T-junction equivalent circuit are presented in section 5.2. The equations required for obtaining the finger length and the main line characteristic impedance of a solitary combline are presented in section 5.3. The process of obtaining the dimensions of a solitary microstrip combline is discussed in section 5.4. The procedure of obtaining the dimensions of the coupled comblines of a diplexer is presented in section 5.5. The computer program developed and used for obtaining the line parameters and the finger lengths is discussed in section 5.6. The method of obtaining the amount of finger overlap of a combline diplexer is presented in section 5.7. The summary of this chapter is presented in section 5.8.

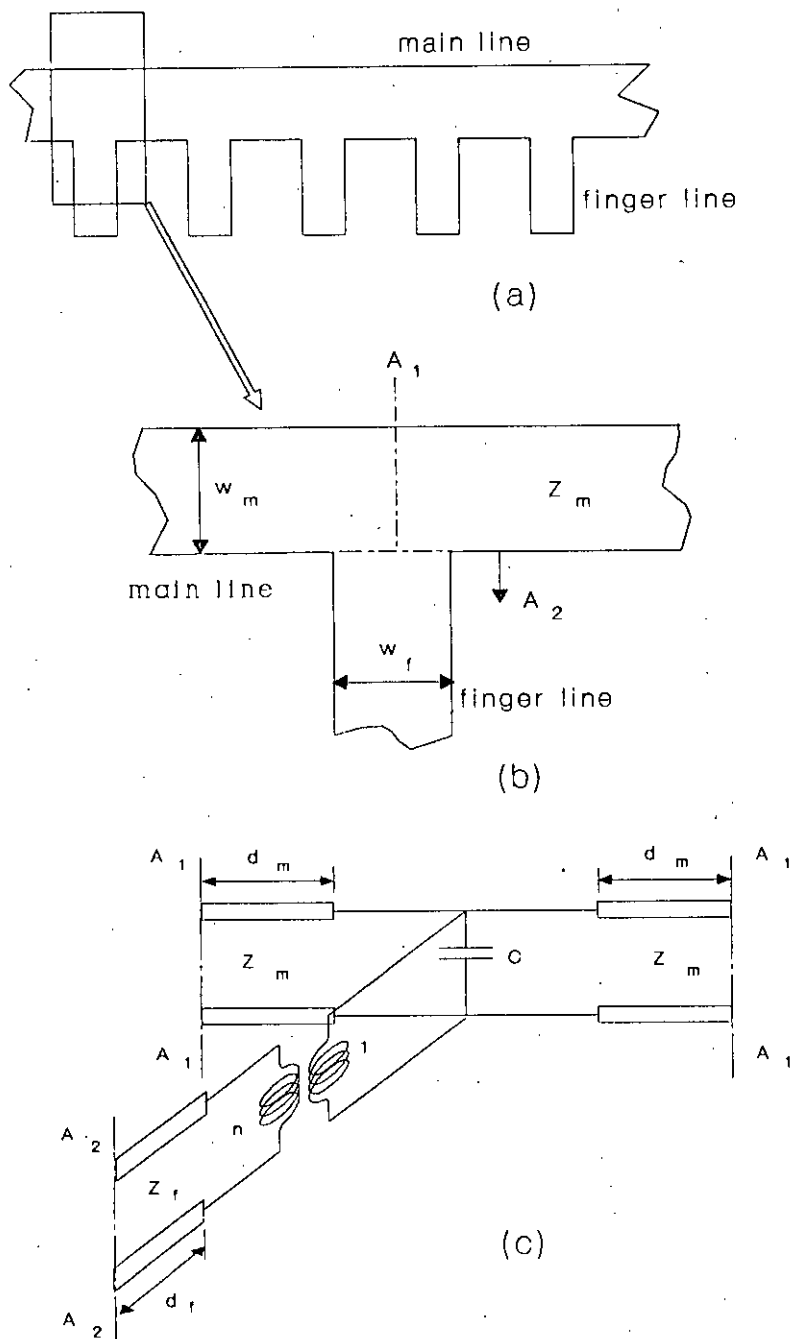


Figure 5.1 Microstrip T-junction equivalent circuit for obtaining equivalent circuit model of a comb- or herringbone- line. (a) A combline, (b) a microstrip T-junction, and (c) equivalent circuit of the T-junction.

5.2 Modeling a solitary combline using the microstrip T-junction equivalent circuit

It is necessary, at this stage, to obtain an equivalent circuit of a solitary (isolated) combline. This is necessary in order to be able to obtain analytical expressions of the characteristic impedance and phase velocity of a combline in terms of the finger periodicity, characteristic impedance of the main line and characteristic impedance of the finger line. Such an equivalent circuit has been presented in reference [5].

From [5] it may be observed that for obtaining such an equivalent circuit the wellknown microstrip T-junction equivalent circuit may be used as the basis. It is known that in a combline, finger lines come out at right angle from the main line and appear periodically. So each junction between a finger and the main line may be treated as a T-junction. An analysis of such a microstrip T-junction was presented by Silvester and Benedek [10] and also by Hammerstead [8]. The equivalent circuit of such a microstrip T-junction used by them is shown in figure 5.1. According to Hammerstead's analysis [8] the impedance offered by the open circuit branch line appears both transformed by the ratio n^2 [8] and displaced by some electrical length from the physical junction. A junction capacitance also appears as shown in figure 5.1. The equations for computing the displacement of reference lines for both main and branch lines were presented by Silvester and Benedek and Hammerstad [8] some of which are presented in section 5.3.

Thus in a herringbone- or comb- line, each junction between a finger and main line is treated as a T-junction. On this basis an equivalent circuit of a combline may be represented by cascaded T-junctions as shown in figure 5.2. A nomenclature of terms which will be used in the following discussion is presented below.

p = finger periodicity

l_f = finger length

d_m = displacement of the main line reference at the junction of the fingers

- d_f = displacement of the finger line reference at the junction
 $\theta = \theta_m = \beta_m(p + 2d_m)$ radians
 = electrical periodicity of the herringbone line
 β_m = propagation constant for the main line (in radians/mm.)
 β_f = propagation constant for finger lines (in radians/mm.)
 β_e = effective propagation constant (in radians/mm.)
 Z_m = characteristic impedance of the main line
 Z_f = characteristic impedance of the finger line
 Z_0 = characteristic impedance of the herringbone – or comb – line
 C = capacitance at the junction for the discontinuity due to fingers
 (negative for $Z_f > 65$ ohms)
 n = transformation ratio
 ω_L = angular velocity at lower end of frequency band (in radian/sec.)
 h = thickness of the substrate (in mm.)
 w_i = width of the main line when $i = m$ and finger line when $i = f$ (in mm.)
 ϵ_r = dielectric constant of the substrate material

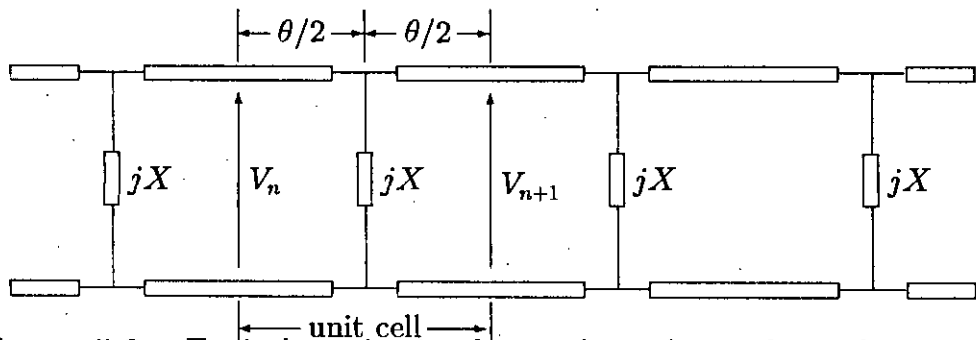


figure 5.2 Equivalent circuit of a comb- or herringbone- line using T-junction model.

For comb lines it may be assumed that the transformation ratio is near to unity [5]. After necessary changes n is the main line reference plane, the effective periodicity for describing the propagation becomes $(p + 2d_m)$. For the finger lines if the reference plane displacement is found to be of significant amount, this is taken into account by replacing l_f by $(l_f + d_f)$. Equations for computing the main line reference displacement d_m , the finger line reference displacement d_f and d_f' are given in section 5.3.

After replacing the finger line with T-junction equivalent circuit of figure 5.1 the equivalent circuit of a comb- or herringbone- line may be drawn as shown in figure 5.2. Here the loading due to the fingers is indicated by the admittance jX and the reference plane displacement is adjusted within the electrical length p . Thus a unit cell of length p is considered with one finger line in the center. The unit cell thus has three parts:

- i) A portion of the main line of effective length $(p + 2d_m)/2$ on the left,
- ii) the reactance due to finger line at the junction in the center, and
- iii) a portion of the main line of effective length $(p + 2d_m)/2$ on the right (as shown in figure 5.1).

The total ABCD matrix of the unit cell is obtained by cascade multiplication of the ABCD matrices for the three sections described above. From the ABCD matrix of the unit cell, the equation of the characteristic impedance of the main line and the equations for the length of the finger lines are obtained.

The detail analysis is available in reference [5]. Here only the useful equations will be presented. Thus following [5] and by considering a unit cell between the n th and $(n + 1)$ th node of the equivalent circuit shown in figure 5.2, the voltage and currents at the two ends of the cell may be represented by the following equations:

$$\begin{bmatrix} V_n \\ I_n \end{bmatrix} = \begin{bmatrix} \cos \frac{\theta}{2} & jZ_m \sin \frac{\theta}{2} \\ jY_m \sin \frac{\theta}{2} & \cos \frac{\theta}{2} \end{bmatrix} \begin{bmatrix} 1 & 0 \\ jX & 1 \end{bmatrix} \begin{bmatrix} \cos \frac{\theta}{2} & jZ_m \sin \frac{\theta}{2} \\ jY_m \sin \frac{\theta}{2} & \cos \frac{\theta}{2} \end{bmatrix} \begin{bmatrix} V_{n+1} \\ I_{n+1} \end{bmatrix} \quad (5.1)$$

$$\begin{bmatrix} V_n \\ I_n \end{bmatrix} = \begin{bmatrix} \cos \theta - \frac{Z_m X}{2} \sin \theta & -j\frac{Z_m^2 X}{2} + j\frac{Z_m^2 X \cos \theta}{2} + jZ_m \sin \theta \\ j\frac{X}{2} + j\frac{X \cos \theta}{2} + jY_m \sin \theta & \cos \theta - \frac{Z_m X}{2} \sin \theta \end{bmatrix} \begin{bmatrix} V_{n+1} \\ I_{n+1} \end{bmatrix} \quad (5.2)$$

Equation 5.2 may be written in terms of ABCD matrix as shown in the following equation:

$$\begin{bmatrix} V_n \\ I_n \end{bmatrix} = \begin{bmatrix} A & B \\ C & D \end{bmatrix} \begin{bmatrix} V_{n+1} \\ I_{n+1} \end{bmatrix} \quad (5.3)$$

Using the eigenvalues of the ABCD matrix it is possible to obtain the analytical expression for the characteristic impedance and phase velocity of a combline.

$$Z_0 = \sqrt{\frac{Z_m^2 (Z_m X \cos \theta + 2 \sin \theta - Z_m X)}{Z_m \cos \theta + 2 \sin \theta + Z_m X}} \quad (5.4)$$

$$(5.5)$$

$$v_{pe} = \frac{\omega p}{\cos^{-1}(\cos \theta - \frac{Z_m X \sin \theta}{2})} \quad (5.6)$$

Here

$$X = \frac{2}{Z_m \sin \theta} (\cos \theta - \cos \beta_e p) \quad (5.7)$$

The expression for finger length of a *herringbone line* may be written as

$$l_f = \frac{1}{\beta_f} \tan^{-1} \left[\frac{Z_f}{n^2 Z_m \sin \theta} (\cos \theta - \cos \beta_e p) \right] \quad (5.8)$$

and the expression for finger length of a *comblines* may be written as

$$l_f = \frac{1}{\beta_f} \tan^{-1} \left[\frac{2 Z_f}{n^2 Z_m \sin \theta} (\cos \theta - \cos \beta_e p) \right] \quad (5.9)$$

It has been shown in [5] that it is possible to make certain approximations regarding θ^2 and higher power of θ so that the following equations can be obtained.

$$Z_0 = Z_m \sqrt{\frac{\theta}{\theta + Z_m X}} \quad (5.10)$$

$$v_{pe} = \frac{\omega p}{\sqrt{\theta(\theta + X Z_m)}} \quad (5.11)$$

Now, eliminating $\sqrt{(\theta + Z_m X)}$ from equations (5.9) and (5.10) one obtains

$$Z_0 = Z_m \frac{\theta v_{pe}}{\omega p} \quad (5.12)$$

$$(5.13)$$

$$\text{or, } Z_0 = Z_m \frac{v_{pe}}{v_{pm}} \frac{p}{(p + 2d_m)}$$

From equation (5.12) one may obtain the main line impedance as follows:

$$Z_m = \frac{Z_0}{(v_{pe}/v_{pm})} \frac{p}{(p + 2d_m)} \quad (5.14)$$

$$(5.15)$$

$$\text{or, } Z_m = \frac{Z_0}{\frac{v_{pe}}{(c/\sqrt{\epsilon_{rem}})}} \frac{p}{(p + 2d_m)}$$

5.3 Necessary equations for obtaining the finger length and main line characteristic impedance of a solitary microstrip combline

The dimensions required to fabricate the diplexer under consideration are coupled length (L_0), length of finger (L_f), width of the main line (w_m), width of the finger line (w_f), thickness of the substrate (h), periodicity of the finger line (p) and the amount of finger overlap. All of the above parameters are shown in Figs. (1.7), (1.8) and (1.9).

Two curves are now required for uniform microstrip lines. The first one is a plot of characteristic impedance Z_i (with $i = m$ or f) against shape ratio (w_i/h) on

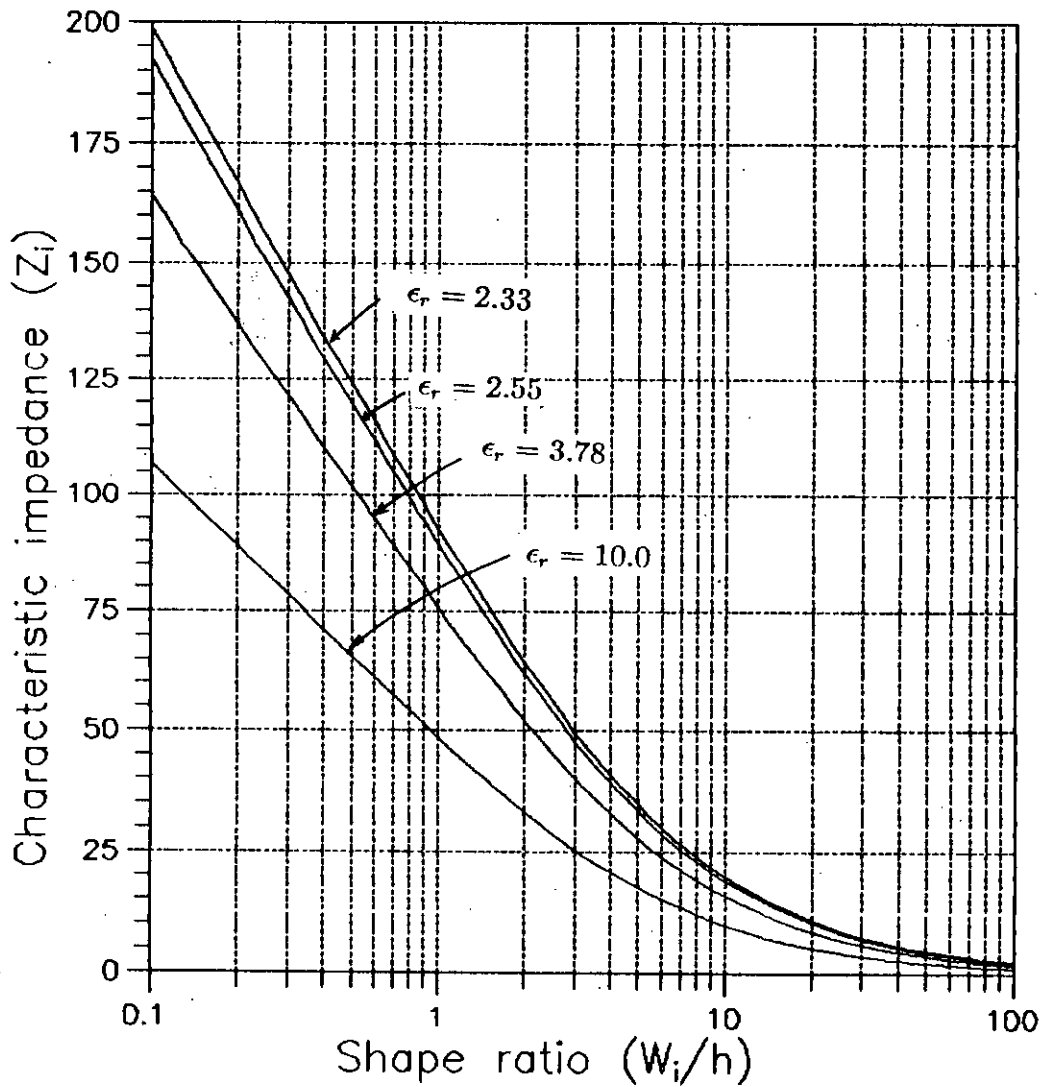


Figure 5.3 Characteristic impedance (Z_i) vs. shape ratio (w_i/h) plots of uniform transmission lines in open microstrip configuration for four different substrate dielectric constant, i.e., for $\epsilon_r = 2.33, 2.55, 3.78$ and 10 .

semilog graph paper and the second one is a plot of the effective dielectric constant ϵ_{rei} against (w_i/h) , also on semilog graph paper. These curves are obtained for the particular value of dielectric constant ϵ_r (of the chosen copper laminated board) using Hammerstad's equations for microstrip lines. These equations are [11]

$$\epsilon_{rei} = [(\epsilon_r + 1) + (\epsilon_r - 1)F]/2 \quad (5.16)$$

$$F = (1 + 12h/w_i)^{-1/2} + 0.04(1 - w_i/h)^2 \quad ; \quad \text{when } w_i/h \leq 1 \quad (5.17)$$

$$F = (1 + 12h/w_i) \quad ; \quad \text{when } w_i/h \geq 1 \quad (5.18)$$

The relationship between effective dielectric constant and the shape ratio is obtained from equations (5.4), (5.5) and (5.6). The relationship is shown graphically in figure 5.3.

The relationship between the impedance and the shape ratio¹ of the main line and finger lines may be obtained from the following equations [11].

for $w_i/h \leq 1$

$$Z_i = [(\eta_0/2) \ln(8h/w_i + 0.25w_i/h)]/\sqrt{\epsilon_{rei}} \quad (5.19)$$

and for $w_i/h \geq 1$

$$Z_i = [\eta_0 w_i/h + 1.393 + 0.667 \ln(w_i/h + 1.444)^{-1}]/\sqrt{\epsilon_{rei}} \quad (5.20)$$

$$\eta_0 = 376.73 \text{ ohms}$$

The subscript i in the above equations is to be replaced by f for finger line and by m for mainline. The exponential relationship between the characteristic impedance (Z_i) and the shape ratio is shown in figure 5.4.

¹The ratio of the *line-width* to the substrate-thickness, (i.e., w_i/h) is known as the *shape ratio*

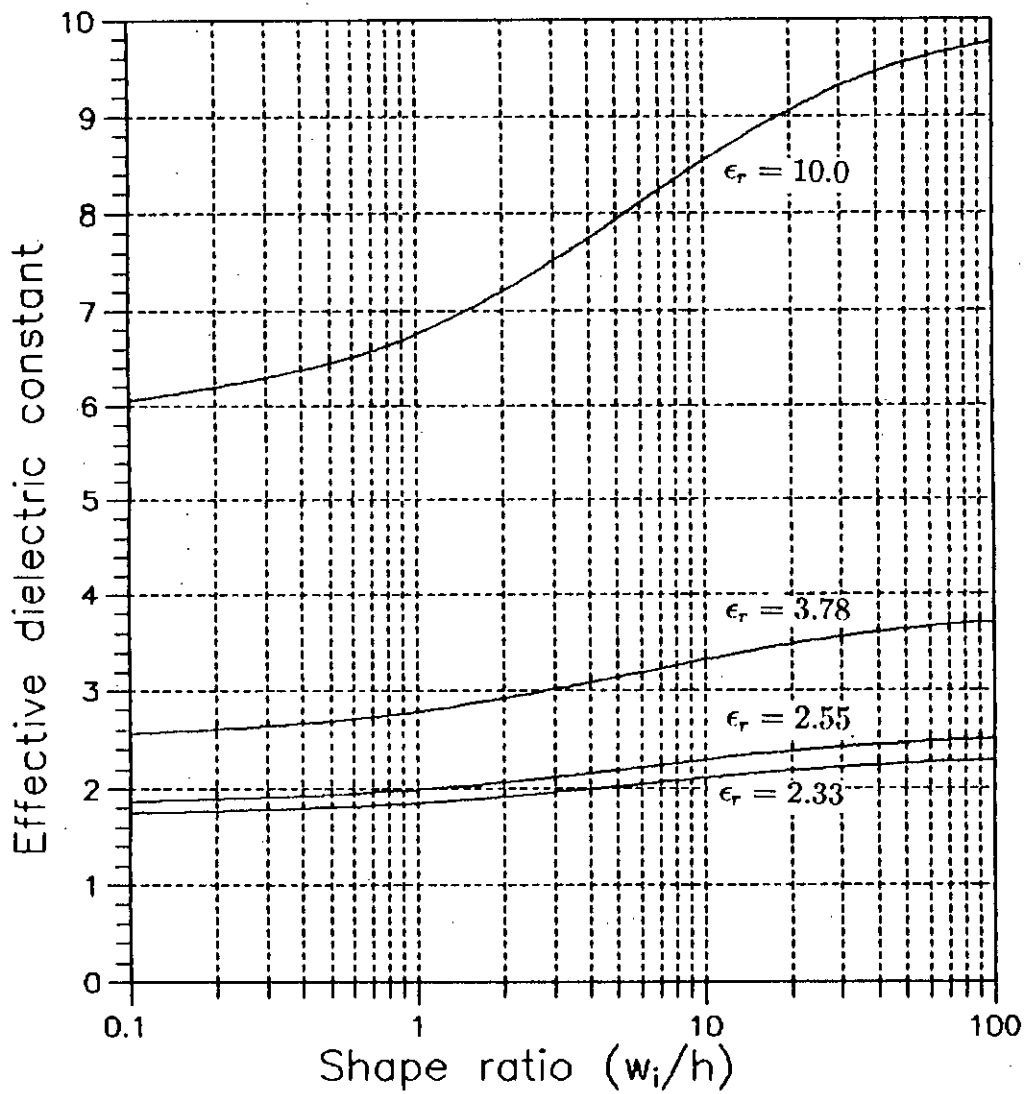


Figure 5.4 *Effective dielectric constant (ϵ_{re}) vs. shape ratio (w_i/h) plots of uniform transmission lines in open microstrip configuration for four different substrate dielectric constant, i.e., for $\epsilon_r = 2.33$, 2.55, 3.78 and 10.*

It is required to assume a value of ϵ_{rem} (the effective dielectric constant of the mainline) as slightly less than ϵ_r (the dielectric constant of the substrate). A value of the mainline impedance Z_m , is then obtained using the following equation.

$$Z_m = Z_0 / [(p + 2d_m)v_{pe} / (c/\sqrt{\epsilon_{rem}})] \quad (5.21)$$

Equation (5.9) is obtained from the model analysis of a combline discussed in section (5.2). The phase velocity v_{pe} and the characteristic impedance Z_0 of the combline should be known beforehand for designing a coupler. Following Hammerstad [8], d_m is written as

$$d_m = D_f(0.05n^2Z_m)/Z_f \quad (5.22)$$

The term D_f used in equation (5.10) is to be obtained from equation (5.12).

Following Hammerstad [8], the displacement of the finger line reference at a junction is given by [5] [6] [11]

$$d_f = D_m[0.076 + 0.2(2D_m/\lambda)^2 + 0.663 \exp(-1.71Z_m/Z_f) - 0.172 \ln(Z_m/Z_f)]Z_m/Z_f \quad (5.23)$$

In equation (5.11) the term λ represents the wave length of the microwave signal under consideration ($\lambda = 2\pi c/\omega_L$).

D_m and D_f used in equations (5.10) and (5.11) are the effective width of the mainline and the finger line respectively. These two notations can be generalized by using the notation D_i where, $i = m$ (for main line) or f (for finger line). The effective width of line i can be obtained from the following equation.

$$D_i = \eta_0 h / (Z_i \sqrt{\epsilon_{rei}}) \quad (5.24)$$

During the first approximate evaluation of Z_m , d_m is assumed to be zero.

The equations required to compute finger length (l_f) of the combline are as follows [5] [6].

For a *herringbone-line*

$$l_f = (1/\beta_f) \tan^{-1} \{ \{ Z_f / (n_2 Z_m \sin \theta_m) \} (\cos \theta_m - \cos \beta_e P) \} \quad (5.25)$$

For a *comblinc*

$$l_f = (1/\beta_f) \tan^{-1} [\{ 2Z_f / (n_2 Z_m \sin \theta_m) \} (\cos \theta_m - \cos \beta_e P)] \quad (5.26)$$

Here, $\theta_m = \omega_L / (c\sqrt{\epsilon_{rem}})(p + 2d_m)$, $\beta_f = \omega_L / (c/\sqrt{\epsilon_{ref}})$ and $\beta_e = \omega_l / v_{pe}$. θ_m and β_f are calculated using ϵ_{rem} and ϵ_{ref} obtained earlier. β_e is calculated using the value of the effective phase velocity of the comblinc $v_{pe} = v_{pi}^u$. At the end, d_f is computed using equation (5.22). The extra finger length for compensating the effect of the finger line reference displacement is computed using the following equation.

$$d_{f'} = \frac{D_m}{2} - d_f \quad (5.27)$$

5.4 Obtaining the dimensions of a solitary microstrip comblinc

The steps required for obtaining the physical dimensions of a microstrip comblinc diplexer is shown in this section. However, before going through the design steps, it is required to identify the parameters which are known or assumed prior to proceeding with computation.

For designing a comblinc in an open microstrip configuration, a suitable value of finger periodicity p and a suitable width (w_f) of finger line are taken first. Selection of a particular copper laminated board gives the dielectric thickness, i.e., the gap h and the dielectric constant (ϵ_r). We choose a copper laminated board with $\epsilon_r = 2.55$ and the substrate thickness of 1.5 mm. Also we choose that for the present example we will have finger widths of 1 mm (suitable for cutting the mask by a 1 mm tool). Thus the finger line characteristic impedance for this case is 107 ohms [5].

The equations presented in section 5.3 may be used for computing the finger length of a solitary microstrip comblinc. The method of finding the dimensions of

a solitary microstrip combline may be used for finding the dimensions of a pair of coupled microstrip combline if few coupling properties are considered. The steps required for obtaining such a pair of coupled microstrip combline which is a diplexer is presented in section 5.6.

5.5 Obtaining the dimensions of a pair of coupled microstrip comblines

The way of obtaining the dimensions of a pair of coupled combline is similar to that of a solitary microstrip combline. A few modifications are required due to the presence of the coupling properties of the two lines. The coupled or mutual capacitance that comes into play due to the finger overlap of the two lines (described in section 5.5) is mainly taken under consideration. The values of the different parameters given in section 5.3 are accepted in obtaining the dimensions of a pair of coupled combline.

The uncoupled characteristic impedances of the two lines are taken as characteristic impedance of the device (Z_0). With this known parameters in hand the following steps are worked through for obtaining the line width (w_f and w_m) and the length of the finger lines (l_f).

Step-I With the known value of relative dielectric constant (ϵ_r) and the characteristic impedance (Z_f), the width-height ratio of the finger lines (w_f/h) is computed from figure 5.3. As the thickness of the substrate (h) is known before hand the width of the finger line (w_f) may be computed.

Step-II Using the known dielectric constant (ϵ_r) and the shape ratio obtained in Step-I, the effective dielectric constant (ϵ_{re}) is obtained from the semilog plot of figure 5.4.

Step-III Now a value of ϵ_{rem} (effective dielectric constant of the main line) is assumed, which should be slightly less than the value of ϵ_{re} obtained in Step-II.

Step-IV Putting the value of ϵ_{rem} (obtained in Step-III) in equation (5.20) the impedance of the main line (Z_m) is now computed. All the terms used in equation (5.20) are known except d_m . However, for the first approximation d_m is taken to be zero. For later iterations the value of d_m comes from Step-V.

Step-V Now d_m is computed with the help of equation (5.21). This d_m is then used to again find the value of main line impedance Z_m using equation (5.20).

Step-VI With the values obtained in the above steps the finger length (l_f) for comb- and herringbone- lines are obtained using equations (5.24) and (5.25) respectively.

Step-VII The Z_m obtained in Step-V is now used to assess the shape ratio (w_m/h) from the semilog plot of figure 5.3. From this step the process is looped back to Step-2 until a steady value of finger length (l_f) is obtained in Step-VI. If a steady value of l_f is obtained then Step-VIII is executed, otherwise the job sequence is switched back to Step-II.

Step-VIII After obtaining l_f it remains to find the value of finger overlap. The amount of finger overlap is determined from figure 5.5. The coupling capacitance is known from equation (3.20) and this capacitance is used to obtain the finger overlap. The widths of the lines, w_m and w_f are also obtained from the shape ratio as h is known.

After completing Step-VIII all the dimensions of the diplexer become known. These dimensions may be used to fabricate a practical device.

5.6 The computer program used in this work for computing the physical dimensions of a diplexer

A computer program named FIND-LF.BAS has been developed to compute the physical dimensions of a diplexer from the optimized \underline{e} vector given as its input. The program is written in BASIC and may be run by using a Quick Basic compiler

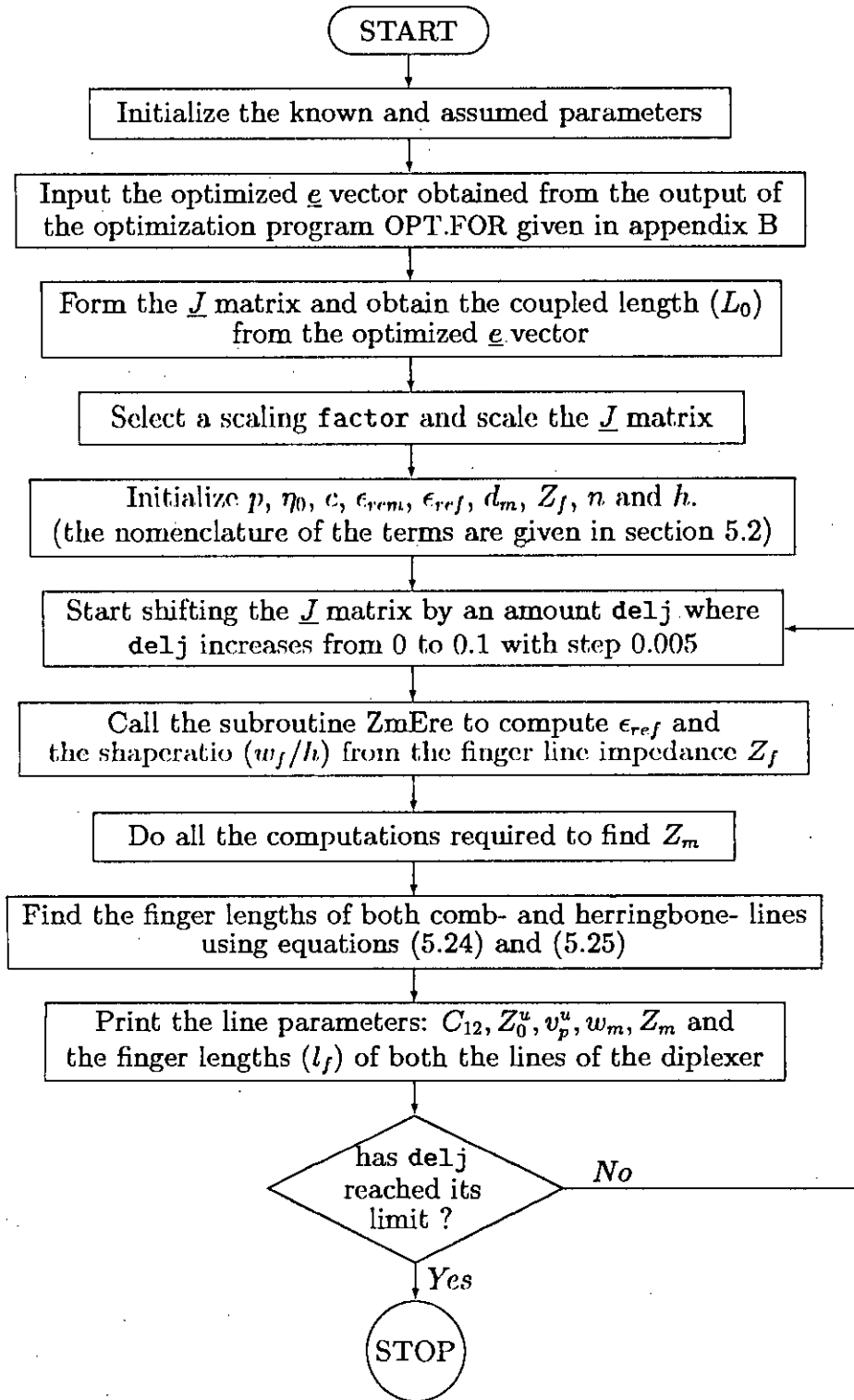


Figure 5.5 Flow-chart of the program FINDLF.BAS developed to find the finger lengths of a diplexer. The program is given in appendix C.

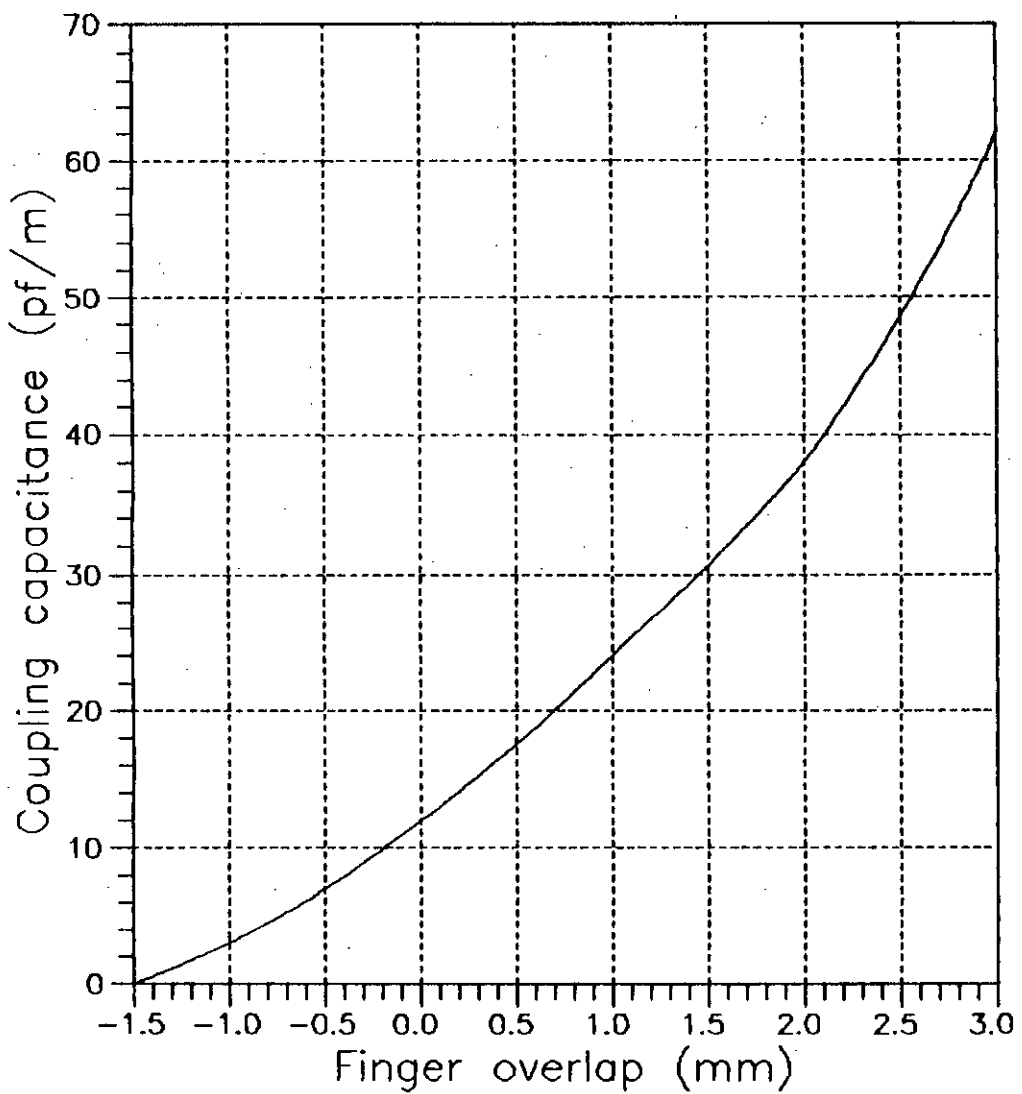


Figure 5.6 Plot of *coupling capacitance vs. finger overlap* for a pair of coupled combines with finger periodicity of 2.4 mm. The finger width was taken as 1 mm, on a 1.5 mm thick dielectric substrate of $\epsilon_r = 2.55$ and finger line impedance = 107 ohms.

or interpreter. The program forms the \underline{J} matrix from the optimized \underline{e} vector and then scales and shifts the \underline{J} matrix according to the rules mentioned in section 3.4. The degree of scaling may be controlled to select a suitable value of coupled length (L_0).

After scaling the \underline{J} matrix the program starts to shift the \underline{J} matrix by an amount Δe_{lj} . With each step of shifting, the program does all the job mentioned in Step-I to Step-VII of section 5.5. Thus the program computes the coupling capacitance, main-line width, main-line impedance and the finger length of both the lines for comb- and herringbone- structures. The program generates a table of data with series of shifted \underline{J} matrix. From this data a suitable value of finger length is chosen for design purpose. The only thing that is left to be found is the amount of finger overlap mentioned in Step-VIII of section 5.5. The finger overlap may be found from a curve showing coupling capacitance against finger overlap. The coupling capacitance is taken from the output of the program and the finger overlap is obtained according to the process mentioned in section 5.7.

The flow-chart of the program FIND_LF.BAS is given in figure 5.5. The program uses a subroutine named ZMERE which handles the job of finding the characteristic impedance of the finger line (Z_f) and the shape ratio (w_f/h). This subroutine actually simulates the search for Z_f and w_f/h in the curves shown in Figs. 5.3 and 5.4 respectively. The program is given in appendix C.

5.7 Relationship between coupling capacitance and finger overlap of a pair of coupled comb lines

The coupling between two adjacent comb lines in a microstrip diplexer is capacitive in nature. Actually this coupling capacitance is achieved with the interpenetration of the finger lines, i.e., with finger overlap as shown in figure 1.9. As can be anticipated from the law of capacitance, the coupling capacitance is proportional to the amount of finger overlap. The behavior between a pair of coupled plain microstrip lines was explained by Bryant and Weiss, Milligan, Garg and Bahl [5] [12]

and others.

The relationship between the coupling capacitance and finger overlap is shown in figure 5.6. This curve shown in this figure is used to find the amount of finger overlap which is a very important design parameter.

5.8 Summary

Using the method presented in an earlier work [6] the equivalent circuit of a solitary combline has been presented. The useful analytical expressions have been presented. Necessary analytical expressions for evaluating the characteristic impedance, effective phase velocity and the finger length of a solitary combline have been presented. The procedure of obtaining the dimensions of a solitary microstrip combline has been presented. Next, the method of obtaining the physical dimensions of a pair of coupled comblines (as used in a diplexer) has been presented. A computer program has been developed to obtain the line parameters of a combline diplexer. The equations and procedure presented in this chapter will be used in designing a microwave forward coupled combline diplexer.

CHAPTER 6

Designing the Diplexer

6.1 Introduction

A design example of a microstrip combline diplexer is presented in this chapter. The \underline{e} vector obtained after optimization in section 4.10 is taken as the design example. For this design example it is necessary to choose a Cu-clad laminate board and the values of a number of design parameters as shown in section 6.2. The practical considerations necessary for designing a diplexer are presented in section 6.3. The factors required to be taken under consideration while scaling and shifting \underline{J} matrix are presented in section 6.4. The process of obtaining suitable coupling capacitances is also presented in section 6.4.

Finally, a complete set of design values, i.e., the physical dimensions of a herringbone- and a comb- line diplexer are presented in section 6.5. These dimensions may be used for fabricating a practical diplexer. The contents of this chapter are summarized in section 6.6.

6.2 Choice of Cu-clad laminate board, finger periodicity, finger line width and lower band edge frequency

For designing a microstrip coupled combline diplexer it is necessary to choose a particular Cu-clad laminate board. For present design work a Cu-clad laminate board having glass woven teflon substrate of thickness $h = 1.5$ mm and substrate dielectric constant $\epsilon_r = 2.55$ has been selected.

Next, the periodicity p of finger lines in the comb- or herringbone- lines of the desired diplexer is chosen to be 2.4 mm. For this finger periodicity, the finger line width w_f is chosen to be 1 mm. This value of finger width will permit to have a gap of 0.2 mm between two adjacent fingers of a pair of coupled comblines. The lower band edge frequency f_L is chosen at 1 GHz (guide wave length $\lambda = c/(f_L\sqrt{\epsilon_r}) = 300/\sqrt{\epsilon_r} = 187.9$ mm).

6.3 Practical considerations for designing

There are several factors which should be taken into consideration for designing a forward coupled microstrip combline diplexer. The optimized \underline{e} vector, and hence, the optimized \underline{J} matrix obtained from computer optimization can not always be directly used to obtain the physical dimensions of a diplexer. The characteristic parameters like coupled and uncoupled capacitances, inductances, phase velocities, characteristic impedances etc. obtained may not be physically realizable. So in order to obtain physically realizable line parameters it is necessary to perform two types of operations: *i*) scaling the \underline{J} matrix and *ii*) shifting the \underline{J} matrix. Details of these two types of operation have been presented in section 3.4.

The scaling of \underline{J} matrix is mainly required for obtaining a suitable coupling capacitance. As mentioned earlier (section 5.7) the coupling capacitance determines the amount of finger overlap of the two comb- or herringbone- lines. For an operating frequency of 1 – 2 GHz it is desired to have finger lengths in the range of 2 to 4 mm due to the difficulties discussed in section 5.7. Scaling is done in such a way that the coupling capacitances (i.e., C_{12} and C_{21}) of the coupled lines of a diplexer (having a substrate dielectric constant come in the range of 20 to 50 pF/m. This is done because, for the selected finger periodicity of 2.4 mm and finger width of 1 mm, finger overlap in the range of 0.75 mm to 2.75 mm (figure 5.6) will be required to achieve this range of coupling capacitance which does not exceed the desired finger

length. With this choice a good amount of separation remains between the finger tip of one line and the other main-line. The derivable values of phase velocities are within the range of 1.5×10^{11} to 2.5×10^{11} mm/s. To keep the above mentioned parameters in the desired ranges the scaling technique of \underline{J} matrix is used.

6.4 Considerations regarding scaling and shifting of \underline{J} matrix

It may be recalled from section 4.10 that the optimized \underline{e} vector for the desired diplexer is:

$$\underline{e}^t = [.598753 \quad .59955 \quad - .215 \quad 6.71651] .$$

From this \underline{e} vector, the \underline{J} matrix may be formed as:

$$\underline{J} = \begin{bmatrix} .598753 & - .215 \\ - .215 & .5995 \end{bmatrix}$$

Here, it is noted that the coupled length of this diplexer is $L_0 = 6.71651$ mm. Using this \underline{J} and coupled length the output power values in dB at the output ports of this diplexer are computed at different frequencies. The computed power plots of the output ports and the computed relative phase plot (phase of port-2 with respect to that of port-1) are presented in figure 6.5.

After obtaining a \underline{J} matrix from the optimized \underline{e} vector, first the \underline{J} matrix is scaled by multiplication (described in section 3.4.1). This operation is done in such a way that the coupled length L_0 comes in the range of 100 to 250 mm for the selected finger width and periodicity values. While multiplying the \underline{J} matrix by a scaling factor it must be kept in mind that the coupled length L_0 also has to be divided by the same scaling factor to keep the characteristics of the diplexer unchanged.

Equation (3.34) may be rewritten for a diplexer as

$$C_{12} = \frac{2 J_{12}}{\omega_L R_{L_i}} \quad (6.1)$$

Table 6.1.a Result of shifting J matrix by an amount Δj . Here Δj is varied from 0 to .028. The finger length given in this Table represents a *herringbone-line* diplexer having coupled length of 201.49 mm. The data in this Table is obtained from the output of the program FIND_LF.BAS given in appendix C

<ul style="list-style-type: none"> • $e^t = [.598753/30 \quad .59955/30 \quad - .215/30 \quad 6.7165 \times 30]$ • Scaling factor $x = 30$ • Coupled length $L_0 = 201.49$ mm • Coupling Capacitance $C_{12} = 45.6244$ pF/m 						
Line	Δj	Z_0^u in ohms	v_p^u in mm/s	w_m in mm	Z_m in ohms	Finger length
1	0	94.18205	5.929957E+11	8.38148	30.90082	8.689165
2	0	94.02293	5.912069E+11	8.38148	30.94054	8.673311
1	.002	84.84923	4.85575E+11	7.28651	34.03586	7.538556
2	.002	84.75304	4.844384E+11	7.35974	34.06441	7.528712
1	.004	78.88539	4.137595E+11	6.527505	37.14206	6.563409
2	.004	78.82041	4.129607E+11	6.527505	37.18158	6.551844
1	.006	74.71554	3.616948E+11	5.847563	40.24923	5.713981
2	.006	74.66849	3.610975E+11	5.789378	40.30153	5.700898
1	.008	71.62367	3.219241E+11	5.291094	43.34304	4.965777
2	.008	71.58794	3.214581E+11	5.291094	43.38229	4.95676
1	.01	69.2338	2.904082E+11	4.78758	46.43505	4.295668
2	.01	69.20568	2.90033E+11	4.78758	46.47418	4.287546
1	.012	67.32819	2.64741E+11	4.331982	49.52473	3.688722
2	.012	67.30547	2.644318E+11	4.288878	49.57897	3.67909
1	.014	65.77152	2.433885E+11	3.959134	52.61246	3.134109
2	.014	65.75275	2.431288E+11	3.959134	52.6344	3.128781
1	.016	64.475	2.253203E+11	3.618376	55.66161	2.624974
2	.016	64.45923	2.250989E+11	3.618376	55.71795	2.617298
1	.018	63.37782	2.098161E+11	3.340182	58.70531	2.151685
2	.018	63.36438	2.096249E+11	3.306947	58.76099	2.144069
1	.02	62.43692	1.963554E+11	3.052697	61.75987	1.706582
2	.02	62.42532	1.961884E+11	3.052697	61.7983	1.70104
1	.022	61.62085	1.845518E+11	2.817995	64.79018	1.859015
2	.022	61.61074	1.844047E+11	2.817995	64.84793	1.864609
1	.024	60.90615	1.74112E+11	2.601337	67.81298	2.131266
2	.024	60.89726	1.739814E+11	2.601337	67.85112	2.13471
1	.026	60.27492	1.648091E+11	2.401337	70.82794	2.401109
2	.026	60.26703	1.646923E+11	2.401337	70.86592	2.404527
1	.028	59.71325	1.564644E+11	2.238992	73.81548	2.667244
2	.028	59.7062	1.563593E+11	2.238992	73.8533	2.67064

Table 6.1.b Continuation of Table 6.1.a. Here Δj is varied from .030 to .060. The data in this table is obtained from the output of the program FIND.LF.BAS given in appendix C.

<ul style="list-style-type: none"> • $\underline{e}^t = [.598753/30 \ .59955/30 \ - .215/30 \ 6.7165 \times 30]$ • Scaling factor $x = 30$ • Coupled length $L_0 = 201.49$ mm • Coupling Capacitance $C_{12} = 45.6244$ pF/m 						
Line	Δj	Z_0^u in ohms	v_p^u in mm/s	w_m in mm	Z_m in ohms	Finger length
1	.03	59.21018	1.489352E+11	2.06685	76.81343	2.932449
2	.03	59.20385	1.488401E+11	2.06685	76.85113	2.935824
1	.032	58.75694	1.421062E+11	1.927119	79.78278	3.194165
2	.032	58.75122	1.420197E+11	1.927119	79.82034	3.197517
1	.034	58.34646	1.358829E+11	1.778955	82.76262	3.454916
2	.034	58.34126	1.35804E+11	1.778955	82.8	3.458243
1	.036	57.97292	1.301875E+11	1.658686	85.71304	3.712414
2	.036	57.96818	1.301151E+11	1.658686	85.7501	3.715689
1	.038	57.63152	1.249549E+11	1.546549	88.6531	3.967822
2	.038	57.62719	1.248882E+11	1.546549	88.69021	3.971104
1	.04	57.31829	1.201303E+11	1.441993	91.58226	4.22123
2	.04	57.3143	1.200688E+11	1.441993	91.61921	4.22449
1	.042	57.02986	1.156676E+11	1.358018	94.47636	4.471549
2	.042	57.02618	1.156105E+11	1.358018	94.51316	4.474789
1	.044	56.76337	1.11527E+11	1.266207	97.37486	4.720742
2	.044	56.75997	1.11474E+11	1.266207	97.41148	4.723959
1	.046	56.51643	1.076748E+11	1.180604	100.258	4.967916
2	.046	56.51327	1.076254E+11	1.180604	100.2945	4.971113
1	.048	56.28694	1.040816E+11	1.111851	103.1083	5.212433
2	.048	56.284	1.040355E+11	1.111851	103.1447	5.215612
1	.05	56.07311	1.00722E+11	1.036683	105.9626	5.455871
2	.05	56.07037	1.006788E+11	1.036683	105.9988	5.459029
1	.052	55.87339	9.757377E+10	.9763111	108.7855	5.696873
2	.052	55.87083	9.753327E+10	.9665967	108.8388	5.700653
1	.054	55.68642	9.461747E+10	.9103065	111.6123	5.936821
2	.054	55.68402	9.457942E+10	.9103065	111.6482	5.939939
1	.056	55.51102	9.1836E+10	.8572944	114.4089	6.174509
2	.056	55.50876	9.180015E+10	.8572944	114.4446	6.177609
1	.058	55.34614	8.92142E+10	.7993361	117.2092	6.411161
2	.058	55.34401	8.918038E+10	.7993361	117.2448	6.414242
1	.060	55.19086	8.673864E+10	.7527865	119.9805	6.6457
2	.060	55.18885	8.670668E+10	.7527865	120.0159	6.648763

It may be seen from the above equation that the coupling capacitance is *directly* proportional to the off-diagonal element of the \underline{J} matrix and *inversely* proportional to the lower band edge frequency of the diplexer. For a fixed band of operating frequency the off-diagonal element of the \underline{J} matrix is to be incremented or decremented if it is desired to respectively increase or decrease the coupling capacitance. For the selected \underline{e} vector the coupling capacitance is found to be:

$$C_{12} = \frac{2 (.215/30)}{2 \pi 1 \times 10^9 50} = 45.6244 \text{ pF/m}$$

The off-diagonal elements of a \underline{J} matrix can be changed by scaling the \underline{J} matrix as indicated in section 6.5.

In the next step the \underline{J} matrix is shifted by adding a small quantity (say, Δj which may be *+ve* or *-ve*) with the diagonal elements of the \underline{J} matrix. This is done to select a desirable value of finger length, because the finger length is a function¹ of the off diagonal elements of the \underline{J} matrix. With each step of \underline{J} matrix shifting, the characteristic parameters and the finger lengths are also computed.

To obtain a suitable finger length the \underline{J} matrix is shifted according to the rule mentioned in section 3.4.2. The \underline{J} matrix is gradually shifted by adding a constantly increasing quantity (Δj) with the diagonal elements of the \underline{J} matrix (i.e., J_{11} and J_{12}). In the process of shifting, at some point, realizable values of coupling capacitances and finger lengths are obtained. The values that come in the process of \underline{J} matrix shifting technique are listed in tables 6.1.a – 6.2.b. The shifting of \underline{J} matrix is done by running the program FIND.LF.BAS (given in appendix C). The data listed in tables 6.1.a – 6.2.b represent the output of this program written in Quick Basic. The change of uncoupled characteristic impedance (Z_0^u), uncoupled phase velocity (v_p^u), main-line width (w_m), the main-line impedance (Z_m) and the finger length (l_f) with the amount of shifting (Δj) are given in table 6.1 for

¹The nature of relationship between the finger length and the amount by which the diagonal elements of \underline{J} are shifted is latter shown in Figs. 6.3 and 6.4

Table 6.2.a Result of shifting J matrix by an amount Δj . Here Δj is varied from 0 to .028. The finger length given in this Table represents a *Comblin*e diplexer having coupled length of 201.49 mm. The data in this Table is obtained from the output of the program FIND_LF.BAS given in appendix C

<ul style="list-style-type: none"> • $e^t = [.598753/30 \quad .59955/30 \quad - .215/30 \quad 6.7165 \times 30]$ • <i>Scaling factor</i> $x = 30$ • <i>Coupled length</i> $L_0 = 201.49$ mm • <i>Coupling Capacitance</i> $C_{12} = 45.6244$ pF/in 						
Line	Δj	Z_0^u in ohms	v_p^u in mm/s	w_m in mm	Z_m in ohms	Finger length
1	0	94.18205	5.929957E+11	8.38148	30.90082	13.49306
2	0	94.02293	5.912069E+11	8.38148	30.94054	13.4687
1	.002	84.84923	4.85575E+11	7.28651	34.03586	11.68929
2	.002	84.75304	4.844384E+11	7.35974	34.06441	11.67472
1	.004	78.88539	4.137595E+11	6.527505	37.14206	10.12594
2	.004	78.82041	4.129607E+11	6.527505	37.18158	10.1073
1	.006	74.71554	3.616948E+11	5.847563	40.24923	8.734396
2	.006	74.66849	3.610975E+11	5.789378	40.30153	8.712143
1	.008	71.62367	3.219241E+11	5.291094	43.34304	7.485154
2	.008	71.58794	3.214581E+11	5.291094	43.38229	7.470037
1	.01	69.2338	2.904082E+11	4.78758	46.43505	6.346313
2	.01	69.20568	2.90033E+11	4.78758	46.47418	6.332463
1	.012	67.32819	2.64741E+11	4.331982	49.52473	5.298165
2	.012	67.30547	2.644318E+11	4.288878	49.57897	5.28099
1	.014	65.77152	2.433885E+11	3.959134	52.61246	4.325912
2	.014	65.75275	2.431288E+11	3.959134	52.6344	4.317562
1	.016	64.475	2.253203E+11	3.618376	55.66161	3.423666
2	.016	64.45923	2.250989E+11	3.618376	55.71795	3.409108
1	.018	63.37782	2.098161E+11	3.340182	58.70531	2.574659
2	.018	63.36438	2.096249E+11	3.306947	58.76099	2.560614
1	.02	62.43692	1.963554E+11	3.052697	61.75987	1.767704
2	.02	62.42532	1.961884E+11	3.052697	61.7983	1.757645
1	.022	61.62085	1.845518E+11	2.817995	64.79018	2.14422
2	.022	61.61074	1.844047E+11	2.817995	64.84793	2.15579
1	.024	60.90615	1.74112E+11	2.601337	67.81298	2.750398
2	.024	60.89726	1.739814E+11	2.601337	67.85112	2.758052
1	.026	60.27492	1.648091E+11	2.401337	70.82794	3.342931
2	.026	60.26703	1.646923E+11	2.401337	70.86592	3.350425
1	.028	59.71325	1.564644E+11	2.238992	73.81548	3.920262
2	.028	59.7062	1.563593E+11	2.238992	73.8533	3.927613

Table 6.2.b Continuation of Table 6.2.a. Here Δj is varied from .030 to .060. The data in this table is obtained from the output of the program FIND.LF.BAS given in appendix C.

<ul style="list-style-type: none"> • $\underline{e}^t = [.598753/30 \ .59955/30 \ - .215/30 \ 6.7165 \times 30]$ • <i>Scaling factor</i> $x = 30$ • <i>Coupled length</i> $L_0 = 201.49$ mm • <i>Coupling Capacitance</i> $C_{12} = 45.6244$ pF/m 						
Line	Δj	Z_0^u in ohms	v_p^u in mm/s	w_m in mm	Z_m in ohms	Finger length
1	.03	59.21018	1.489352E+11	2.06685	76.81343	4.488529
2	.03	59.20385	1.488401E+11	2.06685	76.85113	4.495749
1	.032	58.75694	1.421062E+11	1.927119	79.78278	5.04348
2	.032	58.75122	1.420197E+11	1.927119	79.82034	5.050573
1	.034	58.34646	1.358829E+11	1.778955	82.76262	5.590447
2	.034	58.34126	1.35804E+11	1.778955	82.8	5.597417
1	.036	57.97292	1.301875E+11	1.658686	85.71304	6.125572
2	.036	57.96818	1.301151E+11	1.658686	85.7501	6.132391
1	.038	57.63152	1.249549E+11	1.546549	88.6531	6.651484
2	.038	57.62719	1.248882E+11	1.546549	88.69021	6.658232
1	.04	57.31829	1.201303E+11	1.441993	91.58226	7.168623
2	.04	57.3143	1.200688E+11	1.441993	91.61921	7.175267
1	.042	57.02986	1.156676E+11	1.358018	94.47636	7.675329
2	.042	57.02618	1.156105E+11	1.358018	94.51316	7.681875
1	.044	56.76337	1.11527E+11	1.266207	97.37486	8.175397
2	.044	56.75997	1.11474E+11	1.266207	97.41148	8.181844
1	.046	56.51643	1.076748E+11	1.180604	100.258	8.667416
2	.046	56.51327	1.076254E+11	1.180604	100.2945	8.67377
1	.048	56.28694	1.040816E+11	1.111851	103.1083	9.150455
2	.048	56.284	1.040355E+11	1.111851	103.1447	9.156721
1	.05	56.07311	1.00722E+11	1.036683	105.9626	9.627443
2	.05	56.07037	1.006788E+11	1.036683	105.9988	9.633619
1	.052	55.87339	9.757377E+10	.9763111	108.7855	10.09615
2	.052	55.87083	9.753327E+10	.9665967	108.8388	10.10335
1	.054	55.68642	9.461747E+10	.9103065	111.6123	10.55909
2	.054	55.68402	9.457942E+10	.9103065	111.6482	10.5651
1	.056	55.51102	9.1836E+10	.8572944	114.4089	11.0143
2	.056	55.50876	9.180015E+10	.8572944	114.4446	11.02022
1	.058	55.34614	8.92142E+10	.7993361	117.2092	11.46394
2	.058	55.34401	8.918038E+10	.7993361	117.2448	11.46978
1	.06	55.19086	8.673864E+10	.7527865	119.9805	11.90629
2	.06	55.18885	8.670668E+10	.7527865	120.0159	11.91205

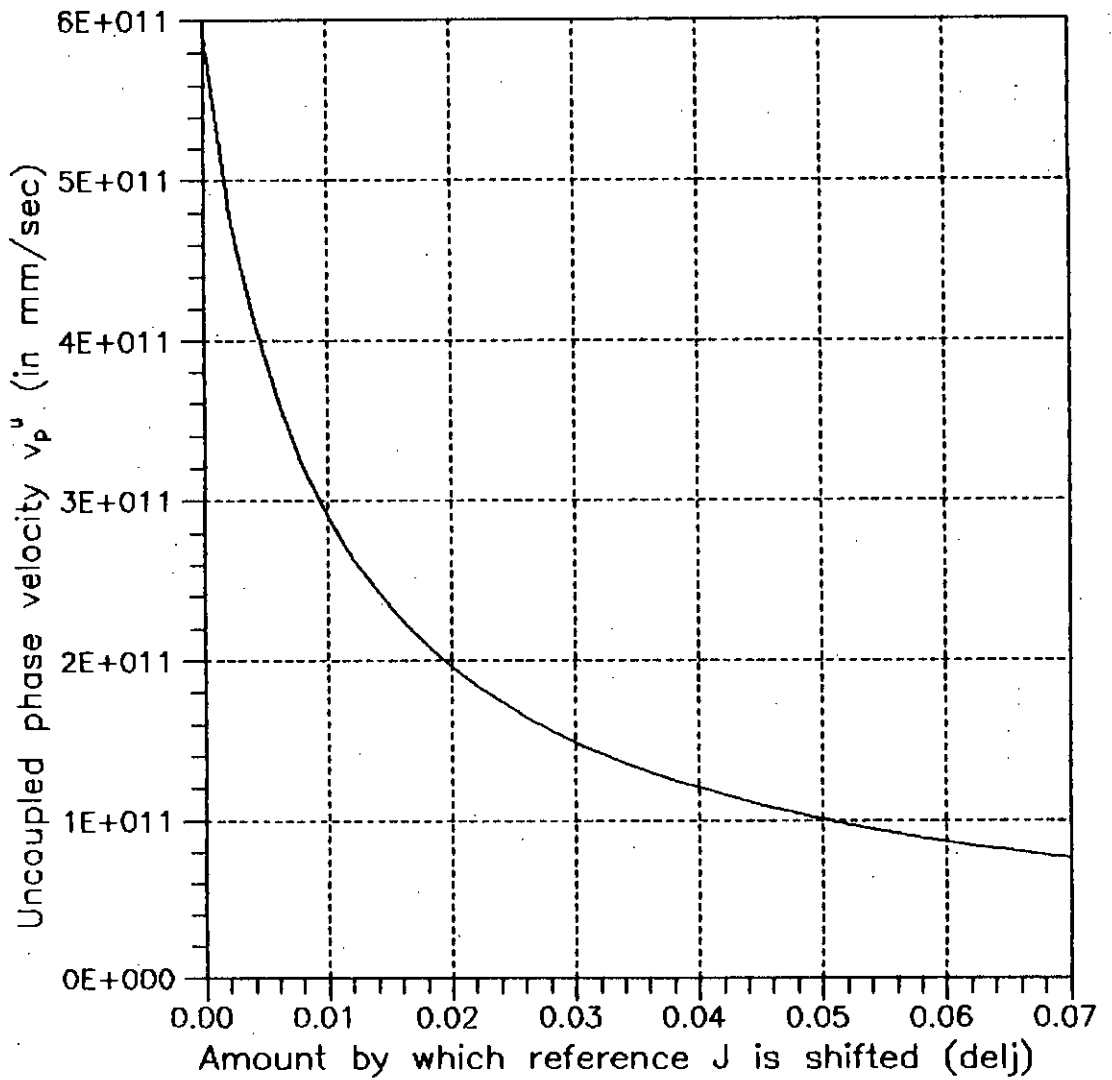


Figure 6.1 The uncoupled phase velocity v_p^u vs. Δj plot of a comb-and-herringbone-line diplexer having coupled length of 201.49 mm. The reference \underline{J} matrix is:

$$\underline{J} = \frac{1}{30} \begin{bmatrix} 0.598753 & -0.215 \\ -0.215 & 0.59955 \end{bmatrix}$$

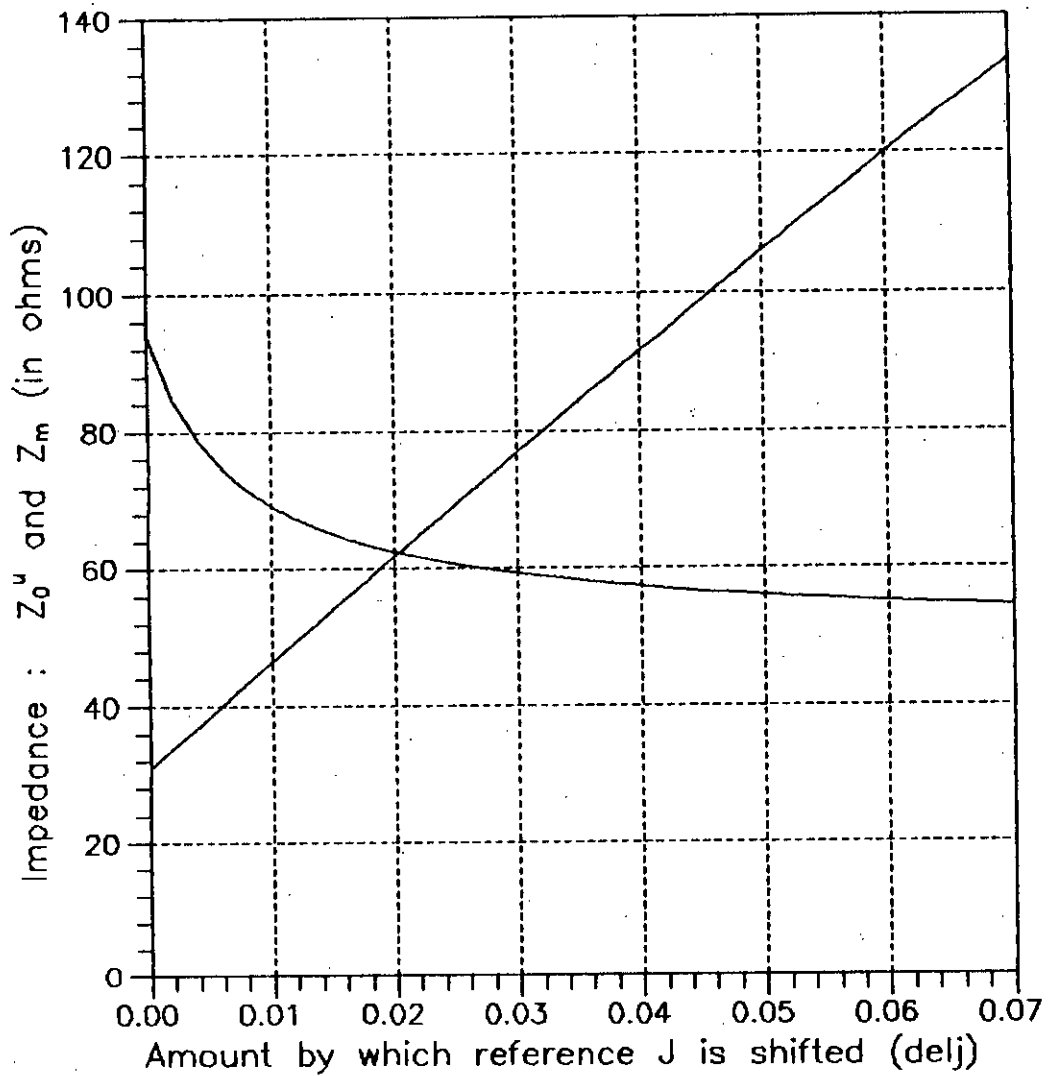


Figure 6.2 The *main line impedance* Z_m and *uncoupled characteristic impedance* Z_0^u vs. Δj plot of a *comb- and herringbone- line diplexer* having coupled length of 201.49 mm. The reference \underline{J} matrix is:

$$\underline{J} = \frac{1}{30} \begin{bmatrix} 0.598753 & -0.215 \\ -0.215 & 0.59955 \end{bmatrix}$$

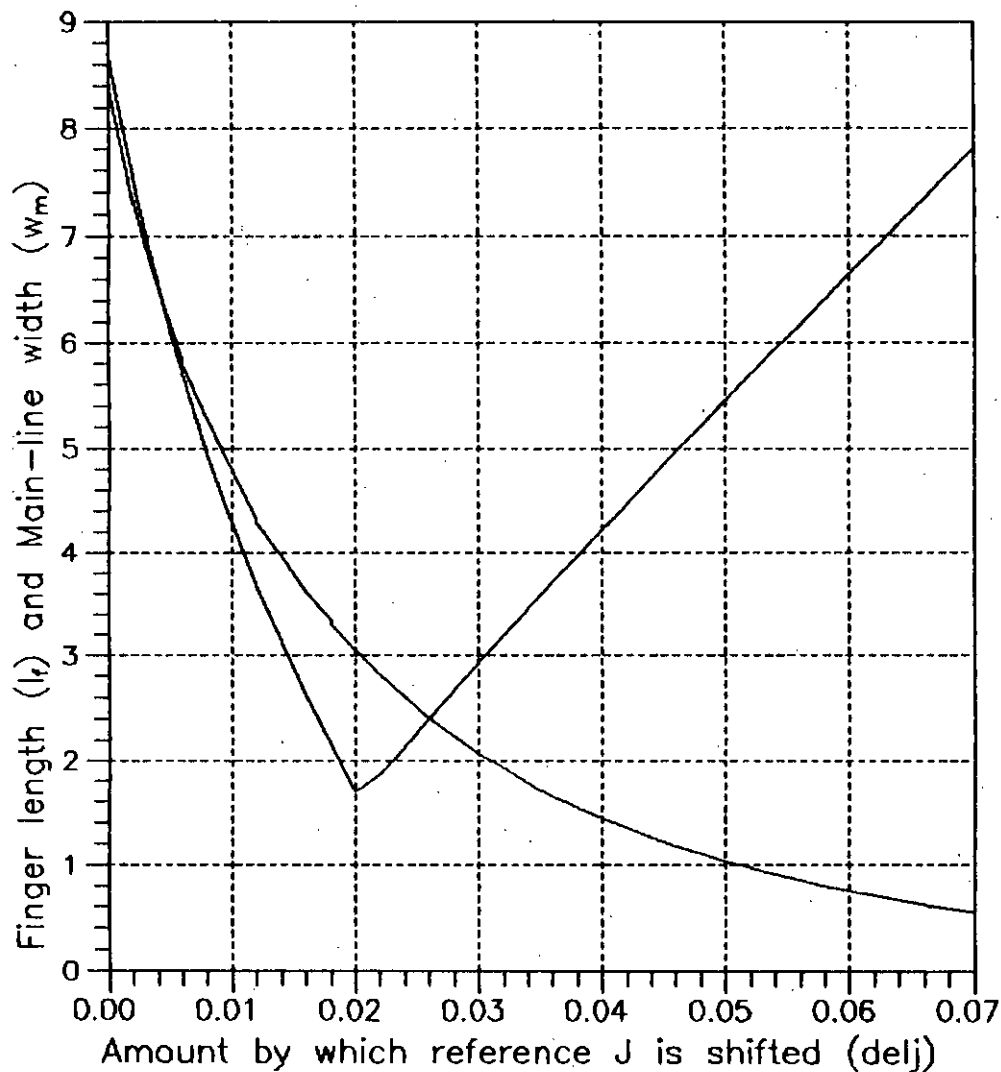


Figure 6.3 The main line width w_m and finger length l_f vs. Δj plot of a herringbone-line diplexer having coupled length of 201.49 mm. The reference \underline{J} matrix is:

$$\underline{J} = \frac{1}{30} \begin{bmatrix} 0.598753 & -0.215 \\ -0.215 & 0.59955 \end{bmatrix}$$

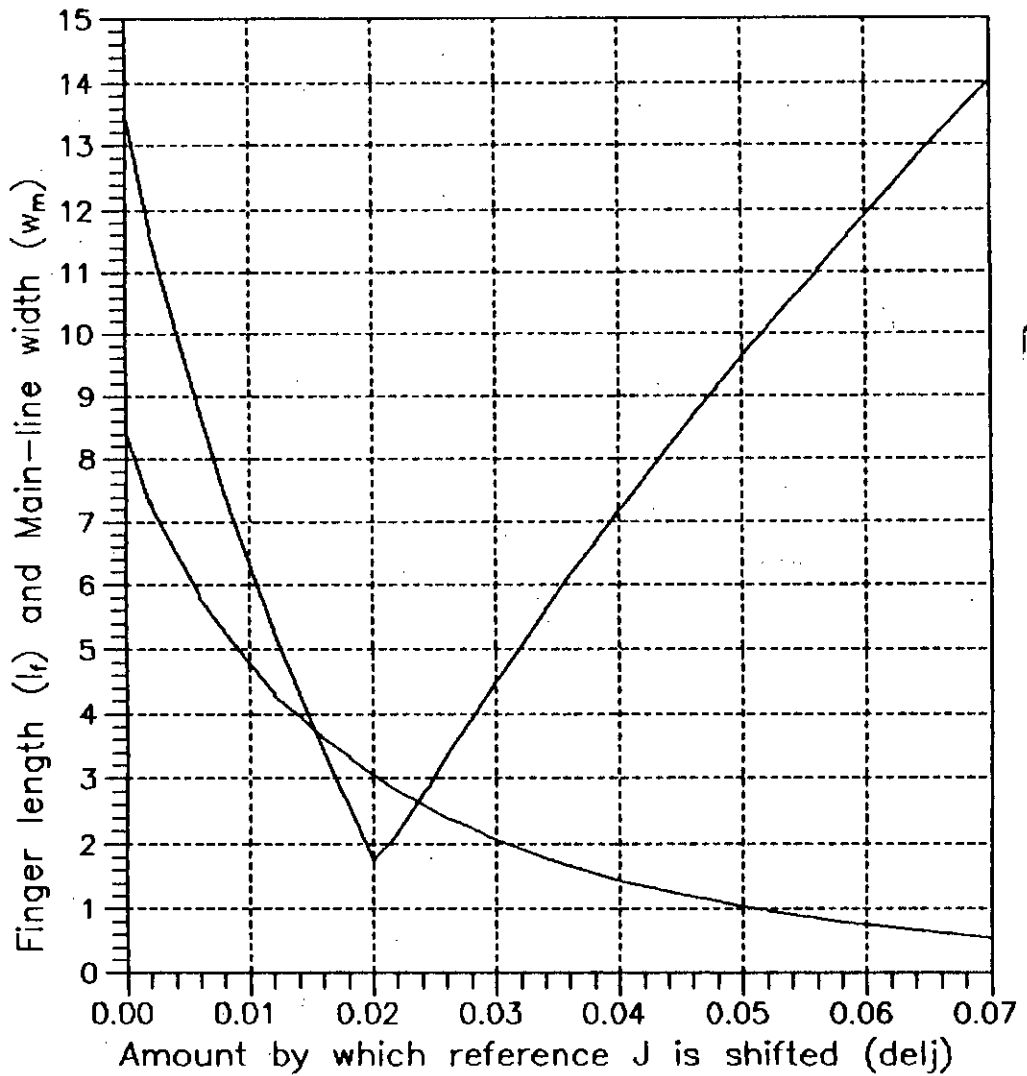
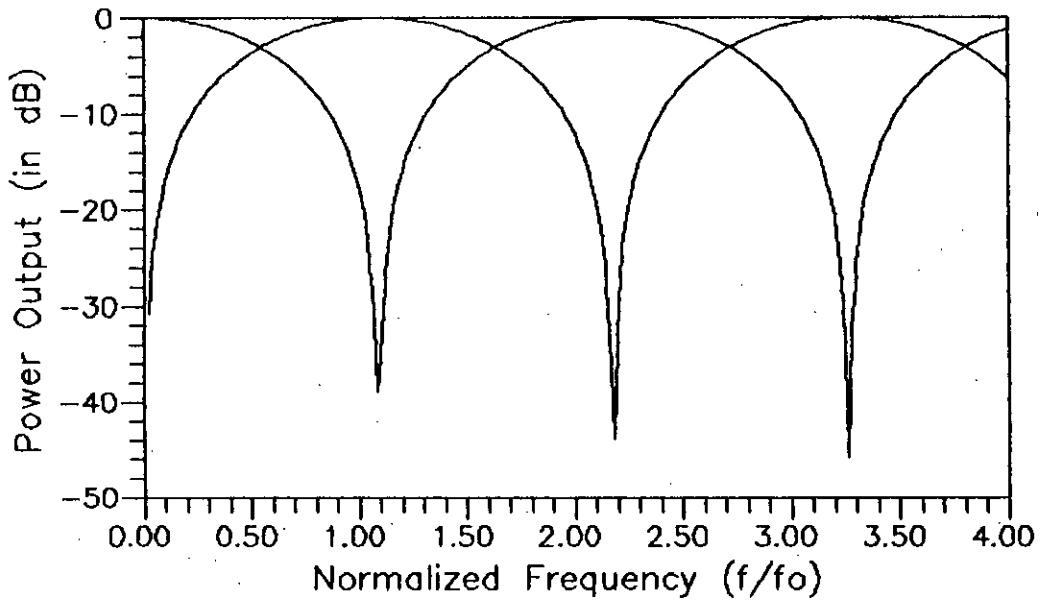
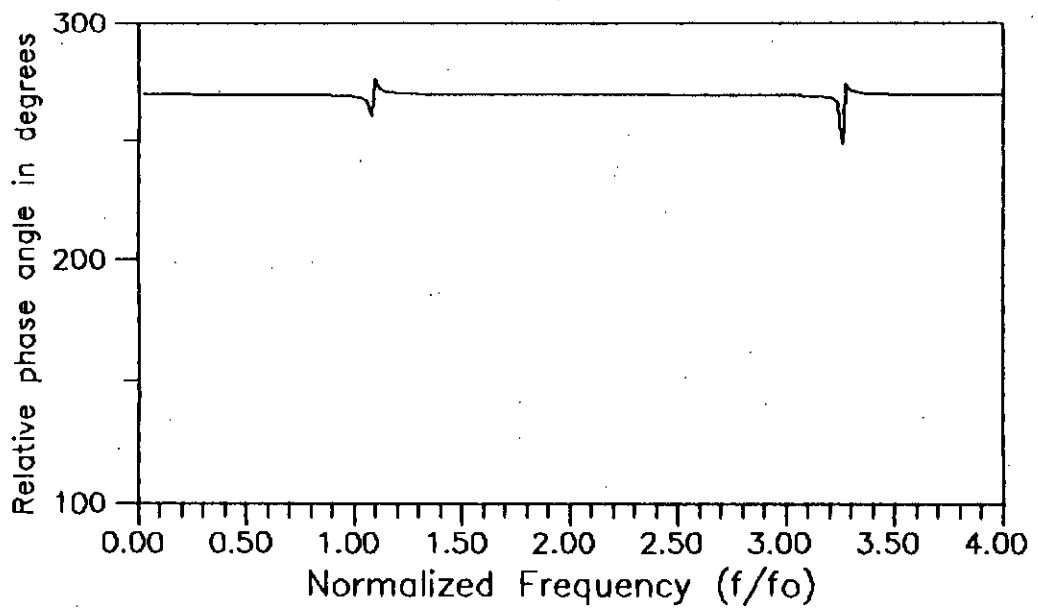


Figure 6.4 The main line width w_m and finger length l_f vs. Δj plot of a *compline* diplexer having coupled length of 201.49 mm. The reference \underline{J} matrix is:

$$\underline{J} = \frac{1}{30} \begin{bmatrix} 0.598753 & -0.215 \\ -0.215 & 0.59955 \end{bmatrix}$$



(a)



(b)

Figure 6.5 The characteristics of the designed diplexer. The corresponding \underline{e} vector is shown in table 6.1 and 6.2. a) Power against frequency plot, b) relative phase angle of channel-2 with respect to

a *comblin*e diplexer. Similar data for *herringbone-line* diplexer are presented in table 6.2. The data presented in tables 6.1.a – 6.2.b have been used for plotting figures 6.1 – 6.4.

The amount by which \underline{J} matrix is shifted (i.e., Δj)² from a reference \underline{J} matrix³ is taken as the x-axis of the plots. The uncoupled phase velocity v_p^u against Δj plot is shown in Fig 6.1. The variation of the *finger length* and the *main line width* with changing Δj is shown in figure 6.2. The variation of *uncoupled characteristic impedance* and *main line impedance* with Δj of a herringbone- and comb- line are shown in Figs. 6.3 and 6.4 respectively.

6.5 The design values

Thirty one values of Δj have been considered for computing the values of Z_0^u , v_p^u , main-line width w_m , Z_m , finger lengths of the two coupled comblines of which both the lines are in comb form (table 6.1). Similarly table 6.2 contains similar values for the coupled combline system with the two lines in herringbone form. For the design of diplexer under consideration either combline (from table 6.1) or herringbone-line (from table 6.2) may be chosen.

Any of the values of Δj which gives finger lengths in the range of 3 to 5 mm may be taken as the accepted amount of shifting to be done. This amount of shifting is performed on the reference, i.e., the optimized and scaled \underline{J} matrix to obtain the final \underline{J} matrix which is used to obtain the dimensions of the diplexer.

In this research, Δj is accepted as 0.036 for *herringbone-line* from table 6.1.b. With this amount of shifting *finger lengths* for line-1 and line-2 are found to be 3.712414 (≈ 3.712) mm and 3.715684 (*approx*3.716) mm respectively. The *mainline width* for herringbone-lines (w_m) are found to be 1.658686 (≈ 1.659) mm for both

² Δj is represented by the variable *delj* in the program FIND.LF.BAS

³The optimized \underline{e} vector obtained from table 4.2.b is used as the *reference J matrix*

Table 6.3 The physical dimensions of a herringbone- and a comb- line diplexer required for fabricating a practical diplexer. The diplexers under consideration have operating bands in ranges of (1 – 1.3) GHz and (2 – 2.3) GHz.

Physical dimensions of diplexer	
Precision upto maximum three decimal digits is considered for the design data presented in this table	
• Coupled length (L_0)	: 201.49 mm.
• Finger line width (w_f)	: 1.0 mm.
• Substrate thickness (h)	: 1.5 mm.
• Finger periodicity (p)	: 2.4 mm.
• Finger overlap	: 2.4 mm.
★ For <i>herringbone-line</i> :	
• Finger length of line-1	: 3.712 mm.
• Finger length of line-2	: 3.716 mm.
• Main-line width (w_m)	: 1.659 mm.
★ For <i>comb-line</i> :	
• Finger length of line-1	: 3.920 mm.
• Finger length of line-2	: 3.928 mm.
• Main-line width (w_m)	: 2.239 mm.

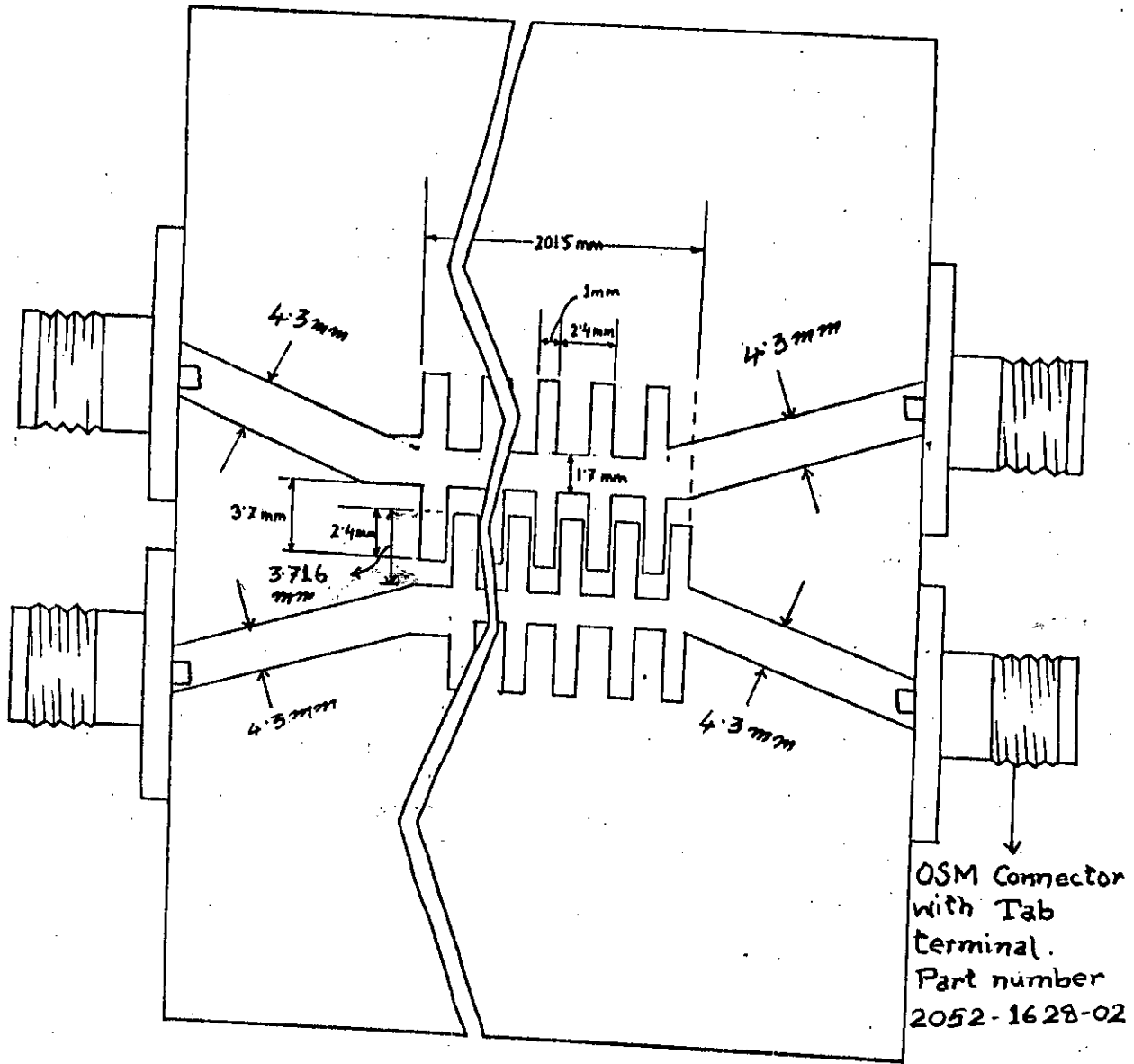


Figure 6.7 The schematic diagram of the *herringbone-line* diplexer with obtained design values as indicated in table 6.3. The figure is drawn in 3:1 scale.

the lines. As mentioned earlier, the *width of the finger lines* are accepted as 1 mm for both the lines. As shown in section 6.4 and tables 6.1 and 6.2, the *coupling capacitance* is found to be 45.6244 pF/m. Using this coupling capacitance the amount of finger overlap is found out with the help of figure 5.6. In this case, the *finger periodicity* has been taken as 2.4 mm and the amount of *finger overlap* is found to be 2.4 mm from the graph (figure 5.6).

For a comb-line diplexer, Δj is accepted as .028 from table 6.2.a. All the other dimensions except the finger length and the main-line width remain the same as that of herringbone-line. The *finger lengths* of line-1 and line-2 are found to be 3.920262 (≈ 3.920) mm and 3.927613 (≈ 3.928) mm respectively from table 6.2.a. From the same table the main-line width of line-1 and line-2 are found to be 73.81548 (≈ 73.815) mm and 73.8533 (≈ 73.853) mm respectively.

The physical dimensions of a diplexer for both herringbone- and comb- line configurations are shown in table 6.3. The designs are schematically presented in figure 6.6. A drawing of the designed diplexer is presented in figures 6.6 and 6.7. This drawing is prepared using 2:1 scale. This drawing shows that this diplexer can be fabricated by using usual photolithographic and etching techniques without any difficulty.

6.6 Summary

The design values of a practical diplexer have been obtained through scaling and shifting of \underline{J} matrix. Finally the physical dimensions of the desired combline diplexer have been presented for realization in the form of two coupled comblines and also in the form of two coupled herringbone-lines.

CHAPTER 7

Discussions and suggestions for future work

7.1 Discussions

A computer optimization based method for designing a microstrip combline diplexer has been presented. This work utilizes the theory of generalized coupled lines. In this work the \underline{g} vector of a diplexer is obtained by computer optimization of the elements of this vector for obtaining the desired bands of operation of the output ports of the diplexer. For this optimization job the \underline{g} vector of a 3dB directional coupler has been taken as a starting point. This starting point is not unique. However, it appears that such a starting point works well for the desired design of a diplexer. It has been observed that the two operating bands of the two ports can not be brought very close to each other, because the behaviour of a pair of coupled combines does not permit to do so. As a result of this, contiguous channel type diplexers can not be realized using this type of coupled combines.

The characteristics of such a diplexer show that the output power level within the operating band of output port-1 is not the same as the input power level. This is because of the fact that in the useful band of output port-1 small amount of power remains at the other output port. Similar explanation holds for the power at the output port-2 within its operating band. This behaviour makes this diplexer somewhat different than the conventional diplexers. However, this does not prohibit the use of such diplexers in communication networks. Even if, within the operating bands of output ports, the same power level as the input port is required then this can be obtained by making an additional arrangement. In this arrangement one

simple solid state identical amplifier can be added at each output port as shown in figure 7.1. The resulting device can still be in one microstrip substrate board. This means that the diplexer along with the solid state amplifiers can be fabricated in Monolithic Microwave Integrated Circuits (MMIC) form.

In selecting the solid state amplifiers care must be taken so that the operating band (flat characteristic) of such an amplifier is wider than the operating band of the corresponding output port. The addition of these solid state amplifiers provides with additional facility of adjusting the output power level to the desired level.

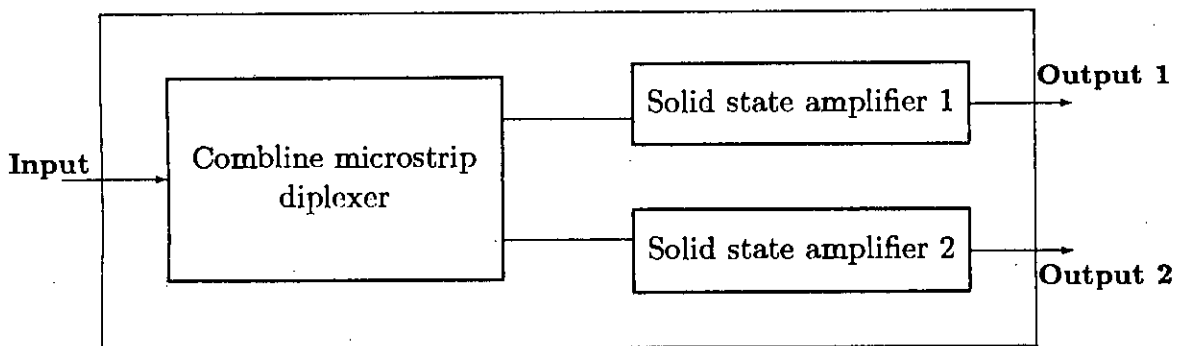


Figure 7.1 The modified diplexer after adding the solid state amplifiers with the output ports. The combine diplexer and the solid state amplifiers are on the same substrate board.

7.2 Suggestions for future work

A suggestion for possible future work for the microstrip diplexer is presented in subsection 7.2.1. Besides this, further extension of the design method of the present type of diplexer are presented in subsections 7.2.2 and 7.2.3.

7.2.1 Developing an analytical design method

As mentioned in section 6.1 the design method presented in this thesis is based on computer optimization. It would be interesting to investigate the possibility of

developing an analytical method. An analytical method will be much more simple in application. It is hoped that if an analytical method could be developed then one would be able to find out the flexibilities in the design. Also, using an analytical method, the computation time required for a design job can be significantly reduced. So developing an analytical method for designing such a diplexer is expected to be very useful for understanding the behaviour of the coupled line system.

7.2.2 Developing a design method for a microstrip combline triplexer

The design procedure of a diplexer presented in this thesis may be extended for designing a triplexer. In case of a triplexer there will be three microstrip lines one of which will be direct and the other two will be coupled lines. The equations of an n -line coupled system presented in chapter 2 are applicable for such a triplexer. It is expected that by extending the same optimization and computation technique it will be possible to develop a design method for a triplexer. For the computational purpose, new programs to find eigenvalues, eigenvectors and scattering matrix will be required. It is worthwhile to investigate whether the same optimization algorithm (i.e., the steepest descent algorithm) works for the triplexer design.

7.2.3 Developing a designing method for microstrip combline quadruplexers, quintoplexers and n -channel multiplexers

If the design of a triplexer seems to work satisfactorily, one may go for designing a quadruplexer. The idea then can be extended for quintoplexer and in general for multiplexers. The mathematical models of these multiplexers will require matrices of higher orders and the computations will naturally be more complicated. The higher the number of channels the more complex is the computational procedure. Besides, the behaviour of the coupled combline system is expected to be quite complicated. The computations for optimization will become more and more time consuming because of the increase in the number of independent variables. As a result a powerful optimization method will be required. Probably the quasi-

Newton method is expected to provide good results. For finding the eigenvalues and eigenvectors of a multiplexer it is advisable to use mathematical routines provided by any programming language or mathematical packages (like Matlab or Mathcad).

Appendix A

List of the computer program for obtaining the power and relative phase characteristics of the ports of a diplexer

```
*****
*
*           Name of the program   : PAL.FOR
*           Language              : FORTRAN77
*           Programmer            : Md. Sayeed Akmal
*
*****
*
* This program may be used to compute the POWER and RELATIVE PHASE
* of the two lines of a diplexer at different frequencies between
* 0 to 4.0 GHZ. This program has been used in this work to create
* data-files for plotting POWER against FREQUENCY and RELATIVE
* PHASE against FREQUENCY characteristics.
*
*****
```

```
COMPLEX C1, C2, C3, C4, S(2,2), SO, CHECK
REAL N, J, L, L1, L2, L3, L4, FO

DIMENSION E(4), J(2,2), B(2), Q(2,2)
* DATA E/.646, -.5523, -.501, 1.536 /
* DATA J/.646, -.2, -.2, .5523 /
```

```
*****
*
* The following \e vectors have been used to make data files
* required for plotting the curves shown in Figs.4.6 to 4.23.
*
*****
```

```
***** Data with only varying E(1)=d1 *****
*
* DATA E/ 1.5, .5, -.2, 6.0 /
* DATA E/ 1.0, .5, -.2, 6.0 /
* DATA E/ 0.75, .5, -.2, 6.0 /
* DATA E/ 0.5, .5, -.2, 6.0 /
```

```

*      DATA E/ 0.25, .5, -.2, 6.0 /
*      DATA E/ 0.0, .5, -.2, 6.0 /

***** Data with only varying E(2)=d2 *****
*      DATA E/ .5, 1.5, -.2, 6.0 /
*      DATA E/ .5, 1.0, -.2, 6.0 /
*      DATA E/ .5, 0.75, -.2, 6.0 /
*      DATA E/ .5, 0.5, -.2, 6.0 /
*      DATA E/ .5, 0.25, -.2, 6.0 /
*      DATA E/ .5, 0.0, -.2, 6.0 /

***** Data with only varying E(3)=c1 *****
*      DATA E/ .50001, .5, -.01, 6.0 /
*      DATA E/ .50001, .5, -.1, 6.0 /
*      DATA E/ .50001, .5, -.3, 6.0 /
*      DATA E/ .50001, .5, -.6, 6.0 /

***** Data with only varying E(4)=Lo *****
*
*      DATA E/ .50001, .5, -.2, 2.0 /
*      DATA E/ .50001, .5, -.2, 6.0 /
*      DATA E/ .50001, .5, -.2, 10.0 /
*      DATA E/ .50001, .5, -.2, 15.0 /

***** Data from the paper *****
*      DATA E/.646, .5523, -.501, 15.36 /

***** Starting e vector *****
*      DATA E/.646, .5523, -.2, 6.7 /

***** Test e vectors *****
DATA E/ 2.0, 1.0, -.2, 6.0 /

J(1,1) = E(1)
J(2,2) = E(2)
J(1,2) = E(3)
J(2,1) = J(1,2)

PI = 3.1415927
ICOUNT = 0
ISIGN = -1

*****
*
*      Computing the EIGENVALUES: B(1) & B(2) of J matrix
*
*****

B1 = (J(1,1)+J(2,2))
B2 = SQRT( ( J(1,1)+J(2,2))**2 - 4.0*( J(1,1)*J(2,2)-J(1,2)
+      *J(2,1) ) )

```

```

      B(1) = (B1 + B2) / 2.0
      B(2) = (B1 - B2) / 2.0

      WRITE(*,10) B(1), B(2)
10    FORMAT( 'Eigenvalues are:   B(1) = ',f10.8, '   B(2) = ',
      +      f10.8 )

*****
*
*      Time to find Eigenvectors of J matrix using B(1) & B(2)
*
*****

      Q(1,1) = 1.0
      Q(2,1) = 1.0

      DO 20 I = 1, 2
          Q(I,2) = ( B(I) - J(1,1) ) / J(1,2)
          N = SQRT( 1.0 + Q(I,2) * Q(I,2) )

*****
*
*      Normalization of Eigenvector elements:
*
*****

          Q(I,1) = 1.0 / N
          Q(I,2) = Q(I,2)/N

20    CONTINUE

      WRITE(*,30) ((Q(I,K), K=1, 2 ), I=1, 2)
30    FORMAT(//'The Eigenvector Q is: ', 2(f20.8), /21x, 2(f20.8))

      L = E(4)
      L1 = L * B(1)
      L2 = L * B(2)

*****
*
*      Open files here if necessary for writing data files of
*      POWER and RELATIVE PHASE against FREQUENCY.
*
*****
*
      OPEN( 8, FILE = 'D:\AKMAL\DAT\fig424B.dat' )
      OPEN( 9, FILE = 'D:\AKMAL\DAT\PHS424B.DAT' )
*
*****

      DO 40 F = .02, 4, .02

```

```

        L3 = L1 * F
        L4 = L2 * F
        C3 = (0,-1) * L3
        C4 = (0,-1) * L4

*      PRINT *, 'L3, L4, C3, C4 ', L3, L4, C3, C4

        C1 = CEXP( C3 )
        C2 = CEXP( C4 )

*      CHECK = ( Q(1,1)**2 ) * C1 + ( Q(2,1)**2)*C2
*      PRINT *, 'CHECK = ',CHECK

*****
*
*      Computing Scattering matrix Soi :
*
*****

        DO 50 I = 1, 2
        DO 50 K = 1, 2
            S(I,K) = Q(1,I) * C1 * Q(1,K) + Q(2,I) * C2 * Q(2,K)
50      CONTINUE

*      WRITE(*, 60) f, ( ( S(I,K), K=1,2), I=1,2 )
60      FORMAT(//'The Forward Scattering matrix Soi : at f= ',
+             f10.8, /12x, 2(f12.8), 5x, 2(f12.2), /12x, 2(f12.8),
+             5x, 2(f12.8), //)

*****
*
*      Computing OUTPUT POWER of the two lines
*
*****

        PO1 = 20.0 * ALOG10( CABS( S(1,1) ) )
*      PHI1 = ATAN( IMAG(S(1,1)) / REAL(S(1,1)) ) * 180/PI

        PO2 = 20.0 * ALOG10( CABS( S(1,2) ) )
*      PHI2 = ATAN( IMAG(S(1,2)) / REAL(S(1,2)) ) * 180/PI

*****
*
*      Computing RELATIVE PHASE between the two lines
*
*****

        PHIR = ATAN( (IMAG(S(1,2))*REAL(S(1,1)) - REAL(S(1,2))*
+             IMAG(S(1,1)) ) / (REAL(S(1,1))*REAL(S(1,2)) +
+             IMAG(S(1,1))*IMAG(S(1,2)) ) ) * 180/PI

```

```

IF (PHIR .LT. 0) NSIGN = -1
IF (PHIR .GT. 0) NSIGN = 1

IF (ISIGN .NE. NSIGN) ICOUNT = ICOUNT + 1

ISIGN = NSIGN

IF ( ICOUNT .EQ. 0 .OR. ICOUNT .EQ. 1) MCOUNT = 1
IF ( ICOUNT .EQ. 2 .OR. ICOUNT .EQ. 3) MCOUNT = 3
IF ( ICOUNT .EQ. 4 .OR. ICOUNT .EQ. 5) MCOUNT = 5
IF ( ICOUNT .EQ. 6 .OR. ICOUNT .EQ. 7) MCOUNT = 7
IF ( ICOUNT .EQ. 8 .OR. ICOUNT .EQ. 9) MCOUNT = 9
IF ( ICOUNT .EQ. 10 .OR. ICOUNT .EQ. 11) MCOUNT = 11
IF ( ICOUNT .EQ. 12 .OR. ICOUNT .EQ. 13) MCOUNT = 13
IF ( ICOUNT .EQ. 14 .OR. ICOUNT .EQ. 15) MCOUNT = 15
IF ( ICOUNT .GT. 15) THEN
  PRINT *, ' Angle Exceeds 1530 degrees.'
  PRINT *, ' To handle this please add more IF statements here.'
  STOP
END IF

PHIRF = (90.0 + PHIR) + MCOUNT * 90.0
*   IF (PHIR .LT. 0.0) PHIRF = (90.0 + PHIR) + 90

*   XX = TAN(PHIR*PI/180.0) - TAN(PHIRF*PI/180.0)

*****
*
*   Writing Frequency, Power and Relative phase in the data files
*
*****

      WRITE(8,*) F, PO1, PO2
      WRITE(9,*) F, PHIRF

*   PRINT*, ICOUNT, PHIR, PHIRF, XX

40   CONTINUE

      END

*****
*
*   END of the program
*
*****
*****

```

Appendix B

List of the computer program for optimizing the e vector of a diplexer

```
*****
*
*           Name of the Program:  OPT:FOR
*           Language   :  FORTRAN77
*           Programmer:  Md. Sayeed Akmal
*
*****
*
*   This is the main optimization program. This program is used to
*   optimize the [e] matrix so that the maximum power may be obtained
*   at the output port of the two lines at two selected bands
*   of frequencies.
*
*   This is the main optimization program. The flowchart of this
*   main program is given in Fig. 4.29(a) and the flowchart of the
*   subroutine ERROR is given in Fig. 4.29(b). Please refer to section
*   4.9 for detailed description of the algorithm of this program.
*
*****

      REAL E(4), U(4), V(4)
      INTEGER COUNT

      TERR = 100.0
      DELX = .00075
      COUNT = 0

***** Some sample e vectors *****

*   DATA E / 0.646, 0.5523, -.2, 6.7 /
*   DATA E / 0.75, 0.5, -.2, 6.0 /

*   DATA E /.5991923, .5991077, -.2046001, 15.3346700 /
*   DATA E /.604177, .6037722, -.2400954, 6.702775 /
*   DATA E /.55, .56, -.20, 6.0 /
*****
*   The optimized e vector .....
*   e = [ .5990006 .5992994 -.215 6.715999 ]
```



```

*
*****
*****
*
*           VERIABLE IDENTIFICATION:
*           -----
*
*   TERR : Temporary Error.
*
*   delx : Value of Increment or Decrement.
*
*   PERR : Previous Error with which recent Error is compared.
*
*   E     : Original E Matrix, [ J11  J22  J12  L ]
*                   or, [ C1  C2  d1  L0 ]
*
*   U     : Holds the currently Optimized E Matrix.
*
*   V     : Temporary Matrix containing the values of U Matrix on
*           which the ERROR Subroutine operates,
*
*****

      DO 110 I = 1, 4
110      U(I) = E(I)

*****
*
*   Open file for writing data for Tables 4.1 and 4.2
*
*   OPEN ( 8, FILE = 'D:\AKMAL\DAT\tAB1.DAT' )
*
*****

300  CALL ERROR ( U, ERR, POWER )

      PERR = ERR
      COUNT = COUNT + 1

      WRITE (*,150) ERR

      PRINT*, 'Iteration = ', COUNT, 'ERROR=', ERR, 'POWER=', POWER
*   PRINT *, 'THE NEW e VECTOR:'
*   WRITE (*,163) U(1), U(2), U(3), U(4)

      WRITE (8,173) COUNT, (U(I),I=1,4), ERR, POWER
173  FORMAT(I4,'& ',4(F8.6,' & '),F9.6,' & ',F9.6,' \\ \hline')

```

```

150  FORMAT (/'ERR: ', F16.10,/ )
160  FORMAT ( 4 (F16.10) )
170  FORMAT ( I3, 6(F12.8) )

      IF (PERR .GE. TERR ) GOTO 600

      DO 120 I = 1, 4
120   V(I) = U(I)

      DO 500 I = 1, 4
      V(I) = U(I) + DELX

      CALL ERROR ( V, ERR, POWER)
      IF ( ERR .LT. PERR ) GOTO 400
      V(I) = U(I) - DELX

      CALL ERROR ( V, ERR, POWER )
      IF ( ERR .LT. PERR ) GOTO 400
      V(I) = U(I)

400   TEMP = U(I)
      U(I) = V(I)
      V(I) = TEMP

500   CONTINUE

      TERR = PERR
      GOTO 300

600   PRINT *, '----- OPTIZATION COMPLETE-----'

      END

```

```

*
*
*       MAIN PROGRAM ENDS HERE.....
*
*****
*****

```

```

SUBROUTINE ERROR ( E, ERR, POWER )

```

```

*****
*
*       SUBROUTINE : ERROR
*
*****

```

```

COMPLEX C1, C2, C3, C4, S(2,2), SO, CHECK
REAL N, J, L, L1, L2, L3, L4

```

```
DIMENSION E(4), J(2,2), B(2), Q(2,2)
```

```
*****
```

```
*      YR is the reference value around which error is computed
```

```
*****
```

```
      YR = 0.1  
      J(1,1) = E(1)  
      J(1,2) = E(3)  
      J(2,1) = E(3)  
      J(2,2) = E(2)
```

```
*****
```

```
*
```

```
      Computing the EIGEN VAUES: B(1) & B(2) of J Matrix
```

```
*
```

```
*****
```

```
      B1 = J(1,1) + J(2,2)  
      B2 = SQRT( B1*B1 - 4.0 * ( J(1,1)*J(2,2) - J(1,2) *  
+      J(2,1) ) )
```

```
      B(1) = ( B1 + B2 ) / 2.0  
      B(2) = ( B1 - B2 ) / 2.0
```

```
*      WRITE (*, 10) B(1), B(2)  
* 10  FORMAT ( ' Eigen Values are:      B(1) = 'F10.8,  
*      +      & B(2) = ', F10.8 )
```

```
*****
```

```
*
```

```
*      Time to find Eigen Vector of J matrix using B(1) & B(2)
```

```
*
```

```
*****
```

```
      Q(1,1) = 1  
      Q(1,2) = 1  
      Q(2,1) = ( B(1)-J(1,1) ) / J(1,2)  
      N = SQRT( 1 + Q(2,1)*Q(2,1) )  
      Q(1,1) = Q(1,1) / N  
      Q(2,1) = Q(2,1) / N  
  
      Q(2,2) = ( B(2) - J(1,1) ) / J(1,2)  
      N = SQRT( 1 + Q(2,2)*Q(2,2) )  
      Q(1,2) = Q(1,2) / N  
      Q(2,2) = Q(2,2) / N
```

```
*****
```

```
*
```

```

*      Use This Segment if you wish to print the values of
*      "Eigen Values" and the "Eigen Vector".....
*

```

```

*****

```

```

*      PRINT*, 'The J matrix:'
*      PRINT*, J(1,1), J(1,2)
*      PRINT*, J(2,1), J(2,2)
*
*      PRINT*, 'Eigen Values: ', B(1), B(2)
*
*      PRINT*, 'The Eigen Vector of the above J matrix : '
*      PRINT*, Q(1,1), Q(1,2)
*      PRINT*, Q(2,1), Q(2,2)
*

```

```

*****

```

```

      L = E(4)
      L1 = L * B(1)
      L2 = L * B(2)

```

```

*****

```

```

*      Initializing errors for line-1 (ER1) and line-2 (ER2)

```

```

*****

```

```

      ER1 = 0
      ER2 = 0

```

```

      DO 100 II = 1, 2

```

```

          IF (II .EQ. 1) THEN
              F1 = 1.0
              F2 = 1.3
          ELSE
              F1 = 2.0
              F2 = 2.3

```

```

          ENDIF

```

```

      DO 40 F = F1, F2, .04

```

```

          L3 = L1 * F
          L4 = L2 * F
          C3 = (0, -1) * L3
          C4 = (0, -1) * L4

```

```

          C1 = CEXP(C3)
          C2 = CEXP(C4)

```

```

*****

```

```

*
*
*

```

```

      Computing SCATTERING MATRIX  Soi :

```

```

*****
      DO 50 I = 1, 2
      DO 50 K = 1, 2
          S(I,K) = Q(1,I) * C1 * Q(I,K) +
+              Q(2,I) * C2 * Q(2,K)
50      CONTINUE

*****
*
*      WRITE(*,60) F, ( ( S(I,K), K=1,2 ), I=1,2 )
* 60      FORMAT(//'The Forward Scattering Matrix SoI : at f = ',
*      +          f4.3, /12x, 2(f12.8), 5x, 2(f12.2), /12x,
*      +          2(f12.8), 5x, 2(f12.8), //)
*
*****
*
*      Computing POWER & ERROR
*
*****

      IF ( II .EQ. 1 ) THEN
          PO2 = 20 * ALOG10( CABS( S(1,2) ) )
          ER2 = ER2 + ABS( YR - PO2 )
      ELSE
          PO1 = 20 * ALOG10( CABS( S(1,1) ) )
          ER1 = ER1 + ABS( YR - PO1 )
      ENDIF

***** Writing in the data file opened earlier *****

      WRITE(8,*) F, PO1, PO2

40      CONTINUE

100     CONTINUE

      ERR = ER1 + ER2
      POWER = PO1 + PO2

      PRINT *, ER1, ER2, ERR, POWER

      RETURN

      END

*****
*
*      End of the subprogram ERROR.
*
*****
*****

```

Appendix C

List of the computer program for obtaining the line parameters of a diplexer from its e vector

Name of the Program: FInD_LF.BAS
Language: BASIC
Programmer: Md. Sayeed Akmal

This program uses the program COMBLINE.BAS as its first part for "calculating combline parameters". The parameters are printed on the screen.

The second segment of the program uses the subprogram ZmRe and computes C(1,2), Zou, Vpu, Wm, Zm and H-Lf for different values of shifting parameter "delj". This output goes to the printer.

There is also an option for opening data file for writing delj, H-Lf, Zm and Vpu for plotting purpose.

```
DECLARE SUB ZmEre (z!, Ere!, sr!)  
DIM Zou(5), Vpu(5), e(4)
```

----- Defining Function COS INVERSE -----

```
DEF fnacos (x) = ATN((SQR(1 - x * x) / x))
```

CLS

The optimized e vector from Table 4.2 :

```
e(1) = .598753:      e(2) = .59955  
e(3) = -.215:      e(4) = 6.71651
```

```
-----  
Length = e(4)  
m(1) = 1:    m(2) = 1:  
Rt(1) = 50:  Rt(2) = 50  
f = 1E+09:  pi = 3.1415926#  
wL = 2 * pi * f
```

```
Factor = 30  
Length = Length * Factor
```

```
----- OPENING FILE FOR WRITING DATA -----
```

```
OPEN "d:\AKMAL\dat\T6co30-1.dat" FOR OUTPUT AS #1  
OPEN "d:\AKMAL\dat\T6co30-2.dat" FOR OUTPUT AS #2  
OPEN "c:\vtex\T6co30.tex" FOR OUTPUT AS #3
```

```
-----  
LPRINT "Factor ="; Factor, "Length ="; Length  
LPRINT "
```

```
"  
LPRINT "      delj      C(1,2)      Zou      Vpu      Wm      Zm      H-Lf"  
LPRINT "      -----      -----      -----      -----      -----      -----      -----"
```

```
"  
FOR delj = 0 TO .07 STEP .002
```

```
-----  
Forming the J matrix from the e vetor:
```

```
j(1, 1) = e(1):    j(1, 2) = e(3)  
j(2, 1) = j(1, 2):  j(2, 2) = e(2)
```

```
----- Scalar Multiplication -----
```

```
FOR i = 1 TO 2  
    FOR k = 1 TO 2  
        j(i, k) = j(i, k) / Factor  
    NEXT k  
    j(i, i) = j(i, i) + delj  
NEXT i
```

```
-----  
FOR i = 1 TO 2
```

```
----- Calculation of Coupled Capacitance & Inductance -----
```

```
C(i, i) = 2 * j(i, i) / (wL * Rt(i) * (1 + m(i) * m(i)))
```

```
L(i, i) = 2 * j(i, i) * m(i) * m(i) * Rt(i) / (wL * (1 + m(i) * m(i)))
```

```
FOR k = 1 TO 2  
IF i <> k THEN
```

```
----- Calculation of Uncoupled Capacitance -----
```

```
    C(i, k) = 2 * j(i, k) / (wL * Rt(i))  
    PRINT , "Mutual Capacitance: C("; i; ", "; k; ") = "; C(i, k)  
END IF
```

```
    NEXT k  
PRINT
```

```
NEXT i
```

```
FOR i = 1 TO 2
```

```
----- Calculation of Uncoupled Capacitance -----
```

```
    CC(i) = C(i, i) - ABS(C(1, 2))
```

```
    PRINT "Uncoupled Capacitance: C("; i; ") = "; CC(i)
```

```
----- Calculation of Uncoupled & Coupled Impedances -----
```

```
    Zou(i) = SQR(ABS(L(i, i) / CC(i)))
```

```
    Zoc(i) = SQR(L(i, i) / C(i, i))
```

```
----- Calculation Uncoupled & Coupled Phase Velocities -----
```

```
    Vpu(i) = 1 / SQR(ABS(L(i, i) * CC(i)))
```

```
    Vpc(i) = 1 / SQR(L(i, i) * C(i, i))
```

```
NEXT i
```

```
PRINT "=====
```

```
PRINT "    Factor = "; Factor, "delj = "; delj
```

```
----- Printing the new [J] matrix -----
```

```
PRINT "The New [J] matrix = ";
```

```
FOR i = 1 TO 2
```

```
    PRINT TAB(22); "i"; " ";
```

```
    FOR k = 1 TO 2
```

```
        PRINT TAB(29 * k - 4 * k * k); j(i, k);
```

```
    NEXT k
```

```
    PRINT TAB(58); "i"
```

```
NEXT i
```

```
PRINT
```

```
PRINT "..... Length = "; Length; "mm"
```


=====

PROGRAM SEGMENT to calculate Zm and Lf
This program is uses a SUBprogram named ZmEre.

=====

----- Initializing values -----

P = 2.4: ETAo = 376.73: C = 3E+11
Erem = 2.55: Eref = 2.55:
pi = 3.141592: dm = 0:
Zf = 107: n = .9: h = 1.5

CALL ZmEre(Zf, Eref, srf)

FOR nn = 1 TO 2 ... nn=1 for line-1 and nn=2 for line-2

wL = 2 * pi * f
Vpm = C / SQR(Erem)
Vpe = Vpu(nn)
Vpf = C / SQR(Eref)
Bm = wL / Vpm
Bf = wL / Vpf
lamb = C / f

FOR i = 1 TO 6

Vpm = C / SQR(Erem)
Bm = wL / Vpm

Zm = (Zou(nn) * P) / ((P + 2 * dm) * (Vpe / Vpm))

zr = Zm / Zf
Be = wL / Vpe
Tm = Bm * (P + 2 * dm)
t = Tm

XX = ABS(COS(t) - COS(Be * P)) / (Zm * SIN(t))
x = 2 * XX

FINGER LENGTH CALCULATION

----- For HERRINGBONE line -----

$$hlf = \text{ATN}(XX * Zf / (n * n)) / Bf$$

----- For COMBLINE line -----

$$clf = \text{ATN}(2 * XX * Zf / (n * n)) / Bf$$

$$fhlf = hlf + dfp$$

$$fclf = clf + dfp$$

----- PRINTING JOBS -----

IF i = 6 THEN

PRINT "=====
 PRINT "Line"; nn; ":";

PRINT , "Coupled Capacitance: C("; nn; ","; nn; ") = "; C(nn, nn)
 PRINT , "Coupled Inductance : L("; nn; ","; nn; ") = "; L(nn, nn)
 PRINT , "Coupled Characteristic Impedance: Zoc("; nn; ") = "; Zoc(nn)
 PRINT , "Coupled Phase Velocity: Vpc("; nn; ") = "; Vpc(nn)
 PRINT
 PRINT , "Mutual Capacitance C(1,2) = "; C(1, 2)
 PRINT , "Uncoupled Characteristic Impedance: Zou("; nn; ") = "; Zou(nn)
 PRINT , "Uncoupled Phase Velocity: Vpu("; nn; ") = "; Vpu(nn)

PRINT "-----"

PRINT "Vpm="; Vpm; TAB(21); "Zm="; Zm; TAB(38); "srm="; srm, "Bm="; Bm
 PRINT "Vpf="; Vpf; TAB(21); "Zf="; Zf; TAB(38); "srf="; srf, "Bf="; Bf
 PRINT "Vpe="; Vpe; TAB(21); "T="; t; TAB(38); "dm="; dm, "hlf="; hlf
 PRINT "df="; df; TAB(21); "dfp="; dfp; TAB(38); "Dm="; Dm
 PRINT "Erem="; Erem; TAB(21); "Eref="; Eref
 PRINT "..... ULTIMATE FINGER LENGTH FOR HERRINGBONE LINE"; nn; " = "; fhlf; "mm.
 PRINT

ELSE

END IF

----- Calling the SUBprogram: ZmEre -----

CALL ZmEre(Zm, Erem, srm)

```

Dmm = (ETAo * h) / (Zm * SQR(Erem))      ...i= m or f...
Dff = (ETAo * h) / (Zf * SQR(Eref))
df1 = .076 + .2 * (2 * Dmm / lamb) ^ 2 + .663 * EXP(-1.71 * zr)
df = Dmm * (df1 - .172 * LOG(zr)) * zr
dfp = Dmm / 2 - df
dm = Dff * (.05 * n * n * zr)

```

```

NEXT i

```

```

Wm = h * srm
k = nn

```

```

LPRINT k; TAB(5);

```

```

LPRINT USING "+.###"; delj;

```

```

LPRINT TAB(11); ABS(C(1, 2)); TAB(25); Zou(k); TAB(35); Vpu(k); TAB(49); Wm; TAB(59); Zm
(*) ; fclf

```

```

PRINT #3, k; " & "; delj; " & "; Zou(k); " & "; Vpu(k); " & "; Wm; " & "; Zm; " & "; fcl
f;\hline"

```

```

IF k = 1 THEN

```

```

    WRITE #1, delj, fclf, Zm, Wm, Zou(k), Vpu(k), C(1, 2)

```

```

ELSE

```

```

    WRITE #2, delj, fclf, Zm, Wm, Zou(k), Vpu(k), C(1, 2)

```

```

END IF

```

```

NEXT nn

```

```

LPRINT

```

```

    INPUT "terminate (y/n) "; t$

```

```

    IF t$ = "y" OR t$ = "Y" THEN GOTO 1000

```

```

NEXT delj

```

```

CLOSE #1: CLOSE #2: CLOSE #3

```

```

1000 END ===== END OF MAIN PROGRAM =====

```

```

----- SUBprogram: ZmEre -----

```

SUBprogram to find W/H & Ere for a certain Zm
SHAPE RATIO : W/H = SR

SUB ZmEre (z, Ere, sr) STATIC

DIM Er(5)

Er(1) = 2.33: Er(2) = 2.55: Er(3) = 3.78: Er(4) = 10

ETAo = 376.73: pi = 3.141593
i = 2: tolerance = .01
delZ = 500

j1 = LOG(.2): j2 = LOG(10)

FOR j = j1 TO j2 STEP .01

sr = EXP(j)
delZold = delZ

IF sr <= 1 THEN

f = 1 / SQR(1 + 12 / sr) + .04 * (1 - sr) ^ 2

Ere = ((Er(i) + 1) + (Er(i) - 1) * f) / 2

Zi = ((ETAo / (2 * pi)) * LOG(8 / sr + .25 * sr)) / SQR(Ere)

ELSE

f = 1 / SQR(1 + 12 / sr)

Ere = ((Er(i) + 1) + (Er(i) - 1) * f) / 2

Zi = (ETAo / (sr + 1.393 + .667 * LOG(sr + 1.444))) / SQR(Ere)

END IF

PRINT "W/H ="; SR; TAB(20); "Zi ="; Zi; TAB(40); "Ere ="; Ere; TAB(60); "Er="; Er(

delZ = ABS(z - Zi)

IF delZ <= tolerance OR delZ > delZold THEN EXIT FOR

NEXT j

PRINT "Zi="; Zi, "sr="; sr, "Ere="; Ere

===== END OF SUBPROGRAM =====
END SUB

REFERENCES

- [1] G. L. Mathaei, L. Young and E. M. T. Jones, "Microwave Filters, Impedance Matching Methods and Coupling structures", McGraw-Hill Book Company, N.Y., 1964, pp. 965-1000.
- [2] J. F. Cline et al, "Design Data for Antenna-Multicoupler Systems", Final Report, SRI Project 2183, Contract AF 19(604)-2247, Stanford Research Institute, Menlo Park, California (September 1959).
- [3] R. E. Collin, "Foundations for Microwave Engineering", McGraw Hill International book Company, 1966, pp. 364 - 366.
- [4] Simon Ramo, John R. Whinnery and Theodore Van Duzer, "Fields and Waves in Communication Electronics", John Willy & Sons, pp. 23 - 60.
- [5] Saiful Islam, "Multiway Mode-interference and warped-mode microwave combline directional couplers", PhD Thesis, Cambridge University, Cambridge, U.K., 1986.
- [6] Saiful Islam, "The Design of Microwave Forward Directional Couplers Using Microstrip Comblines", Microwave Journal (USA), vol. 31, No. 11, November 1988, pp. 83 - 100.
- [7] Saiful Islam, "Multiway Uniform Comblines Directional Couplers for Microwave Frequencies", IEEE Transactions on Microwave Theory and Techniques, vol.36, 6 June 1988, pp. 985 - 993.
- [8] Erik O. Hammerstead, "Equations for Microwave Circuit Design", Proceedings of 5th European Microwave Conference, Hamburg, 1975, pp. 268 - 272.
- [9] Saiful Islam and J. E. Carroll, "A Symmetric Quitoplexer Using Planar Microstrip Coupled Comblines", Proceedings of the International Conference on Millimeter Wave and Microwave ICOMM-90, Defence Electronics Applications Laboratory, Tata-McGraw Hill Publishing Company Ltd., New Delhi, 1990, pp. 453 - 457.
- [10] P. Silvester and P. Benedek, "Equivalent Capacitance of Microstrip Open Circuits", IEEE Trans. MTT-20, pp. 511 - 516.

- [11] Saiful Islam, "An Analysis and A Design Technique for Microstrip Comblines", *Microwave Journal (USA)*, vol. 32, No. 11, November 1989, pp. 79 – 91.
- [12] R. Garg and I. J. Bahl, "Characteristics of Coupled Microstrip lines", *IEEE Transaction on MTT*, Vol. MTT-27, No. 7, July 1979, pp. 700 – 705.
- [13] William H. Press, Brian P. Flannery, Saul A. Teukolsky and William T. Vetterling, "Numerical Recipes the art of scientific computing", Cambridge University press, 1986, pp. 274 – 333.
- [14] J. D. Rhodes and Ralph Levy, "Design of General Manifold Multiplexers", vol. MTT-27, No. 2, February 1979, pp. 111 – 120.
- [15] J. D. Rhodes and Ralph Levy, "A Generalized Multiplexer Theory", *IEEE Transactions on Microwave Theory and Techniques*, vol. 32, MTT-27, No.2, February 1979, pp. 99 – 110.
- [16] J. L. Haine and J. D. Rhodes, "Direct Design Formulas for Asymmetric Bandpass Channel Diplexers", *IEEE Transactions on Microwave Theory and Techniques*, vol. MTT-25, No. 10, October 1977, pp. 807 – 813.
- [17] E. G. Cristal and G. L. Matthaei, "A Technique for the design of Multiplexers Having Contiguous Channels", *IEEE Transaction, PGMTT-12*, January 1964, pp. 88 – 93.
- [18] J. E. Carroll and P. R. Rigg, "Matrix Theory for n-line Microwave Coupler Design", *IEE Proceedings MOA*, vol. 127, No. 6, December 1980, pp. 315 – 322.
- [19] Saiful Islam and J. E. Carroll, "Warped Mode Multiway Comblines Directional Couplers", *IEE proceedings Microwave antennas and Propagation*, vol. 133, No. 2, April 1986, pp. 81 – 90.
- [20] B. A. Herscher and J. E. Carroll, "Design Technique for Multiport Comblines Couplers with Single Port Excited," *IEE Proceedings MOA*, Vol. 129, No. 2, April 1982, pp. 61 – 67.
- [21] Charles S. Beightler, Don T. Phillips and Douglass J. Wilde, "Foundations of Optimization" Prentice-hall, Inc., Englewood Cliffs, N. J. 07632, pp. 170 – 263.